UNIVERSIDADE DA BEIRA INTERIOR
Ciências

Synthesis of 5-methylene(thio)ureas (thio)barbiturates as potential xanthine oxidase inhibitors

Eunice Cerdeira Soares Cavalheiro

Dissertação para obtenção do Grau de Mestre em
Química Medicinal
(2º ciclo de estudos)

Orientador: Prof. Doutor Samuel Martins Silvestre
Co-orientador:Prof. Doutora Vânia Moreira

Covilhã, fevereiro de 2017

Folha em branco

Para os meus pais,

Folha em branco

Agradecimentos/ Acknowledges

Em primeiro lugar gostaria de agradecer ao Professor Doutor Samuel Silvestre e ao Professor Doutor Paulo Almeida pela possibilidade de desenvolver este projeto e por toda a orientação, apoio, disponibilidade e confiança durante ao longo de todo o processo.

Also I would like to express my gratitude to Professor Dr. Vânia Moreira and Dr. Leena Keuruleinen for allowing me to carry out part of the organic synthesis of this project on the Drug Discovery group of the Division of Pharmaceutical Chemistry and Technology of the Faculty of Pharmacy of the University of Helsinki, Finland. I would like to thank all the continuous support, guidance and kindness during development of this project

Agradeço a todos os meus colegas e amigos de laboratório Mafalda Catarro, João Serrano, Joana Figueiredo e João Marques por todo o auxílio e por todos os bons momentos passados. Gostaria de prestar um agradecimento também a Sara Garcia, companheira de aventuras do programa Erasmus e grande amiga, pelo apoio nos momentos mais difíceis e pela motivação durante o processo de escrita da tese.

Por último gostaria de agradecer à minha família, com especial atenção aos meus pais, irmão e avós que me apoiaram durante todo o meu período académico, encorajando-me a continuar os meus estudos e a conquistar muitas vitórias na vida.

Folha em branco

Resumo Alargado

Os ácidos barbitúricos apresentam um papel muito importante na descoberta de novos fármacos devido ao enorme espetro de atividades biológicas que os seus derivados possuem. Quimicamente, estes compostos são pirimidino-2,4,6-trionas contendo cinco átomos (três oxigénios e dois azotos) com afinidade para estabelecer ligações não-covalentes e com o ião metálico dos locais ativos de vários alvos biológicos tornando-os ligandos polifuncionais versáteis. Contudo, as atividades farmacológicas dependem principalmente do grupo substituinte ligado no carbono 5 do anel pirimidínico da molécula. Nexte contexto, o metileno do anel pirimidínico é um grupo ativado, tendo capacidade para perder um dos seus dois protões gerando diversas formas de ressonância quando desprotonado. Estes compostos exibem dois tipos de tautomerismo, ceto-enol e lactama-lactim, através da transferência de átomos de hidrogénio, tanto do grupo metileno como do grupo imino, para os átomos de oxigénio. O método mais usado na preparação de ácidos barbitúricos consiste numa condensação entre ureias e malonatos.

O Barbital é um hipnótico e foi o primeiro ácido barbitúrico a ser comercializado. Após o lançamento deste fármaco clínico, o interesse em sintetizar novos derivados barbitúricos cresceu exponencialmente, o que levou à descoberta de outros fármacos não só com ação hipnótica, mas também com ação antiepilética e anestésica. Atualmente existem compostos barbitúricos com propriedades anticancerígenas, antibacterianas, antioxidantes entre outras. Devido às propriedades gerais acima referidas, muito comuns em pirimidinas, os ácidos barbitúricos podem ser utilizados na síntese de diversos derivados e de vários compostos *O*- e *N*-heterocíclicos através de diferentes métodos sintéticos, envolvendo nomeadamente a adição de Michael e de reações de Manich, Knoevenagel, Biginelli e de Hantzch.

A xantina oxidase (XO) é uma oxidoreductase envolvida no processo metabólico de uma grande variedade de purinas, pirimidinas, entre outros. Através de reações de hidroxilação, esta enzima transforma a hipoxantina em xantina, seguida da sua oxidação em ácido úrico. A produção excessiva deste último metabolito e consequente acumulação e deposição sob a forma de cristais em determinados locais do organismo leva a um tipo de inflamação denominado gota. Neste âmbito, a XO é o alvo terapêutico mais comum no tratamento da gota sendo importante a sua inibição. O alopurinol, um análogo purínico, é um fármaco que inibe esta enzima. Contudo, este apresenta vários efeitos secundários, sendo necessário o desenvolvimento de inibidores seletivos e potentes. No desenvolvimento de novos compostos surgiram duas classes de inibidores: análogos purínicos e não-purínicos. Dentro da primeira classe foram sintetizados vários análogos de adeninas, guaninas, pirimidinas, pteridonas e xantinas. Embora se registassem bons resultados inibitórios, estes

análogos não mostraram boa seletividade, podendo interferir com outras enzimas do organismo. Assim, nasceu a necessidade de desenvolver novos compostos não-purínicos seletivos, sendo que, atualmente, se conhece uma extensa variedade de inibidores reportados como, por exemplo, derivados pirazole-carboxílicos, flavonoides e flavonas. O fármaco febuxostat é um inibidor não-purínico da XO, tendo maior potência e seletividade que o alopurinol. A síntese de moléculas híbridas através do rearranjo do *core* de dois derivados inibidores de classes químicas diferentes permitiu obter compostos com uma boa ação inibitória da XO.

Neste contexto, este trabalho visa a síntese de derivados de ácido barbitúrico e tiobarbituricos e sua avaliação como potenciais inibidores da XO.

Nesta dissertação são apresentados os resultados da síntese de derivados (tio)barbitúricos 5-metileno(tio)ureias e de (tio)barbituricos 5-(2-nitro)benzilidenos, precursores de pirimido [4,5-*d*]pirimidinas, os produtos finais desejados. Sabendo que alguns derivados de ácidos barbitúricos possuem efeitos inibitórios da XO, foi estudada a ação inibitória da XO, a atividade antioxidante e os efeitos na proliferação celular. Adicionalmente, foi realizado o estudo de *docking* molecular visando a previsão das energias de ligação e as possíveis interações dos compostos obtidos com o local ativo da XO.

O processo de obtenção dos novos barbitúricos 5-metilenoureias e seus tio-análogos baseou-se numa síntese de um só passo (*one-pot*), pela mistura de ácido barbitúrico ou os seus tio- e *N,N*-análogos, trialquil *orto*-formato e ureia ou tioureia em ácido acético em refluxo. Relativamente à preparação de (tio)barbituricos 5-(2-nitro)benzilidenos, esta sucedeu-se reagindo o respetivo ácido barbitúrico com 2-nitroaldeido em água. Todos os compostos sintetizados foram estruturalmente caracterizados por espectrometria infravermelho, ressonância magnética nuclear (RMN) de protão e de carbono, HSQC (*Heteronuclear Single Quantum Coherence*) e HMBC (*Heteronuclear Multiple Bond Correlation*), análise de massa e determinou-se igualmente os pontos de fusão dos compostos.

O teste da atividade antioxidante das moléculas obtidas foi realizado utilizando o método 2,2-difenil-1-picrilidrazil (DPPH). Os resultados demonstraram que tanto as (tio)barbitúricos metileno(tio)ureas tanto os (tio)barbitúricos 5-(2-nitro)benzilidenos não apresentaram bom poder redutor concluindo que estes derivados barbitúricos pouca atividade antioxidante. Dentro dos compostos testados, o [(4,6-dioxo-1,3-difenil-2-sulfanilideno-1,3-diazinano-5-ilideno)metil]tioureia e o [(1,3-dimetil-2,4,6-trioxo-1,3-diazinano-5-ilideno)metil]tioureia apresentaram alguma atividade antioxidante.

No ensaio enzimático de *screening*, utilizando XO de bovino, verificou-se que os compostos sintetizados aparentemente muito pouca atividade inibitória, visto que os resultados mostraram valores de inibição extremamente baixos, à exceção do 1,3-dimetil-5-

[[2-nitrofenil)metilideno]-1,3-difenil-2-sulfanilideno-1,3-diazinano-4,6-dione que revelou uma inibição de cerca de 60%.

A avaliação do efeito anti proliferativo foi realizada através do método colorimétrico do brometo de 3-(4,5-dimetiltiazol-2-il)-2,5-difeniltetrazolio (MTT) após a cultura celular da linha celular humana do cancro da mama (MCF-7). Os compostos sintetizados não mostraram atividade citotóxica relevante verificando-se valores de viabilidade celular bastante elevados.

Relativamente ao estudo computacional, após a realização do *docking* das moléculas sintetizadas, verificou-se que as energias de ligação no sítio ativo da enzima XO encontravam-se próximas das energias dos compostos de referência (alopurinol e febuxoxtat). Dentro da serie de compostos produzidos, aquele que demonstrou menor energia de ligação foi o composto [(4,6-dioxo-1,3-difenil-2-sulfanilideno-1,3-diazinan-5-ilideno)metil]urea.

Palavras-chave

Ácidos 5-Metileno(tio)ureias (tio)barbitúricos, antioxidantes, inibidores da xantina oxidase, atividade antiproliferativa, docking molecular

Abstract

Barbituric acids have an important role on the development of new drugs due to their various biological effects. Nowadays, these derivatives can be used as sedatives, hypnotics, anticonvulsants and anesthetics. Moreover, they possess antibacterial, antioxidant and anticancer activities. Most of these pharmacological properties are generally due to different side groups attached on C5 of the pyrimidine ring. By means of their general chemical and physical properties, barbituric acid and its thio-analogue are great precursors for the synthesis of several heterocyclic bioactive compounds. Some studies indicate that barbiturate derivatives can also inhibit xanthine oxidase (XO). This enzyme plays an important role in purines metabolism by transforming hypoxanthine to xanthine and then to uric acid. As the overproduction of uric acid is linked to gout disease, it is of high interest to inhibit XO.

In this context, during the attempts to synthetize pyrimido [4,5-*d*]pyrimidine-5,7-diones and 7-thione analogues using (thio)barbituric acid and their 1,3-diphenyl and dimethyl analogues, new 5-methylene(thio)urea (thio)barbiturate compounds were prepared by one-pot reaction with ureas or thioureas and trialkyl *ortho*-formates in acetic acid. 5-(2-Nitro)benzilidene derivatives were synthesised as well. All these precursors were structurally characterized by Infrared (IR) spectroscopy, ^{1}H, ^{13}C NMR, HMBC and HSQC and MS-analysis. Antioxidant evaluation though the 2,2-diphenyl-1-picrylhydrazyl (DPPH) method was performed in all synthesised compounds, however no promising antioxidant activity was revealed. These derivatives were also tested as XO inhibitors, revealing insignificant inhibitory activity towards this enzyme, excepting 1,3-dimethyl-5-[(2-nitrophenyl)methylidene]-1,3-diazinane-2,4,6-trione which revealed 60% of inhibitory activity at 30μM. In addition, a cell proliferation assay in breast cancer cell line (MCF-7) through the colorimetric 3-(4,5-dimethylthiazol-2-yl)-2,5-diphenyltetrazolium bromide (MTT) method showed that these derivatives do not have relevant cytotoxic effects.Additionally, it was performed molecular docking studies in order to predict the binding energies and possible interactions with XO enzyme verifying that 5-methylenethiourea thiobarbiturates presented the lowest binding energy among the other synthesised compounds.

Keywords

5-methylene(thio)urea (thio)barbiturates, antioxidants, xanthine oxidase inhibitors antiproliferative activity, molecular docking

Index

1. Introduction....1
1.1. Xanthine Oxidase....1
1.1.1. Inhibitors of Xanthine Oxidase....2
1.1.1.1. Purine analogues inhibitors....3
1.1.1.2. Non-Purine analogues inhibitors....5
1.2. Barbituric Acid and Derivatives....10
1.2.1. Synthesis of barbituric acids and heterocyclic compounds....12
1.2.2. Pharmacological activities of barbiturate derivatives....17
2. Aims....20
3. Results and Discussion....21
3.1. Synthesis....21
3.1.1. Synthesis and characterization of starting materials....22
3.1.2. Synthesis and characterization of 5-methylene(thio)urea (thio)barbiturates....23
3.1.3. Synthesis and Characterization of 5-arylidene (thio)barbiturates....28
3.1.4. Synthetic attempts for the preparation of pyrimido [4,5-*d*]pyrimidines....31
3.1.5. Synthesis of predicted pyrimido [4,5-*b*]quinolines from 5-(2-nitro)benzylidenes....34
3.2. Antioxidant activity....36
3.3. Xanthine Oxidase inhibition....40
3.4. Anti-proliferative evaluation....42
3.5. Molecular Docking....44
4. Conclusions and Future Perspectives....49
5.1. Synthesis....50
5.1.1. General Data....50
5.1.2. Synthesis of 1,3-diphenylthiobarbituric acid....50
5.1.3. General procedure for the preparation of 5-methylene(thio)ureas (thio)barbiturates....51
5.1.4. General procedure for the preparation of 5-arylidene thiobarbituric acids....54

5.1.5. Preparation of the 5-[(2-nitrophenyl)methyl]-2-thioxoidene-1,3-diazinane-4,6-dione 55
5.1.6. Procedure attempts for the preparation of pyrimido [4,5-*d*]pyrimidines 56
5.1.7. General procedure for the preparation of spiro-indole (thio)barbiturates 58
5.2. Biological Studies 59
5.2.1. Antioxidant assay: DPPH (1,1-diphenyl-2-picrylhydrazyl) free radical scavenging activity 59
5.2.1.1. Preparation of compound solutions 60
5.2.2.1. DPPH Assay 60
5.2.2. *In vitro* xanthine oxidase inhibition assays 60
5.3.1.1. Preparation of compounds solutions 60
5.3.1.2. Xanthine oxidase inhibition assay 61
5.2.3. Cell studies 61
5.2.3.1. Cell cultures 61
5.2.3.2. Preparation of compounds solutions 61
5.2.3.3. MTT cell proliferation assay 62
5.2.3.4. Statistics 62
5.4. Molecular Docking 62
6. References 63
6. Publications 70
7. Attachments 71

Figures Index

Figure 1| Diagram of the mechanism of action of XO. Oxidation of hypoxanthine and xanthine at molybdenum site and of the NADH at FAD site. The redox reaction between NAD^+ and molecular oxygen takes place at FAD site [2, 3, 6].....2

Figure 2| Structure of Allopurinol 3

Figure 3| A - structure of the adenine analogue 8-azaadenine; B - Structure of the guanine analogue phenyl-substituted 9-phenylguanidine; C – Structure of 3-nitrobenzoyl 9-deazaguanine 3

Figure 4| Structures of pyrazolo[3,4-*d*]pyrimidines derivatives; A - *N*-phenyl substituted pyrazolo[3,4-d]pyrimidines, B - *N*-(4'-Carboxyphenyl)-*N*-(2',3',4',6'-tetra-O-acetyl-ß-D-glucopyranozyl) pyraxolo[3,4-d]pyrimidine [13] 4

Figure 5| A - structure of phenyl-substituted 4(*3H*)-pteridones; B – structure of pteridine derivatives; C – structure of lumazine derivatives.....4

Figure 6| Chemical structures of hypoxanthine and xanthine analogues with XO inhibitory activity [11, 15].....5

Figure 7|Structures of Febuxostat (A) and Y-700 (B), potent inhibitors of XO 6

Figure 8| Potent carboxylic acids derivatives inhibitors of the XO; A -5-phenylisoxazole-3-carboxylic acid, B - 1-hydroxy-4-methyl-2-phenyl-1*H*-imidazole-5-carboxylic acid, C - 2-phenyl-4-methyl-1,3-selenazole-5-carboxylic acid 7

Figure 9 | Chemical Structures of 1-acetyl-3,5-diaryl-4,5-dihydro(1*H*)pyrazole (A) and *N*-(1,3-diaryl-3-oxopropyl)amide derivatives 8

Figure 10| Structures of different classes of flavonoids which presents inhibitory activity of XO.....9

Figure 11| Isosteric replacement on flavone backbone with a quinolone and key interactions of flavones for XO inhibition[24] 10

Figure 12| Design strategy of naphtoflavone derivatives from molecular hybridization of a naphtopyran and a azaflavone [25]..... 10

Figure 13| Chemical structures of barbituric and thiobarbituric acids derivatives used as drugs 18

Figure 14| Chemical Structure of the potent MMP inhibitor Ro-28-2653 18

Figure 15| Structures of the starting materials: thiobarbituric acid (1a), 1,3-diphenyl thiobarbituric acid (1b), barbituric acid (1c) and1,3-dimethyl barbituric acid (1d)..... 22

Figure 16 | Structure of the spiro-indole (thio)barbiturate derivatives 36

Figure 18| A – Real main interactions between Y-700 and XO68; B – Docked Y-700 structure interaction with XO; C- Docked test compound (2c) interactions win XO with the lowest binding energy value from all tested compounds; B and C were obtained by docking analysis through AutoDock Tools 1.5.6. software. 46

Schemes Index

Scheme 1| Transformation of xanthine to uric acid (adapted)[5] 2

Scheme 2| Original synthesis of barbituric acid 11

Scheme 3| Molecular structure of barbituric acid and ressonance forms of its deprotonation 11

Scheme 4| Synthesis of barbituric and thiobarbituric acids 14

Scheme 5| Synthesis of furopyrimidones (A) and chromeno[2,3-*d*]pyrimidines (B) 15

Scheme 6| Synthesis of pyrimido [4,5-*d*]pyrimidines by Biginelli Reaction 16

Scheme 7| Synthesis of hydropyrimido[4,5-*b*]quinolone (A), pyrazolopyridopyrimidines (B) and pyrimido [4,5-*b*]quinolones (C) through Hantzsh Reaction 16

Scheme 8| Synthetic strategy for the preparation of pyrimido [4,5-*d*]pyrimidines 21

Scheme 9| Preparation of the precursor 1,3-diphenyl thiobarbituric acid (1b) 22

Scheme 10| A- Preparation of the precursors 5-methyleneureas and thioureas from (thio)barbiturates; B- Proposed reaction mechanism to obtain the synthetized compounds .....**Erro! Marcador não definido.**

Scheme 11| A- Preparation of the precursors 5-methyleneureas and 5-methylenethioureas from (thio)barbiturates (2); B- Proposed reaction mechanism of synthetized compounds..... 29

Scheme 12| Synthetic strategies for the preparation attempts of pyrimido [4,5-*d*]pyrimidines from 5-methylene(thio)ureas thiobarbituric acid derivatives (4) 31

Scheme 13| Method D- Synthetic attempt for the preparation of pyrimido [4,5-*d*]pyrimidines from 5-(4-bromo)benzylidene thiobarbituric acid; Method E- Attempt for the preparation of pyrimido [4,5-*d*]pyrimidines 33

Scheme 14| A- Proposed preparation of pyrimido [4,5-*b*]quinolones; B- Proposed reaction mechanism of the formation for compounds 8a-c 35

Scheme 15| Reduction of the methylene double bond of the compound 3b..... 36

Graphics Index

Graphic 1| DPPH free radical scavenging activity of the synthesized compounds 37

Graphic 2! Effect of compounds concentration and determination of the IC_{50} of the the DPPH scavenging activity in the positive control (Trolox) and compounds 2d and 2h 40

Graphic 3| XO inhibition screening activity of the synthesized compounds at 30 μM 41

Graphic 4| Dose-response curves of the compounds 2a, 2b and 3d compared with allopurinol 42

Graphic 5| Effect of the synthesized compounds in MCF-7 cell viability at 30 μM. *p<0,05 in relation to a negative control (t-Student test) 44

Tables Index

Table 1| Physical and analytical data of the synthesized derivatives 2(a-h) 24

Table 2| ^{1}H and ^{13}C NMR spectra data of the synthesized compounds 2(a-h)..... 26

Table 3| Physical and analytical data of the synthesized arylidene (thio)barbituric acids derivatives (3) 29

Table 4| ^{1}H and ^{13}C NMR spectra data of the synthesized arylidene (thio)barbituric derivatives (3) 30

Table 5| DPPH radical scavenging screening assay and determination of half inhibition concentrations (IC_{50}) in the compounds 2d and 2h 38

Table 6| XO inhibitory activity assay and determination of IC_{50} values on the compounds 2a, 2b and 3d..... 41

Table 7| Molecular docking results of the synthesized compounds with XO 47

Acronyms Index

5-FU	5-Fluorouracil
BSA	Bovine serum albumin
DEMM	Diethyl ethoxymethylenemalonate
DEPT	Distortionless enhancement by polarization transfer
DCM	Dichloromethane
DMSO	Dimethyl sulfoxide
DNA	Deoxyribonucleic acid
DPPH	2,2-Diphenyl-1-picrylhydrazyl
FAD	Flavin adenine dinucleotide
FTIR	Fourier transform infrared
HMBC	Heteronuclear multiple bond correlation
HSQC	Heteronuclear single quantum coherence
IR	Infrared
m.p.	Melting point
MetAP-1	Methionine aminopeptidase-1
MCR	Multicomponent reactions
MMP	Matrix metalloproteinase
Mo	Molybdenium
MTT	3-(4,5-Dimethylthiazol-2-yl)-2,5-diphenyltetrazolium bromide
NAD	Nicotinamide adenine dinucleoride
NMR	Nuclear magnetic resonance
PDB	Protein data bank
TEBAC	Bemzyltriethylammonium chloride
THF	Tetrahydrofuran
TLC	Thin layer chromatography
XDH	Xanthine dehydrogenase

XO	Xanthine oxidase
XOR	Xanthine oxidoreductase
Y-700	1-[3-Cyano-4-(2,2-dimethylpropoxy)phenyl]-1*H*pyrazole-4-carboxylic acid

1. Introduction

1.1. Xanthine Oxidase

Xanthine oxidoreductase (XOR) enzymes have been isolated from a range of organisms and catalyse the transformation of a wide variety of purines, pyrimidines, pterins and aldehyde substrates through a hydroxylation process. All these proteins have similar molecular weight and composition of redox centres.[1] XOR has long been known to be present in cows' milk and was first purified from this source in 1902 and has been detected in several organisms, from bacteria to man. It is widely distributed throughout various organs including liver, gut, lung, kidney, heart, brain and in the plasma. These enzymes have consequently become a model for structural and mechanistic studies of molybdoenzymes in general.[2,3] Xanthine dehydrogenase (XDH) and xanthine oxidase (XO) are the two forms of XOR and they are involved on the purine metabolic pathway of degradation of purines in higher animals, catalysing the oxidation of hypoxanthine to xanthine and xanthine to uric acid (scheme 1). These two forms are products of the same gene and the enzyme originally synthesized in its XDH form though, it can readily be converted to XO either by proteolysis or by oxidation of cysteine (Cys) residues to form dissulfide bridges.[4]

XO is a homodimer with a molecular mass of 290kDa. Considering that it belongs to molybdenum-protein family, XO contains one molybdenum metal, one of the flavin adenine dinucleotide (FAD) and two iron-sulfur (Fe_2S_2) redox centres of the ferredoxin type in each of its two independent subunits. This enzyme possesses two separated substrate-binding sites.[5] Electrons are donated from substrates to the molybdenum site of XO and are equilibrated between the redox centres before being passed to NAD^+ or to molecular oxygen at the FAD site. During the reduction of NAD^+ to NADH, molecular oxygen acts as an electron acceptor, producing superoxide anion radical and hydrogen peroxide.[5, 6] These interactions are summarized in the figure 1.

As mentioned before, uric acid is produced by degradation of purines through the action of XO. This metabolite is ionized to urate at physiological pH, which has limited solubility in water. Therefore, the overproduction and/or inadequate excretion of uric acid results in hyperuricemia. Hence, it can lead to the deposition of urate crystals in various locals, particularly on the joints, the connective tissues and kidney. This inflammation state is denominated by gout. [7,8]

XO also plays a role in ischemia-reperfusion injury. During ischemia, the energy of the cell falls and transmembrane gradients break down leading into a rise in levels of intracellular calcium which activate the protease that converts XDH into XO. Concomitantly, purines are catabolized and hypoxanthine is accumulated. When molecular oxygen is available its reaction with XO and hypoxanthine leads to the generation of reactive oxygen species (ROS)

mentioned previously. Superoxide anion and other formed radicals are destructive agents causing tissue damages. [6]

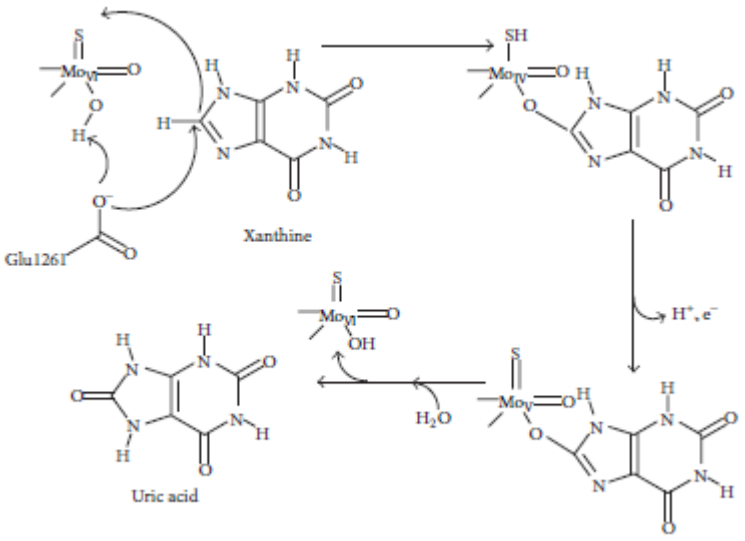

Scheme 1| Transformation of xanthine to uric acid (adapted)[5]

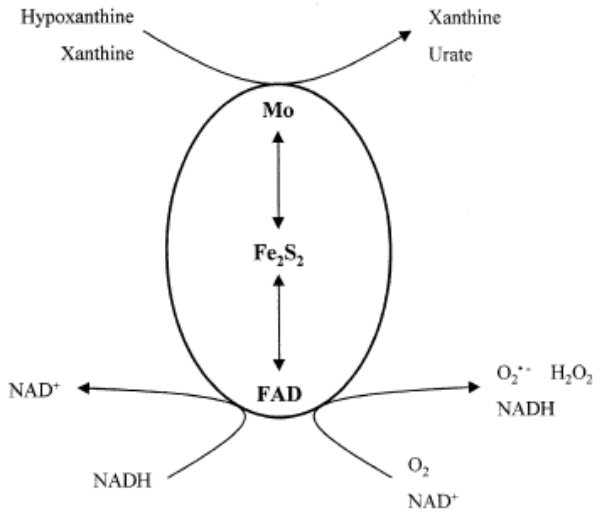

Figure 1| Diagram of the mechanism of action of XO. Oxidation of hypoxanthine and xanthine at molybdenum site and of the NADH at FAD site. The redox reaction between NAD^+ and molecular oxygen takes place at FAD site [2, 3, 6]

1.1.1. Inhibitors of Xanthine Oxidase

Xanthine Oxidase is considered the most promising target for therapeutic treatment of gout, oxidative damage, inflammation and even for cancer. Allopurinol (figure 2) is a potent XO inhibitor with purine moiety and it is the most commonly drug used in therapy for

chronic gout. However, several side effects have been reported as hypersensitivity reactions, gastrointestinal upset and skin rashes. Toxicity symptoms of this drug include fever, eosinophilia (increase of eosinophilic leukocytes in the peripheral blood), hepatitis and renal function failure which can lead to a fatal outcome. [9,10] Therefore, there is a need for the development of novel compounds with better safety profiles and to relieve associated side effects. The discovery and optimisation of new XO inhibitors having structures related to purines or other different molecules have been undertaken. Most of the compounds are nitrogen or oxygen heterocycles. Moreover, miscellaneous structures can also be found as XO inhibitors. [11]

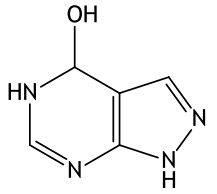

Figure 2| Structure of Allopurinol

1.1.1.1. Purine analogues inhibitors

Due to the fact that XO substrates (hypoxanthine and xanthine) are purines, the synthesis of purine-analogues turned out to be interesting on the development of potent XO inhibitors. Several studies reported adenine and guanine based analogues behaving as excellent suppressors of enzyme. For example, 8-azaadenine and phenyl-substituted 9-phenylguanines exhibited a considerable increase in their binding with the enzyme (figure 3). The guanine derivatives and their thio-analogues showed elevated inhibition results if a hydrophobic phenyl group is present in *N*-9. In a recent study, a new guanine analogue, 3-nitrobenzoyl 9-deazaguanine, presented to be thirty times more potent than allopurinol. [11, 12]

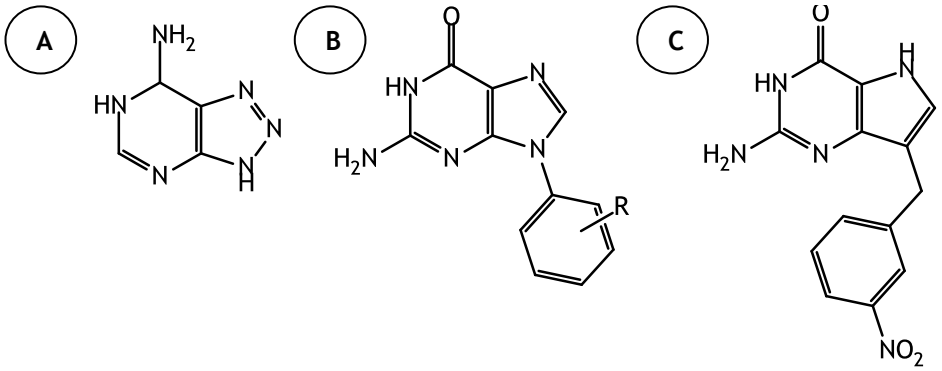

Figure 3| A - structure of the adenine analogue 8-azaadenine; B - Structure of the guanine analogue phenyl-substituted 9-phenylguanidine; C – Structure of 3-nitrobenzoyl 9-deazaguanine

Some *N*-aryl-5-amino-pyrazole[3,4-*d*] pyrimidines derivatives, structurally related to allopurinol, have been reported as potent inhibitors of XO, and the increase of the inhibitory action was due to the addition of a pyrimidine ring on the nitrogen at position 7, as well as the presence of electron-withdrawing groups (CF_3, NO_2 and CN) at *para*-position of the aryl ring mentioned. Moreover, the introduction of a sugar substitutent at the amine on carbon 4 showed the strongest activity (figure 4).[13]

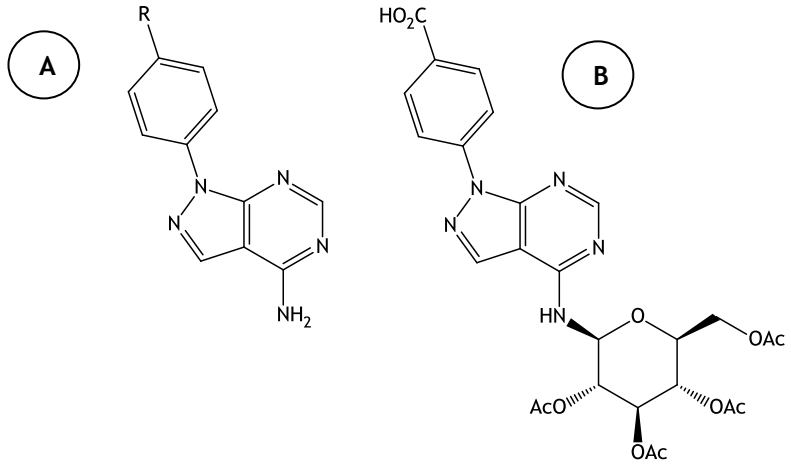

Figure 4| Structures of pyrazolo[3,4-d]pyrimidines derivatives; A - *N*-phenyl substituted pyrazolo[3,4-d]pyrimidines, B - *N*-(4'-Carboxyphenyl)-*N*-(2',3',4',6'-tetra-O-acetyl-ß-D-glucopyranozyl) pyraxolo[3,4-d]pyrimidine [13]

Various pteridone, pteridine and lumazine derivatives (figure 5) were found to have inhibitory effects in XO. It was postulated that the strong activity of phenyl-substituted 4(*3H*)-pteridones was due to the interaction of the aryl group with a hydrophobic region at the active site of the enzyme. Pteridine and lumazine compounds containing a hydroxylated side chain at position 6 revealed to be the most potent inhibitors among the other derivatives. The tautomerism effect on lumazine compounds can be associated to a moderate inhibition action as well. [14]

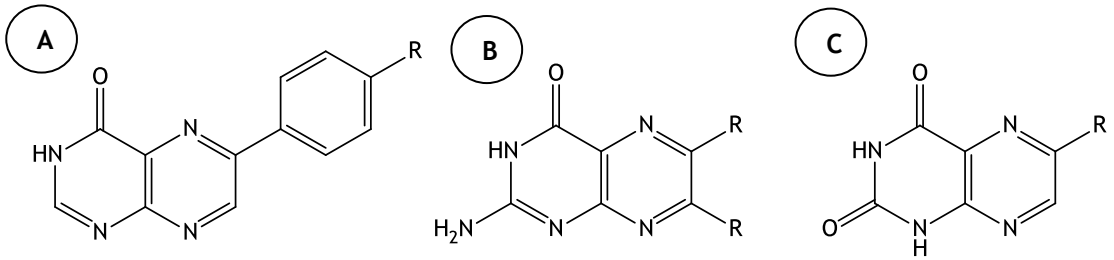

Figure 5| A - structure of phenyl-substituted 4(*3H*)-pteridones; B – structure of pteridine derivatives; C – structure of lumazine derivatives

Hypoxanthine and xanthine analogues (figure 6) also had a role on the discovery of new inhibitory agents of XO. It was shown that their inhibitory activity was higher than the

previous derivatives mentioned before. Structural characteristics which enhance the inhibition of this enzyme are:

- 8-Aryl substituent in the heterocycle system, turning into a linear molecule increasing the affinity to the XO afterwards;
- The presence of a nitrogen at position 1 is essential to the inhibitory properties;
- The replacement of the nitrogen at the position-7 to a C-NO_2 group leads to an analogue with excellent IC_{50} values;
- The insertion of a phenyl ring into the 2 or 3 position can increase the inhibitory potency;
- The introduction of arylaldehyde hydrazones at position 6 of the *7H*-purine markedly increases their activities as inhibitors of XO.

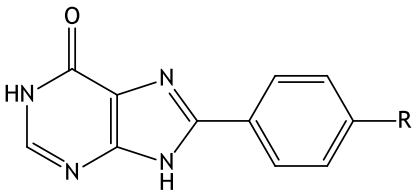

8-arylhypoxanthines

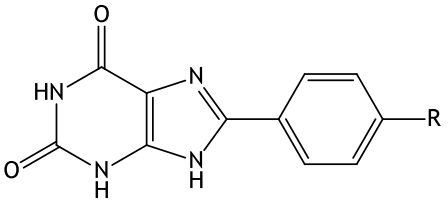

8-arylxanthines

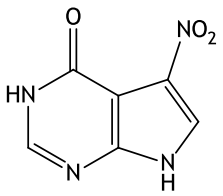

5-nitropyrrolo[2,3]pyrimidin-4-one

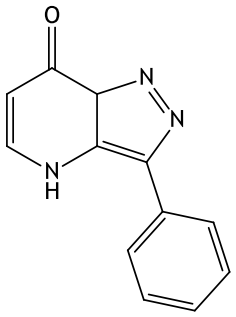

3-phenylpyrazolo[1,5]pyrimidin-7-one

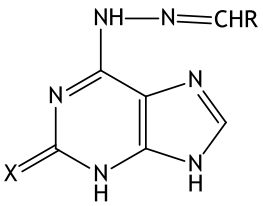

6-alkylidenehydrazino-7*H*-purines

Figure 6| Chemical structures of hypoxanthine and xanthine analogues with XO inhibitory activity [11, 15]

1.1.1.2. Non-Purine analogues inhibitors

Although purine analogues exhibits great inhibitory effects in XO enzyme, they may interfere with other enzymes present in the organism, leading to undesirable effects. Hence, extensive research on the discovery of non-purine analogues started to take place. Since then, a wide range of compounds have been reported.

Febuxostat (figure 7A) is a thiazolecarboxylic acid derivative, selective for inhibition of both reduced and oxidised forms of XO, exerting a mixed-type inhibition. The mechanism of action is mediated by high binding affinity of this drug to the enzyme in a molecular channel leading to the molybdenum-pterin active site. Moreover, the binding of febuxostat persists independent of the redox state of the molybdenum cofactor and is able to block the endogenous substrate access. The absence of a purine backbone in its chemical structure displays an insignificant effect on purine and pyrimidine metabolic enzymes. This drug has greater potency and longer lasting hypouricemia activity due to its capability of inhibit the two XOR forms (XDH and XO). [16, 17] Likewise, pyrazolecarboxylic acid derivatives, as the potent inhibitory drug Y-700 (figure 7B), exhibits the same structural core as febuxostat.[18] These two well-known drugs became relevant on the discovery of new five-membered carboxylic acids where the main changes relied on the insertion of 5 membered isosteres of pyrazole and thiazoles. Derivatives of 5-phenylisoxazole-3-carboxylic acid, 1-hydroxy-4-methyl-2-phenyl-1*H*-imidazole-5-carboxylic acid and 2-phenyl-4-methyl-1,3-selenazole-5-carboxylic acid (figure 8) are some examples of potent inhibitors of the XO. Both febuxostat and Y-700 as the mentioned derivatives possess the same structural features regarding the interaction inside the binding site of XO such as: 1) the replacement of the 4-hydroxypyrimidine ring, which was metabolized by the enzyme, to a carboxylic acid at position-4 of the five-membered ring enhancing the coordination with the molybdenum; 2) the phenyl group excluding the possibility of the compound conversion to unnatural nucleotides as allopurinol; 3) the presence of butoxy or isobutoxy groups at 4'-position of the phenyl ring enhancing the inhibitory activity contrary to other alkoxy ones; 4) a ciano group at 3-position of the five-membered ring, allowing a π bond potentiated the inhibitory activity; 5) the combination of a ciano and a butoxy group as refered previously revealed very important for XO inhibitory acids.[18, 19, 20, 21]

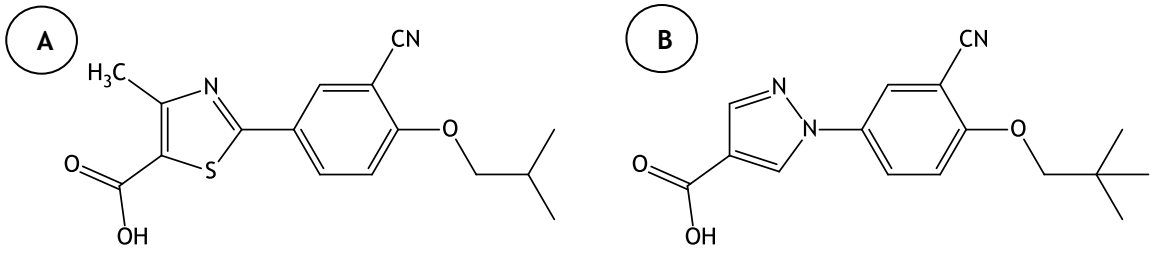

Figure 7|Structures of Febuxostat (A) and Y-700 (B), potent inhibitors of XO

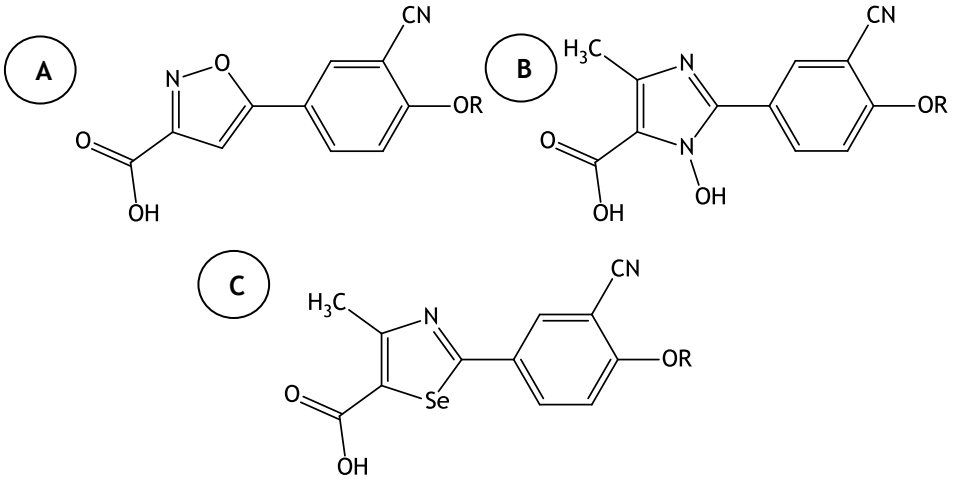

Figure 8| Potent carboxylic acids derivatives inhibitors of the XO; A -5-phenylisoxazole-3-carboxylic acid, B - 1-hydroxy-4-methyl-2-phenyl-1*H*-imidazole-5-carboxylic acid, C - 2-phenyl-4-methyl-1,3-selenazole-5-carboxylic acid

Throughout the discovery of new non-purine inhibitors of the XO, a rational design of 1-acetyl-3,5-diaryl-4,5-dihydro(*1H*)pyrazoles compounds was investigated (figure 9A) based on the following considerations: maintenance of all important groups or functionalities like two(hetero)aromatic rings joined by a central linker which is essential to the 5-membered ring and a site for hydroxylation near the molybdenum metal; presence of a carbonyl group on the 5-membered ring that might impart binding interactions with amino acids of the active site and easy synthesis. The evaluation of the inhibitory activity of these compounds in the enzyme revealed good results leading to some structure-activity conclusions. The placement of a 1-naphtyl or a 2-furyl group on ring A increased the inhibitory effect, being the second group more potent than the first one. On ring B, the introduction of the groups mentioned above decrease the activity being the phenyl groups more effective and their substitution into a heteroaryl one, such as 4-pyridyl group, drastically enhance the inhibitory activity. The presence of deactivating substituents in the phenyl group of ring B also potentiate their activity. It was also concluded that the presence of *N*-acetyl group on the 5-membered ring is essential for the inhibitory activity of the XO. [22]

Following the structural considerations previously described for the design of 1-acetyl-3,5-diaryl-4,5-dihydro(*1H*)pyrazoles, new *N*-(1,3-diaryl-3-oxopropyl)amides were synthesised showing good XO inhibition values. The figure 9B presents the chemical structure of these amide derivatives and their XO inhibition was greater using the same substituents on rings A and B of 1-acetyl-3,5-diaryl-4,5-dihydro(*1H*)pyrazoles. It was revealed as well that the lengthening of the linker between the two rings decreased the XO inhibition activity due to greater flexibility of the molecule. [23]

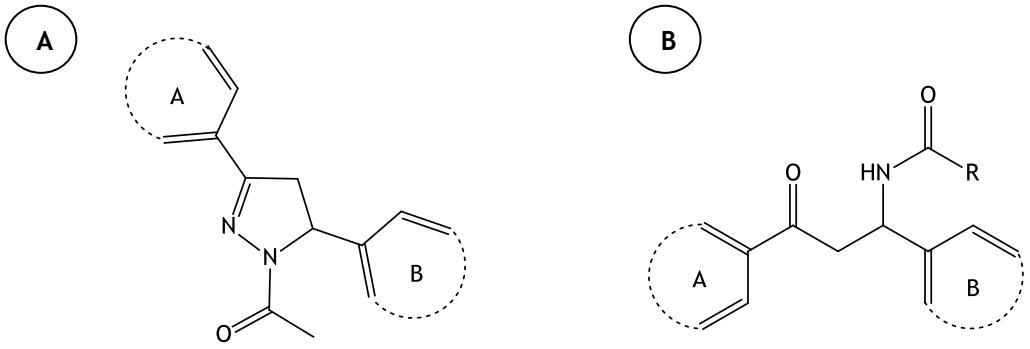

Figure 9 | Chemical Structures of 1-acetyl-3,5-diaryl-4,5-dihydro(1*H*)pyrazole (A) and *N*-(1,3-diaryl-3-oxopropyl)amide derivatives

Flavonoids represent a class of secondary metabolites from natural products sources possessing a diverse array of biological and pharmacological activities. Numerous reports highlight the inhibitory potential of XO of two flavonoids chemical classes: flavonols and flavones. Quercetin and luteolin are some examples of flavonols and flavones exhibiting inhibitory action in XO (figure 10). Structure requirements are necessary for XO inhibition as such the presence of hydroxyl groups on C-5 and C-7. The introduction of hydroxyl groups on both carbons or simple on C-7 demonstrated similar type of binding the XO, suggesting that both derivatives enter on the binding site cavity orientated in similar way. A strong electrostatic interaction of the negatively charged oxygen of the C-7 hydroxyl group is ensured enhancing the 2-phenyl moiety to interact with the enzyme. The presence of a hydroxyl group at C-6 also increases considerably the inhibitory effect. The existence of a double bond between C-2 and C-3 is also very important for the inhibition of XO. Molecules rigidity towards planar structures have a major importance on the inhibitory action of these compounds and substituted C-4 compounds display higher effects than the unsubstituted ones.[11]

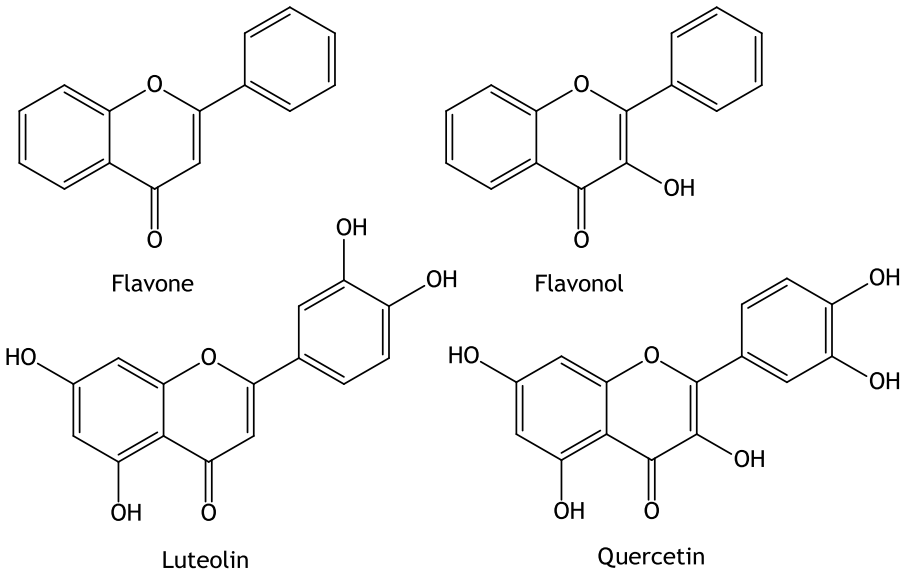

Figure 10| Structures of different classes of flavonoids which presents inhibitory activity of XO

In the past few years, the flavone framework has been used as lead structure for further optimization and design of new compounds. Through the replacement of this structural core into a quinolone ring by bioisosterism, 2-aryl-4-quinolones, also denominated as azaflavones, were produced keeping in view the shape and structural features of flavones responsible for their inhibitory potential (figure 11). The research of the XO inhibitory potential in 2-aryl-4-quinolones derivatives revealed interesting observations on the influence of electronic and steric factors at the 2-phenyl ring. Generally, electronic factors such as the introduction of activating groups like methoxy group at *para*- position on the phenyl ring remarkable enhanced the inhibitory activity due to the greater rigidity of the molecule towards the planar structure. Deactivating groups did not exhibit promising inhibition activity. Apart from the electronic factors, steric ones also influenced the molecules activity. Replacing the 2-phenyl ring with a monocyclic hetero-aryl such as thiophenol and pyrimidil rings, increased significantly the XO inhibition effect. [24]

Naphtoflavone derivatives are another example of the usage of the flavone backbone on the investigation of new potential XO inhibitory molecules. This derivative consists on the rearrangement of two different molecules with XO inhibitory activity, naphtopyran and flavone itself keeping intact the most important requisites for XO inhibition that are the non-substituted C-3 and over planarity (figures 11 and 12). These hybrid molecules revealed significant XO inhibitory activity. The nature and the positioning of substituents on the phenyl group at 2-position were important factures of the inhibitory potential of naphtoflavone derivatives. Mono-substituents on this group increased inhibitory activity whether the substitute was electron withdrawing or electron donating whereas non-substitute or di-substitute decreased the inhibitory effect. The preference order for positioning of the substituents is identical to the previous flavone analogues (*para*> *ortho*> *meta*). The inhibitory potential was remarkably advantaged in substituents at *para*-position with a

stronger inductive nature in comparison to substituents with stronger resonance and hyper conjugation nature. [25]

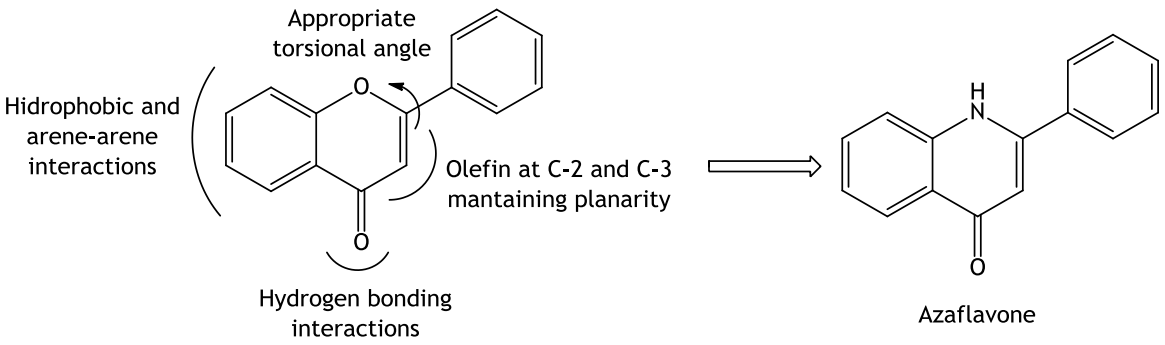

Figure 11| Isosteric replacement on flavone backbone with a quinolone and key interactions of flavones for XO inhibition[24]

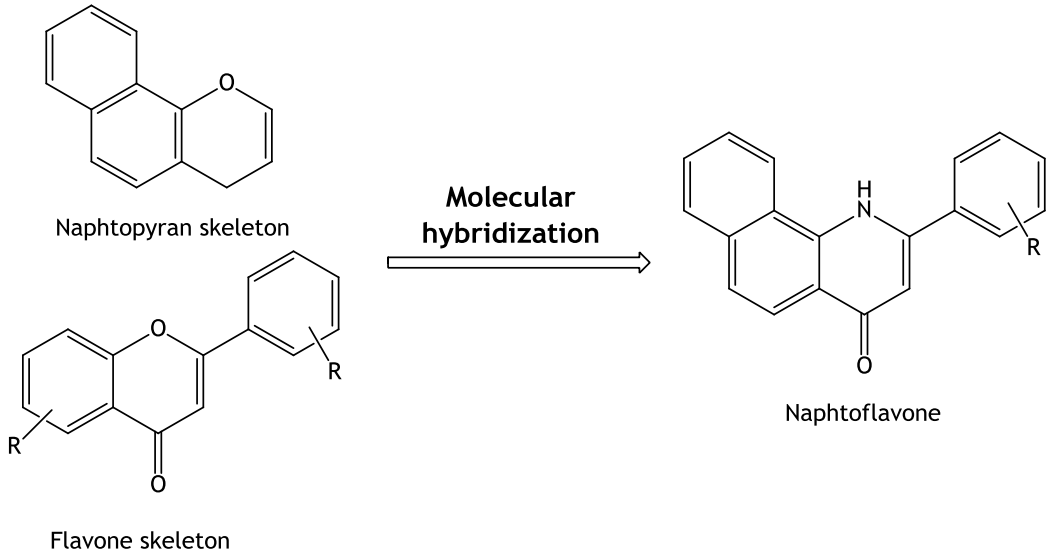

Figure 12| Design strategy of naphtoflavone derivatives from molecular hybridization of a naphtopyran and a azaflavone [25]

1.2. Barbituric Acid and Derivatives

Barbituric acid was first discovered by Adolph von Baeyer in 1864 through a condensation reaction of urea with malonic acid (Scheme 2).[26] Based on these two starting compounds,

several synthetic techniques were studied in order to synthesise this molecule. Although it was determined to be without therapeutic significance, this discovery subsequently led to the preparation of many derivatives of this molecule, commonly known as barbiturates, fuelling the discoveries of a broad new class of therapeutics that would quickly dominate the medical and social circles in the early 20th century.[27]

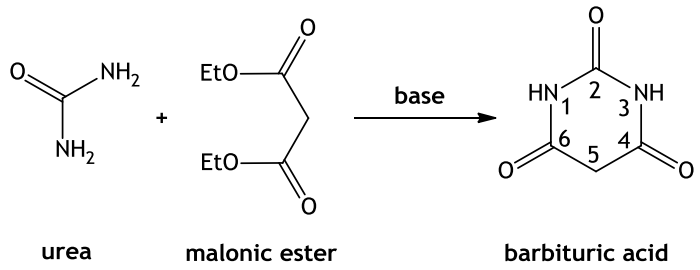

Scheme 2| Original synthesis of barbituric acid

Chemically, barbiturates are pyrimidine 2,4,6(*1H,3H,5H*)-triones. The barbituric acid exists in the solid state containing five atoms (three oxygens and two nitrogens) with potential metal binding sites, or coordination roles, being able to create the possibility for the formation of supramolecular arrangements through the donor-acceptor mechanism of protons in the building block arrangements. The activated methylene group (carbon-5, representing the alpha carbon, which is bonded to two other carbonyl groups) presents the most acidic hydrogen, having the ability to lose one of its protons promoting resonance delocalization that stabilize the pyrimidine ring through the formation of a barbituric anion with a planar carbanion (Scheme 3).[28-31]

Barbituric acid itself do not have biological activity and their pharmacological properties mainly depend on side groups attached to the position-5 of the pyrimidine ring. These substituents also provide interesting solvatochromic and coordination properties. Due to their metal binding capacity, barbituric acids can also be used as disperse fluorescent dyes.[28]

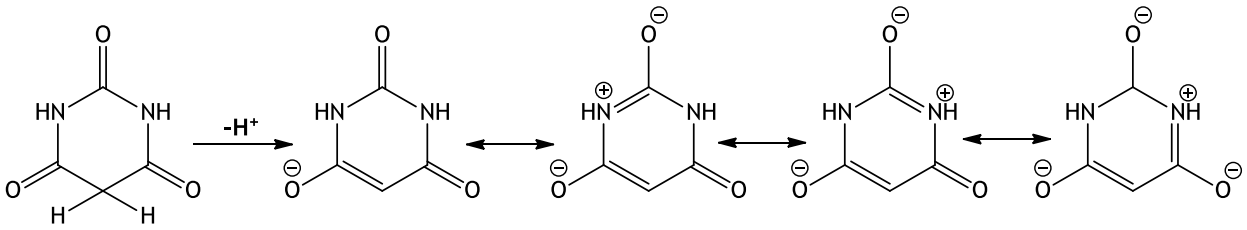

Scheme 3| Molecular structure of barbituric acid and ressonance forms of its deprotonation

Moreover, barbituric acids also possess multiple sites for the creation of non-covalent bonds, namely hydrogen bonding. In the crystalline state, they show several modes of hydrogen bonds formed between the NH and the CO groups. These non-covalent bonds are responsible for layer packing in the crystal lattice and for the construction of supramolecular assemblies. Weak Van der Walls interactions in the carbonyl group of the pyrimidine ring have also an important role in the three-dimensional packing of the molecules in the crystal structure. These intermolecular interactions, together with the hydrogen bonds, are responsible for the barbituric acids polymorphism, which is consequently responsible for the biological availability of the compounds.[29]

Barbiturates, have received great attention of pharmaceutical community for more than a century due to their various biological and medical properties. Thus, barbiturates are employed as depressants for the central nervous system, sedative hypnotics, anticonvulsants and anesthetics.[29] Some of these derivatives also exhibit antibacterial, anti-tubercular, anticancer activities.[28] Recently, barbituric acid derivatives have also received great attention for nanosciences, coordination and supramolecular applications besides being used extensively in therapy for many diseases.

1.2.1. Synthesis of barbituric acids and heterocyclic compounds

Barbiturates are a popular class of heterocycles with a widely range of applications. The construction of heterocyclic molecules and building blocks can be limited and methods based on Multicomponent Reactions (MCR) have proved quite efficient on breaking the borders to their synthesis. MCR is generally defined as any process in which more than two reactants combine in one pot to form a product that incorporates structural features of each starting material. Besides generating structural complexity in a single step, such reactions offer the advantage of simplicity and synthetic efficiency over stepwise sequential approaches. Additionally they are selective, synthetically convergent and atom economic, thus avoiding complicated purification procedures and allowing saving both solvents and reagents. MCR has played a central role in the development of modern synthetic methodologies for drug discovery research. [32, 33]

The scheme 4 presents several methodologies for the synthesis of barbituric acids and their derivatives. The discovery and further medical introduction of barbituric acids led to the synthesis of a huge number of these compounds derivatives. The most standard and industrialized procedure towards barbiturates is the Michael method, which is based on the condensation of urea with the appropriate diethylmalonate in the presence of sodium ethoxide in anhydrous alcohol.[34] Malonic acid, malonyl dichlorides (Scheme 4A) and malonic esters are examples of the most used malonates in the preparation of barbiturics. Likewise, this procedure can be adopted for the preparation of alkyl or dialkylbarbituric acids through

condensation of different 2-substituted or 2,2-disubstituted malonates with urea (Scheme 4B). The reaction between 1,3-disubstituted ureas and 2,2-dialkylmalonates in tetrahydrofuran (THF) solution leads to the formation of crystalline barbiturates, also known as 1,3,5,5-tetrasubstituted pyrimidine-2,4,6(*1H,3H,5H*)-trione (Scheme 4C).[30]

An alternative synthetic method involving an alkali hydroxide as a condensing agent and liquid ammonia as solvent lead to the production of dialkylbarbituric acids (Scheme 4D).

Similarly, the presence of this condensing agent and solvent revealed good yields of barbituric acids by reacting ethyl carbonate with malonamides, C-alkylmalonamides or C,C-dialkylmalonamides.[34]

The replacement of an oxygen into a sulphur in the 2-position of the pyrimidine ring leads to an additional scaffold of derivatives denominated as thiobarbituric acids. Some synthetic methodology of thiobarbituric derivatives are identical to barbiturates involving, in this situation, the thioureas. Diethyl ethoxymethlylenemalonate (DEMM) has very often been exploited in the preparation of pyrimidines, which involve the addition of thioureas and their *N,N*-substituted analogues on DEMM in a solution of reactants in concentrated hydrochloric acid and ethanol resulting into the correspondent thiobarbituric acids (Scheme 4E). [35]

Other reproducible procedure consisting in the reaction of C-functionalized malonates with thioureas in the presence of dimethyl sulfoxide (DMSO) and potassium *tert*-butoxide generates thiobarbiturates in good yields (Scheme 4F).[36]

The chemical synthesis by microwave approaches have been increasingly explored for the preparation of barbituric acid and its thio-analog and their derivatives. The microwave irradiation of a mixture of a diaryl thiourea, malonic acid and acetyl chloride for just a few seconds resulted in 90-95% of the desired product (Scheme 4G).[37] This method provides faster and cleaner reactions with higher yields because of the direct “in core” heating of the mixture. It is possible to use solvents with lower boiling points under pressure and heated in superior temperatures than their boiling point and the microwave heating also is more energy efficient than the classic oiling bath due to the direct molecular heating and inverted temperature gradients.[38]

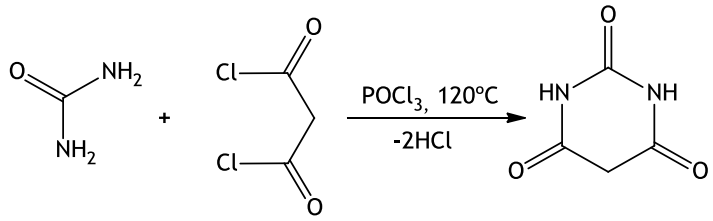

(A)

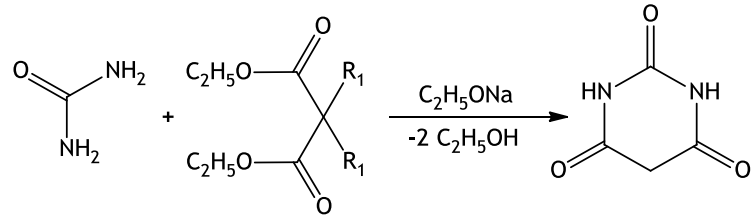

(B)

R= H, aAlkyl

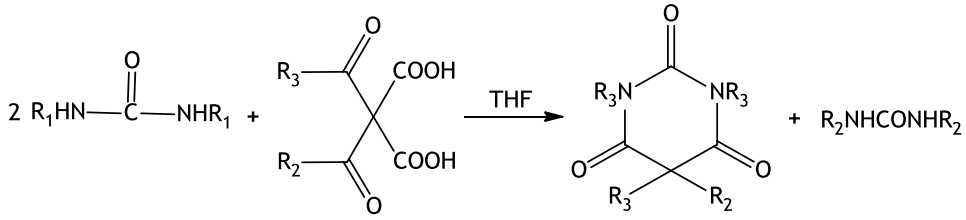

(C)

R_1, R_2 = H, Alkyl, Aryl; R_3= C_6H_{11}, *i*-Pr, *p*-tolyl

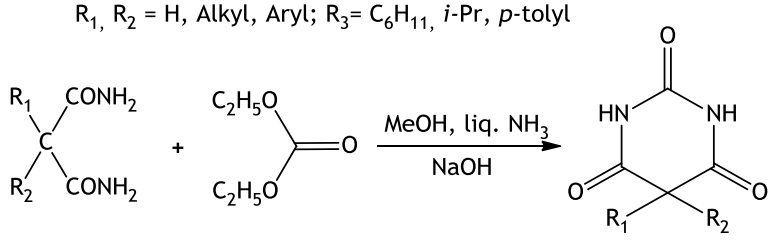

(D)

R_1, R_2 = H, Alkyl, Allyl, etc.

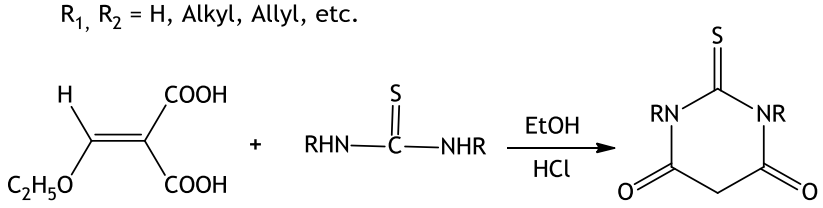

(E)

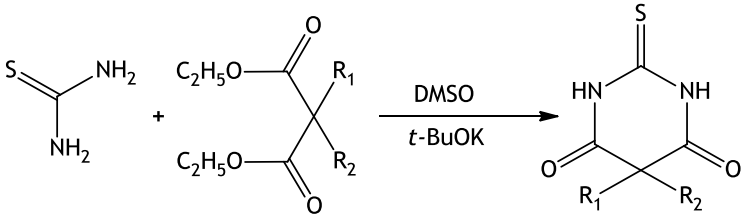

(F)

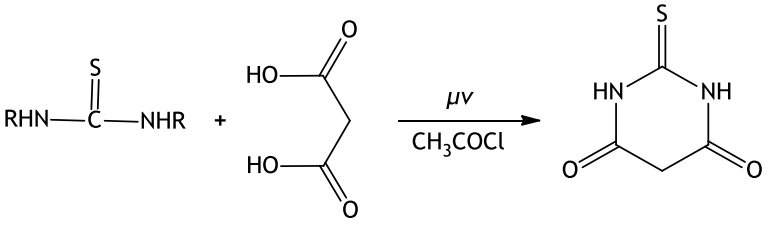

(G)

Scheme 4| **Synthesis of barbituric and thiobarbituric acids**

The chemical synthesis by microwave approaches have been increasingly explored for the preparation of barbituric acid and its thio-analog and their derivatives. The microwave irradiation of a mixture of a diaryl thiourea, malonic acid and acetyl chloride for just a few seconds resulted in 90-95% of the desired product (Scheme 4G).[37] This method provides faster and cleaner reactions with higher yields because of the direct "in core" heating of the mixture. It is possible to use solvents with lower boiling points under pressure and heated in superior temperatures than their boiling point and the microwave heating also is more energy efficient than the classic oiling bath due to the direct molecular heating and inverted temperature gradients.[38]

As mentioned before, barbituric acids are widely included in the synthesis of various novel organic compounds over the past years using MCR strategies. Manich reactions can be used in a based MCR on barbituric and thiobarbituric acids allowing the introduction of an aminomethyl group in the 1- and/or 3-position of the barbituric acid and at the 5-position (using formaldehyde as a reagent with piperidine). One-pot synthesis of substituted compounds using Manich reaction can also performed under microwave irradiation, giving excellent yields within a few minutes of irradiation.[39]

5- And 6-membered *O*-heterocyclic compounds can be synthetized via Knoevenagel Reaction from barbituric acids. One-pot three-component reactions of 1,3-dimethylbarbituric acid, isocyanides and aldehydes can afford furopyrimidones (Scheme 5A).[40, 41] Microwave-assisted reactions as well as ultrasound methods between aromatic aldehydes, nitriles and barbituric acids produce 4H-pyrano[3,2-*d*]pyrimidines. One-pot cyclocondensation using 1,3-dimethylbarbituric acid with aldehydes and dimenone, indane-1,3-dione or *β*-naphtol in the presence of $InCl_3$ or P_2O_5 under solvent-free conditions produce chromeno[2,3-*d*]pyrimidines (Scheme 5B), diazobenzo[*b*]fluorenones and azabenzo[α]anthracenediones derivatives, respectively.[39, 40]

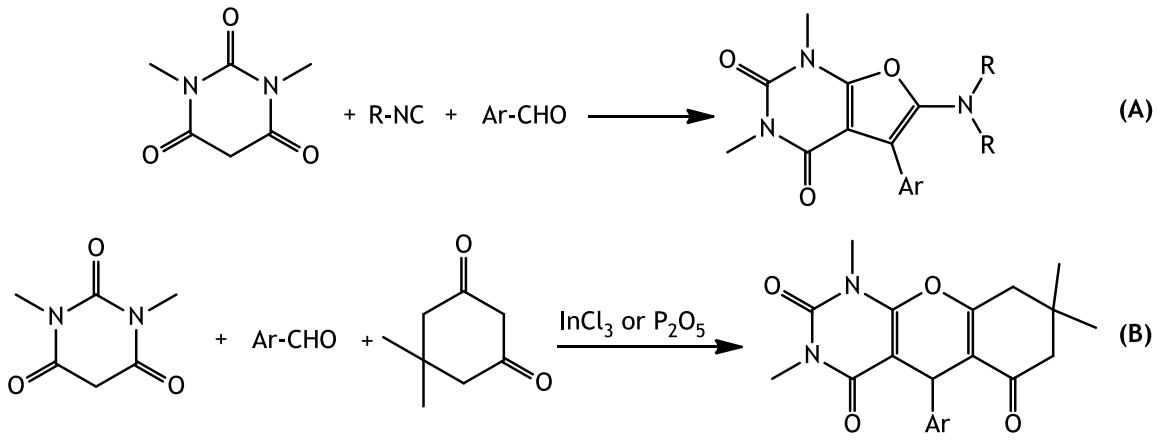

Scheme 5| Synthesis of furopyrimidones (A) and chromeno[2,3-*d*]pyrimidines (B)

A three-component reaction between barbituric acid, aldehyde and (thio)urea by a Biginelli reaction, under solvent-free microwave conditions, affords pyrimido [4,5-*d*] pyrimidines (Scheme 6). The reaction is also promoted either in water. [42]

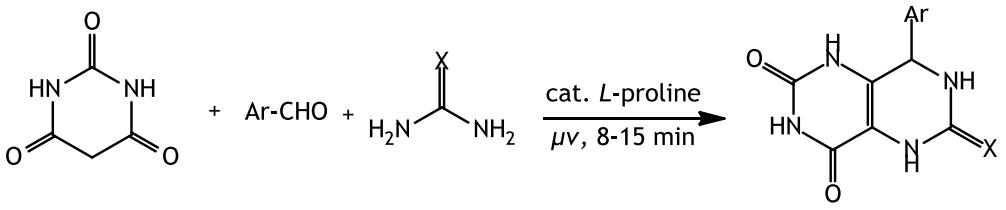

Scheme 6| Synthesis of pyrimido [4,5-*d*]pyrimidines by Biginelli Reaction

Barbituric acids can be used on the synthesis of polihydroquinoline derivatives through the Hantzsch condensation. The original procedure involves mixing an aldehyde with ethyl acetoacetate and ammonia in acetic acid or in refluxing alcohol affording 1,4-dihydropyridines. However, this known route suffers from several disadvantages such harsh refluxing conditions, long reaction times and low product yields. Aiming the development of more efficient and environmentally benign Hantzsch reactions, microwave irradiations, ultrasonic irradiation and the use of solar energy have been reported.[39, 43] A one-pot reaction between (thio)barbituric acid, aldehyde and amino derivatives such as naphtylamines generates hydropyrimido[4,5-*b*]quinoline derivatives controlled by ultrasound irradiation (Scheme 7A). A reaction involving aminopyrazole, aldehyde and barbituric acid in water under microwave irradiation affords pyrazolopyridopyrimidines. The temperature optimization procedure and the search for the best catalytic system allowed selecting one equivalent of *p*-toluenesulfonic acid (*p*-TSA) and 140ºC as optimum conditions for the synthesis (Scheme 7B). Different microwave approaches have also been applied for the synthesis of pyrimido [4,5-*b*]quinolones (Scheme 7C) and pyrido dipyrimidine derivatives using anilines or aminouracils, respectively, along with aldehydes and barbituric acid.[39]

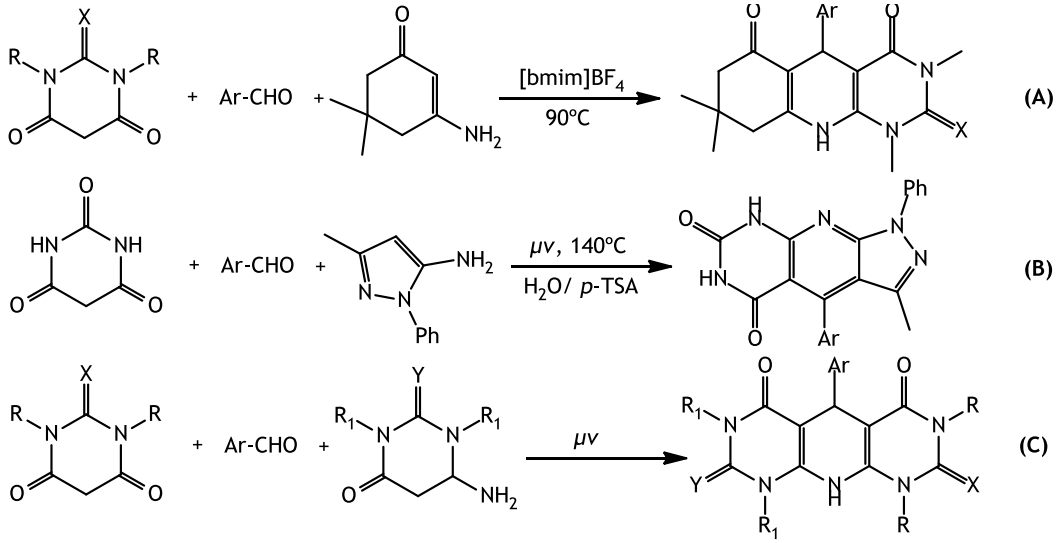

Scheme 7| **Synthesis of hydropyrimido[4,5-*b*]quinolone (A), pyrazolopyridopyrimidines (B) and pyrimido [4,5-*b*]quinolones (C) through Hantzsh Reaction**

1.2.2. Pharmacological activities of barbiturate derivatives

The first of the barbiturates to come to the market was diethyl-barbituric acid, also known as Barbital (figure 13), as a hypnotic, giving profound changes in the pharmacological approach to psychiatric and neurological disorders. Furthermore, barbital had sedative and anticonvulsant properties, calming down manic patients and helping melancholic patients to sleep as well as inducing insomniacs to sleep effectively.[44]

The interest on the synthesis of barbituric derivatives was greatly stimulated after the discovery of the therapeutic activities of barbital. By means of small modifications, thousands of different barbituric agents were produced. One of the most widely used subsequently was phenobarbital (figure 13) on substituting one of the ethyl groups by a phenyl radical. This molecule was employed in therapy as a hypnotic with more prolonged pharmacological action than its predecessor soon becoming the "king of the barbiturates". Moreover, this drug opened up the way to another important clinical application of barbiturates, namely the treatment of epilepsy. Later, new barbiturates such as butobarbital, amobarbital, secobarbital and pentobarbital brought substantial advantages compared with the two classical drugs referred like greater potency and duration of action, as well as a wider therapeutic range. [44]

In addition to the excellent hypnotic effect of phenobarbital, Hauptmann reported that a patient with epilepsy had fewer seizures when given phenobarbital for sedation concluding that this drug had significant anticonvulsant properties.[44,45] It was the first effective barbituric drug for the treatment of epilepsy and rapidly recognized as a better and safer antiepileptic drug than bromides. In the following years several barbituric derivatives were studied in the field of epilepsy, the most important being mephobarbital (figure 13), a *N*-methyl derivative of phenobarbital with chirality on the 5-position carbon of the molecule. This asymmetric molecule was regarded as a prodrug to phenobarbital with similar antiepileptic efficacy, however it is well absorbed after oral administration and may enter the brain more readily than its predecessor.[45]

Beyond hypnotic and anticonvulsant properties, barbiturates were found to be useful as anesthetics. The first one to be used systematically in anesthesia was sodium-butyl-(2-bromo-allyl)-barbiturate and subsequently, as new barbiturates were synthesized for their oral administration as sedatives, sodium salts of the same drugs were formulated, which could be administrated intravenously and used as anesthetics. Sodium amobarbital and sodium pentobarbital are some examples of drugs within this pharmacological feature. The introduction of thiobarbiturates through the addition of a sulfur group to pentobarbital, revolutionized the intravenous anesthesia. The sulfur derivative of pentobarbital (Thiopental) rapidly displaced the rest of the barbiturates as an anesthetic partly due to the swiftness of

its onset along with its short action period (figure 13). Methohexital showed to be more potent than thiopental and to lead to quicker recovery in patients afterwards.[44]

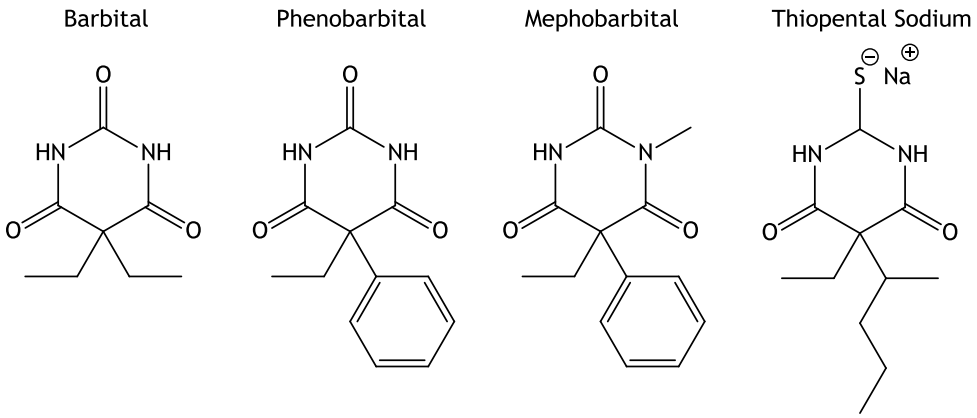

Figure 13| Chemical structures of barbituric and thiobarbituric acids derivatives used as drugs

Besides the hypnotic, anticonvulsionant and anesthetic properties, barbiturates possess a wide range of other biological activities such as inhibiting matrix metalloproteinases (MMP) like collagenase-3 (MMP-13)[46] and gelatinases A and B (MMPs-2 and -9)[47] and cytochrome P450 enzymes (CYP2C19 and CYP2C9)[48].

Ro-28-2653 (figure14), a pyrimidine-2,4,6-trione derivative, represents an attractive new class of orally available selective MMPs inhibitors with potent anti-tumoral, antiangiogenic and anti-invasive activities.[49]

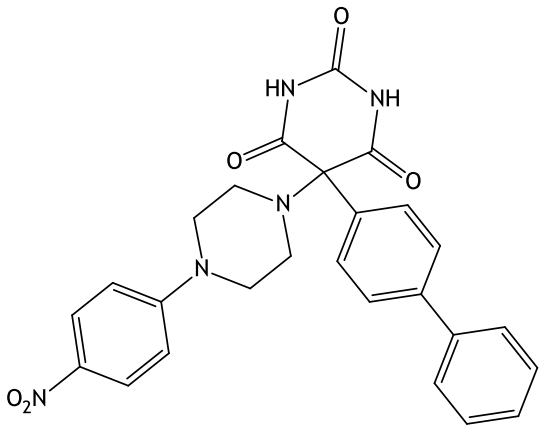

Figure 14| Chemical Structure of the potent MMP inhibitor Ro-28-2653

Some studies reported that arylidene barbiturates can exhibit antioxidant, antibacterial activities and inhibit urease. The presence of a hydroxyl group at *para*- or *ortho*-position of the phenyl group attached in the carbon-5 of the pyrimidine ring seems to be important for these properties.[50]

It has also been reported several barbiturate derivatives with potential anticancer properties. In this context, some barbituric acid derivatives presented great potency and selectivity in inhibiting the human methionine aminopeptidase-1 (MetAP-1) leading to the arrest of cell division and induction of apoptosis in leukemia cells.[51] Nucleobase based barbiturate derivatives (hybrid molecules on the basis of nucleobase and barbituric acid) and spiro-quinolines with barbituric acid significantly attenuated the cytotoxicity activity against several cancer cell lines.[52,53] Aside from the great anticancer properties, arylhydrazone barbiturates, complexed with Ag^{I}, afforded good binding interactions with BSA (bovine serum albumin) and DNA and exhibited remarkable antibacterial activity.[54]

In summary, (thio)barbituric acid is a very important precursor to afford promising drugs with different and great biological actions. Among the great spectrum of pharmacological activities, some (thio)barbituric derivatives can show inhibitory effects in XO due to the structural core of the (thio)barbituric moiety, which present some analogies to purines.

2. Aims

This project aimed the synthesis of a serie of pyrimido [4,5-*d*]pyrimidines-5,7-diones and 7-thiones analogues, starting from (thio)barbituric acids and their 1,3-alkyl and aryl derivatives, and its evaluation as potential xanthine oxidase inhibitors.

Several new 5-methylene(thio)urea barbiturates, precursors of these six-membered bicyclic compounds, were prepared by a one-pot reaction using *ortho*-alkyl formate, (thio)barbituric acid and their 1,3-alkyl and aryl derivatives and (thio)urea. These compounds were further purified and their complete structural characterization was performed. Although several cyclization trials to synthesize the final desired products were proceeded, it was not possible to obtain the pyrimido [4,5-*d*]pyrimidines-5,7-diones and 7-thione analogues. Previous studies indicate that some C5-subtituted (thio)barbiturates are able to inhibit xanthine oxidase. Accordingly to this, it was proposed to evaluate the biological activity of 5-methylene(thio)urea (thio)barbiturates as potential xanthine oxidase inhibitors. Antioxidant properties were also studied through the 2,2-diphenyl-1-picrylhydrazyl (DPPH) assays as well as their cytotoxicity in a human breast carcinoma (MCF-7) cell line using the colorimetric 3-(4,5-dimethylthiazol-2-yl)-2,5-diphenyltetrazolium bromide (MTT) assay.

In order to predict binding energies and possible interactions in xanthine oxidase of the synthesized precursors, molecular docking studies were performed using the enzyme mentioned.

3. Results and Discussion

3.1. Synthesis

As referred before, initially this project consisted on the development of new pyrimido[4,5-*d*]pyrimidines-4,5-diones and 7-thione analogues starting from barbituric and thiobarbituric acid and theirs 1,3- aryl and alkyl derivatives. In order to synthesize the desired products a new strategy was followed, starting with the preparation of different 5-substituted barbiturate precursors, 5-methylene(thio)urea and 5-benzylidene (thio)barbiturates (**2** and **3**) and proceeding to their further cyclization (**4**) (Scheme 8). All these precursors were successfully synthetized and the complete structural characterization was performed. However, after several ring closing attempts, the synthesis of the aimed compounds was not accomplished.

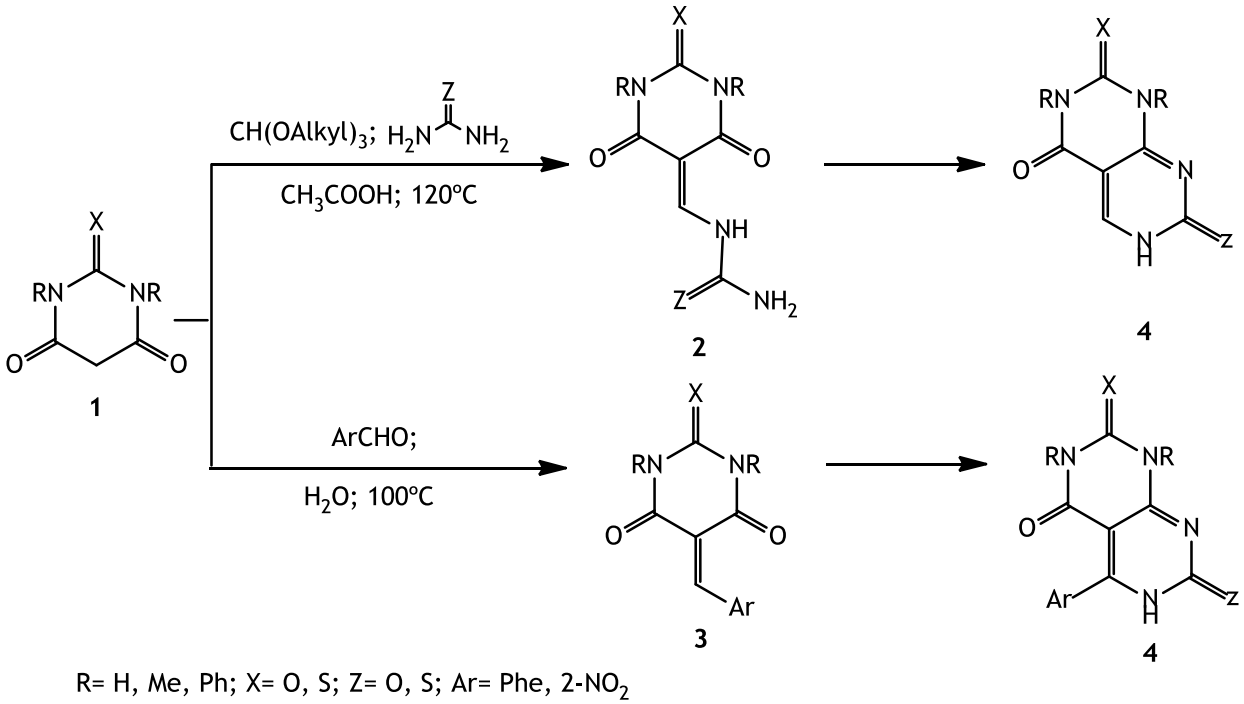

Scheme 8| Synthetic strategy for the preparation of pyrimido [4,5-*d*]pyrimidines

3.1.1. Synthesis and characterization of starting materials

The starting materials used for the synthesis of the desired pyrimido [4,5-*d*]pyrimidines were: thiobarbituric acid (**1a**), barbituric acid (**1c**), 1,3-dimethyl barbituric (**1d**) acid and 1,3-diphenyl thiobarbituric acid (**1b**) (figure 15). All these compounds were acquired by commercial firms less the last one cited.

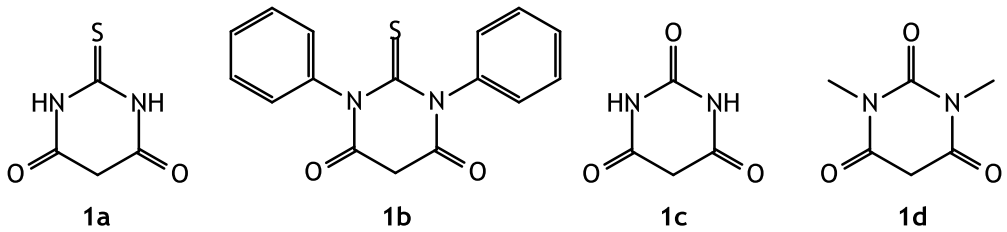

Figure 15| Structures of the starting materials: thiobarbituric acid (1a), 1,3-diphenyl thiobarbituric acid (1b), barbituric acid (1c) and1,3-dimethyl barbituric acid (1d)

The 1,3-diphenyl thiobarbituric acid (**1b**) was prepared by the condensation of malonic acid with a dinucleophile – diphenylthiourea (**7**) – with acetyl chloride (Scheme 9). A rocked mass was obtained which was recrystallized with acetic acid leading into green needled crystals. The diphenylthiourea was also synthetized in laboratory by mixing aniline (**5**) and isothiocyanate (**6**) in dichloromethane (DCM) at room temperature. White crystals were formed which were further used to the reaction mentioned before.

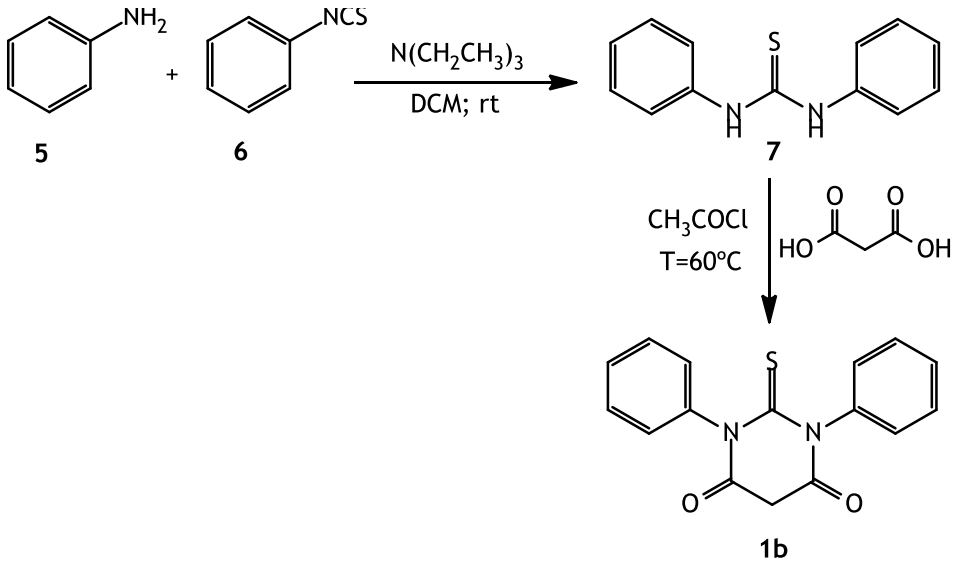

Scheme 9| Preparation of the precursor 1,3-diphenyl thiobarbituric acid (**1b**)

3.1.2. Synthesis and characterization of 5-methylene(thio)urea (thio)barbiturates

The preparation of 5-methylene(thio)urea (thio)barbituric acid derivatives (**2**) was effected by one-pot reaction with the barbituric and thiobarbituric acids (**1c** and **1a**) or their 1,3-aryl and alkyl derivatives (**1b** and **1d**), trimethyl- or triethyl *ortho*-formate and (thio)urea in *n*-butanol at 120ºC (Scheme 10). Coloured and pure solids were obtained after cooling and filtering the reactional mixture once it was completed. The reaction begins with a keto-enol tautomerism forming an enol. The activated methylene in carbon 5 of the (thio)barbiturates attacks the central carbon of *ortho*-formate through an electrophilic addiction (A_E). Subsequently there is a nucleophilic substitution with the acid of an alkoky, forming a carbamide. All compounds were characterized by ^{1}H NMR, ^{13}C NMR, Infrared spectra and Mass Analysis (tables 1 and 2). Their melting points were also determined. All data are consistent with the expected structures.

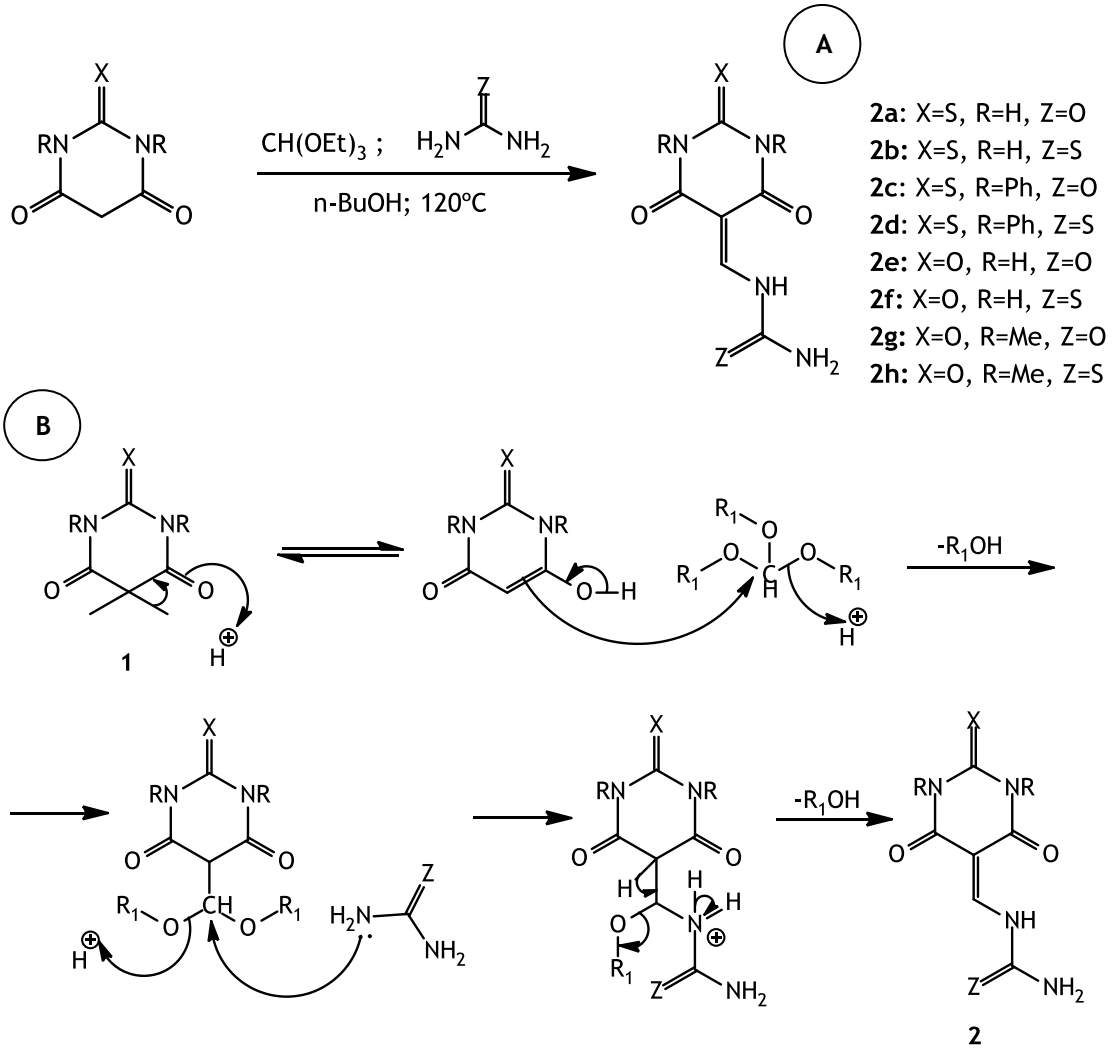

Scheme 10| Preparation of the precursors 5-methyleneureas and thioureas from (thio)barbiturates; B- Proposed reaction mechanism to obtain the synthetized compounds

Table 1| Physical and analytical data of the synthesized derivatives **2(a-h)**

Compound	Yield (%)	Colour	m.p(°C)	FTIR (cm^{-1})	m/z
2a	77	Reddish	Decomposes	3406 (NH), 3147 (CH alkene), 2889, 1730 (C=O), 1693 (C=O), 1643, 1529 (NH), 1375 (C-N), 1259, 1149 (C=S), 815 – 757 (CH alkene)	214.01576 Calculated* ($C_6N_4O_3SH_6$) 214.01606
2b	74	Reddish	Decomposes	3284, 3136 (CH alkene), 1695 (C=O), 1664 (C=C), 1574 (NH), 1506 (NH), 1413 (C=S), 1259, 1143 (C=S), 804 804 (CH=CR_2)	299.99336 Calculated* : ($C_6N_4O_2S_2H_6$) 299,99321
2c	79	Yellow	261-265	3469 (NH amide), 3182 (CH alkene), 1735 (C=O), 1649 (C=C), 1560 (NH), 756-692 (CH ar)	366.07856 Calculated* : ($C_{18}N_4O_3SH_{14}$) 366.07866
2d	85	Orange	259-261	3442 (NH amide), 3263, 3172 (CH alkene), 3051 (CH alkene), 1685 (C=O), 1654 (C=C), 1591 (NH amide), 1402 (C-N amide), 1321, 1217 (C=S), 823-688 (CH ar)	382.05556 Calculated* : ($C_{18}N_4O_2S_2H_{14}$) 382.05581
2e	71	Yellow	316-318	3411(NH amide), 3172 (CH alkene), 1733-1703 (C=O), 1629 (C=C ar), 1569 (NH amide), 1384 (C-N)	198.13672 Calculated* : ($C_6N_4O_4H_6$) 198,03890
2f	86	Yellow	317-320	3358 (NH amide) 2808 (CH alkane), 1733-1701 (C=O), 1645 (C=O amide), 1571 (NH amide), 1407 (C-N),	214.0860 Calculated* ($C_6N_4O_3SH_6$) 214.01606
2g	52	Beige	248-250	3371 (NH amide), 3197 (CH akane), 1704 (C=O), 1666-1635 (C=C alkene), 1560 (NH amide), 1406 (C-N), 1247 (C=S)	226.07006 Calculated* : ($C_8N_4O_4H_{10}$) 226.07020
2h	89	Beige	267-270	3290 (NH amide), 1716 (C=O), 1635 (C=C alkene), 1589 (NH amide), 1429 (C-N)	242.04716 Calculated* : ($C_8N_4O_3SH_{10}$) 242.04736

*The theoretic value of M/z was calculated by using the Chemdraw Pro 12.0 Software

Regarding the Infra-Red spectra results (table 1), all synthetized compounds showed absorption bands representative of the NH groups at 3100 - 3400 cm^{-1} and 1591 – 1504 cm^{-1}, as well as 1735 – 1690 cm^{-1} for C=O groups. Characteristic bands around 1670 and 1629 were presented on spectra, representing the carbon double bonds of alkenes and aromatic groups as well as the C-H bonds from these ones at 684 – 804 cm^{-1}. The C=S bands can be attributed at 1217 – 1143 range.

According to the ^{1}H NMR data (Table 2), all spectra signals from each compound were located around lower fields. It was verified the presence of common signals in all compounds spectra, such as the NH_2 protons from the urea and thiourea attached to the methylene group on the carbon-5 of the (thio)barbituric acids derivatives, showing two singlets in the lower field. Depending on the side group, carbonyl or C=S groups, there were some differences on NH_2 signal ranges, being 7.46 – 7.88 ppm (**2a, 2c, 2e** and **2g**) and 9.44 – 9.72 ppm (**2b, 2d, 2f** and **2h**) respectively. The same occurred with the NH signals from the thiobarbituric (**2a** and **2b**), located at 12.13 – 12.27 ppm, and barbituric (**2e** and **2f**), in 10.97 – 11.15 ppm, moieties. They presented two singlets although these signals could appear overlapped. It was also verified the multiplicity of the CH group, which makes the linkage between (thio)barbituric and urea or thiourea. A duplet signal appeared in all spetra data at 8.51 – 8.67 ppm range in **2a, 2c, 2e** and **2g** compounds, with urea moiety, and at 9.08 – 9.28 ppm range in **2b, 2d, 2f** and **2h** compounds, with thiourea moiety. On the 1,3-diphenyl thiobarbituric acid derivatives (**2c** and **2d**) spectra, it was shown the correspondent signals from aromatic rings around 7.24 and 7.49 ppm. Correspondent peaks characteristic from methyl groups of 1,3-dimethylbarbituric acid compounds (**2g** and **2h**) could be seen around 3.20 ppm. In the ^{13}C NMR spectra of the compounds, the signals also appeared at lower field values due to the resonance carbon of the carbonyl and C=S groups. In all compound spectra it was possible to visualise similar chemical shifts for the mentioned groups, being located around 160 ppm and 180 ppm respectively. For 1,3-diphenyl compounds, it was also be verified characteristic signals of the aromatic carbons around 128 and 140 ppm.

Table 2 ^{1}H and ^{13}C NMR spectra data of the synthesized compounds **2(a-h)**

Compound	Barbituric moiety (X=S or O)			C5-group (Z=S or O)		
	NH(CX)	(CX)N-C_6H_5	(CX)N-CH_3	C-CH-NH	CH-NH-(CZ)	-(CZ)-NH_2
2a	12.19, singlet 12.13, singlet	-----	----	8.54, duplet *J*= 13.1 Hz	11.24, duplet *J*= 13.2 Hz	7.88, singlet 7.56, singlet
	178.5 (C=S); 161.3 (C=O), 163.0 (C=O); 96.1 (C_5)					151.0 (CH); 152.0 (C=O)
2b	12.27, singlet 12.18, singlet	-----	----	9.11, duplet *J*= 6.30 Hz	11,94, duplet *J*= 6.30 Hz	9.64, singlet 9.52, singlet
	178.9 (C=S); 161.8 (C=O), 163.4 (C=O); 98.3 (C_5)					153.0 (CH); 181.7 (C=S)
2c	------	7.24 – 7.45 multiplet	----	8.67, duplet *J*= 6.30	11.48, duplet *J*= 6.60 Hz	7.76, singlet 7,58, singlet
	181.3 (C=S); C=O: 161.5 (C=O), 162.5 (C=O); 97.2 (C_5); 128.4 (CH_{ar}), 128.9 (CH_{ar}), 129.2 (CH_{ar}), 129.3 (CH_{ar}), 129.6 (CH_{ar});139.7 (C_{ar}); 140.3 (C_{ar})					152.8 (CH); 151.7 (C=O),
2d	-------	7.27 – 7.49 multiplet	----	9.28, duplet *J*= 11.7 Hz	12.13, duplet *J*= 6.30 Hz	9.72, singlet 9.44, singlet
	181.3 (C=S); 161.2 (C=O), 162.5 (C=O); 99.0 (C_5); CH_{ar}:128.4 (CH_{ar}), 128.5 (CH_{ar}), 129.2 (CH_{ar}), 129.3 (CH_{ar}), 129.5 (CH_{ar});139.8 (C_{ar}); 140.5 (C_{ar})					154.4 (CH); 181.6 (C=S)
2e	11.06, singlet 10.97, singlet	-----	----	8.51, duplet *J*= Hz	11.10, duplet *J*= Hz	7.83, singlet 7.46, singlet
	151.0 (C=O), 163.9 (C=O), 165.6 (C=O); 95.5 (C_5)					150.3 (CH); 152.7 (C=O)

2f	11.15, singlet 11.03, singlet	-----	----	9.08, duplet *J*= 6.15 Hz	11.84, duplet *J*= 6.15 Hz	9.53, singlet 9.45, singlet
	152.7 (C=O), 163.7 (C=O), 165.6 (C=O); 97.4 (C_5)					150.9 (CH); 181.9 (C=S)
2g	------	-----	3.18, singlet 3.16, singlet	8.61, duplet *J*=6.45 Hz	11.23, duplet *J*= 6.60 Hz	7.82, singlet 7.47, singlet
	152.0 (C=O), 162.4 (C=O); 163.7 (C=O); C_5: 95.4 (C_5); 27.5 (CH_3), 28.1 (CH_3)					151.1 (CH); 151.7 (C=O)
2h	-------	-----	3.20, singlet 3.18, singlet	9.19, duplet *J*= 6.30 Hz	11.95, duplet *J*= 6.15 Hz	9.59, singlet 9.48, singlet
	152.8 (C=O),162.2 (C=O); 167.8 (C=O); 97.3 (C_5); 27.7 (CH_3), 28.3 (CH_3)					151.6 (CH); 181.5 (C=S)

3.1.3. Synthesis and Characterization of 5-arylidene (thio)barbiturates

The 5-arylidene (thio)barbiturates (**3**) were prepared by the condensation of (thio)barbituric acids or their 1,3-aryl and alkyl derivatives (**1**) and different benzaldehydes with water through a Knoevenagel reaction (Scheme 11). Initially, the activated (thio)barbituric methylene suffers a deprotonation and an enol intermediate is formed which attacks the carbonyl carbon of the aldehyde resulting in an aldol. This aldol undergoes further elimination of one molecule of water. Accordingly with this reaction, several pure substituted 5-benzylidene (thio)barbiturates were synthesized in good yields. Their purification procedure was based in washing the formed precipitate with cold water and ethyl ether. 5-Benzylidene substituted (thio)barbituric acids and their 1,3-diaryl and alkyl analogues were prepared in good yields and purity (table 3). These synthesised precursors were colourful powders and their melting points and NMR spectra of some compounds were in accordance with the literature as well as all spectra data.[59]

The IR spectrum of the compounds showed absorption due to –NH stretching at 3255 cm^{-1}, the carbonyl groups at approximately 1700 cm^{-1}, the double carbon bonds around 1627 cm^{-1} and 1600 cm^{-1} range, the nitro group band is presented between 1569-1540 cm^{-1}. The aromatic –CH bands were around 778 cm^{-1} and 728 cm^{-1} values (Table 3)

Relatively to the ^{1}H NMR signals obtained (table 4), it was identified the signals of the phenyl ring at lower fields which are characteristic of this group. The compound **3a** presented well defined NH and aromatic signals. In the compound **3c**, a multiplet on the aromatic range was shown due to the presence of several aromatic protons of the benzyl group in the pyrimidine ring and benzylidene moiety. On the contrary, it was possible to identify the aromatic proton signals well defined in compounds **3b** and **3d**, showing double-triplets and double-duplets due to the interaction to the vicinal proton and the long-range coupling. The spectra also showed the presence of the methylene proton at lower field values being ranged between 8.63 and 8.70 ppm in all synthetized compounds. In the lowest field it was possible to verify the signals, singlets of multiplicity, of the protons that are directly linked to the nitrogen atom of the pyrimidine ring. In compound **3d**, it was verified the presence of two singlets at 3.07 and 3.26 ppm, which represented the methyl group attached on the nitrogen of the pyrimidine group.

In ^{13}C NMR (table 4), there were presented the typical signals of the carbonyl and C=S groups in the pyrimidine ring at 159.2 –160.8 ppm and 179.1-181.9 ppm respectively. The signal of the methylene group appeared around 153.3 ppm and 155.5 ppm values. On the benzyl group, it was determined the CH, between 124.0-134.5ppm values, and quaternary carbons, one carbon linked to the methylene group and other to the nitro group, around a range of 131.6-132.2 ppm and 146 ppm values. It was also possible to visualize the signal of the methylene around 153.3 and 155.5 ppm and the carbon-5 of the pyrimidine ring at 120.0 and 121.7 ppm values.

The brominated derivative was prepared only for synthesis purposes and it was not considered in the biological evaluation

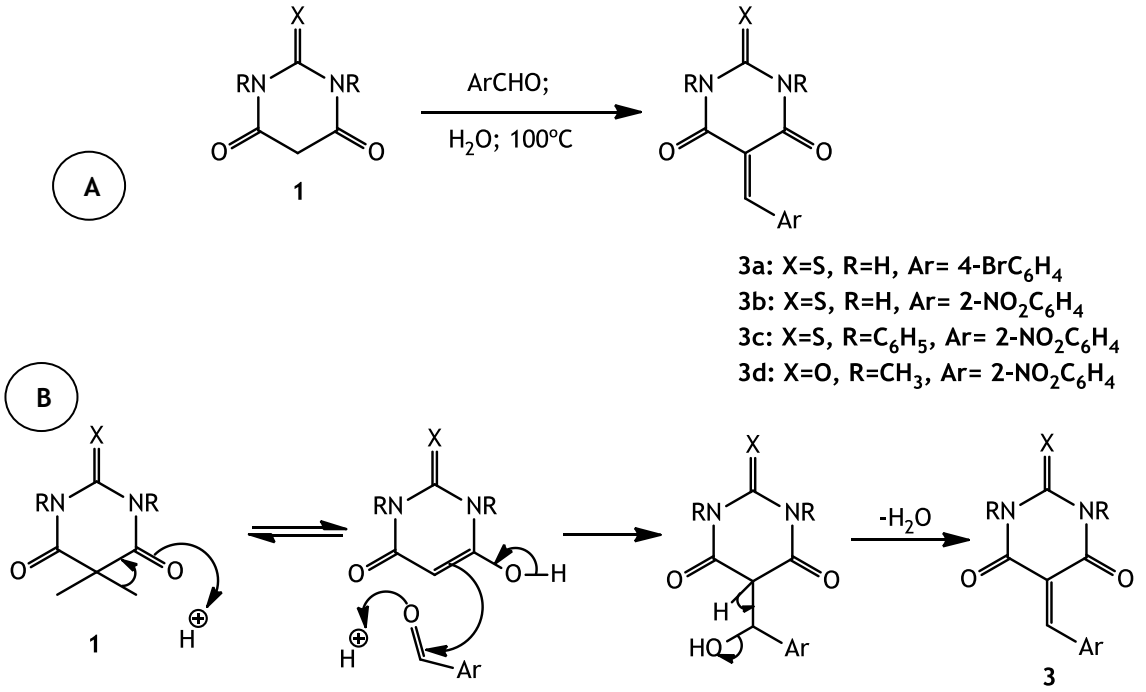

Scheme 11| A- Preparation of the precursors 5-methyleneureas and 5-methylenethioureas from (thio)barbiturates (2); B- Proposed reaction mechanism of synthetized compounds

Table 3| Physical and analytical data of the synthesized arylidene (thio)barbituric acids derivatives **(3)**

Compound	Benzylidene moiety	Colour	Yield (%)	m.p. (°C)	FTIR (cm^{-1})
3a	4-Br	Yellow	71	293-294 Lit:292-293[55]	3240 (N-H amide), 3095 (CH_{ar}), 1739 (C=O), 1620 (C=C), 1562, 852-787 (CH_{ar})
3b	2-NO_2	Yellow	89	239-241 Lit:246-250[56]	3255(N-H amide), 3157 (CH_{ar}), 1719 (C=O), 1693 (C=O amide), 1627 (C=C), 1604 (C=C), 1540 (N=O), 1352 (C-N), 1204 (N=O), 785-733 (CH_{ar})
3c	2-NO_2	Yellow	90	235 Lit:232[57]	3032 (CH_{ar}), 1717 (C=O), 1692 (C=O amide), 1625 (C=C ar), 1607 (C=C), 1520 (N=O), 1396 (C-N), 1354-1326 (N=O), 768-723 (CH_{ar})
3d	2-NO_2	Yellow	93	158-159 Lit:159-161[58]	1664 (C=O), 1603 (C=C), 1569 (N=O), 1377 (CH_3),1323, 788-737 (CHar)

Table 4| ^{1}H and ^{13}C NMR spectra data of the synthesized arylidene (thio)barbituric derivatives **(3)**

Compound	Barbituric moiety (X=S or O)			Arylidene moiety	
	NH(CX)	(CX)N-C_6H_5	(CX)N-CH_3	C-CH-Ar	CH_{ar}
3a	12.39, singlet 12.50, singlet	-----	----	8.31, singlet	7.74 - 8.30
	178.7 (C=S), 162.7 (C=O), 160.4 (C=O), 119.8 (C_5)			153.0 (CH), 134.4 (CH_{ar}),131.1 (CH_{ar}),131.7 (C_{ar}), 127.9 (C_{ar}-Br)	
3b	12.56, singlet 12.33, singlet	-----	----	8.63, singlet	7.62 – 8.24
	179.1 (C=S),159.2 (C=O), 160.6 (C=O);120.6 (C_5)			153.3 (CH), 124.0 (CH_{ar}),130.3 (CH_{ar}), 130.4 (CH_{ar}), 133.7 (CH_{ar}), 131.6 (C_{ar}), 146.3 (C_{ar})	
3c	------	7.62 - 8.19	----	8.80, singlet	7.62 - 8.19
	181.9 (C=S), 159.3 (C=O), 160.8 (C=O), 121.7 (C_5), 128.6 (CH_{ar}), 128.8 (CH_{ar}), 129.3 (CH_{ar}), 129.4 (CH_{ar}), 129.5 (CH_{ar}), 140.2(C_{ar}), 140.5 (C_{ar})			155.5 (CH), 124.6 (CH_{ar}), 130.6 (CH_{ar}), 130.9 (CH_{ar}),134.5 (CH_{ar}),132.2 (C_{ar}), 146.7 (C_{ar})	
3d	-------	----	3.07, singlet 3.26, singlet	8.70, singlet	7.53 - 7.80
	151.2 (C=O), 160.4 (C=O), 161.7 (C=O), 120.6 (C_{ar}), 28.3 (CH_3), 28.9 (CH_3)			154.1 (CH), 124.5 (CH_{ar}), 130.5 (CH_{ar}), 130.6 (CH_{ar}), 134.4 (CH_{ar}), 132.5 (C_{ar}), 146.6 (C_{ar})	

3.1.4. Synthetic attempts for the preparation of pyrimido [4,5-*d*]pyrimidines

Following the preparation of different precursors described, it was envisaged the synthesis of the desired pyrimido [4,5-*d*]pyrimidines. In the scheme below is indicated several attempts that were performed in order to accomplish the proposed final compounds without success (Sheme 12).

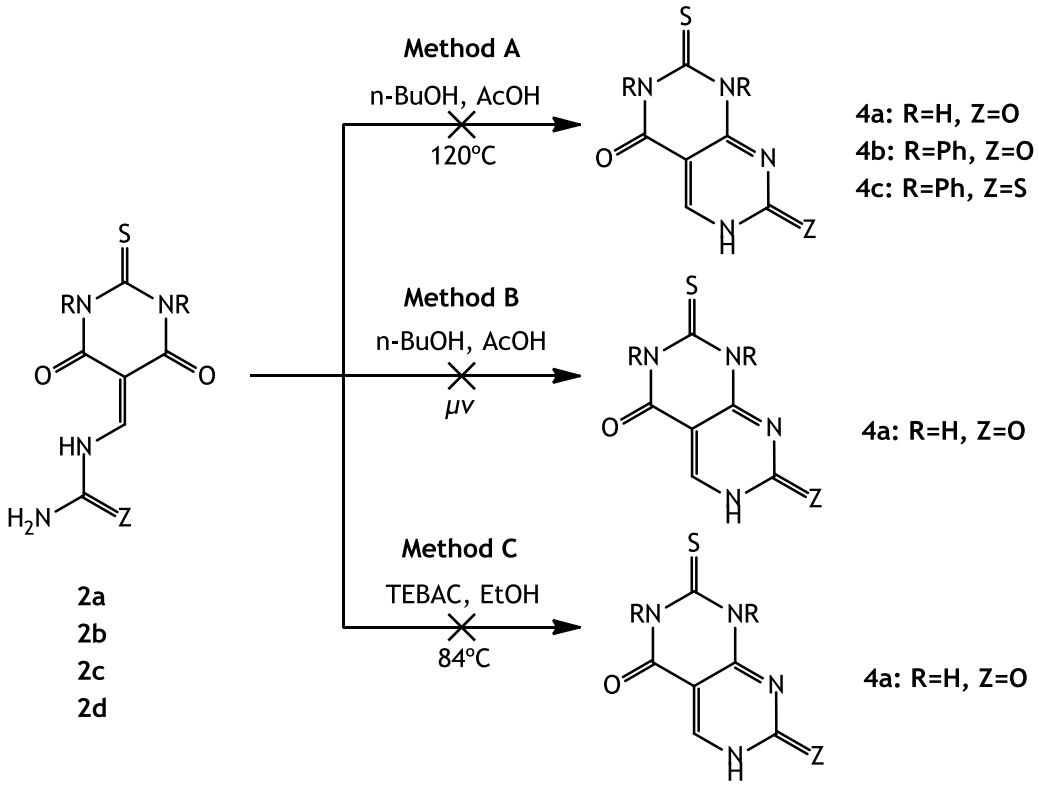

Scheme 12| Synthetic strategies for the preparation attempts of pyrimido [4,5-*d*]pyrimidines from 5-methylene(thio)ureas thiobarbituric acid derivatives **(4)**

5-substituted barbituric and thiobarbituric acids possess fewer acidic protons than their precursors, being less acidic and having higher pKa than unsubstituted barbituric and thiobarbituric acids. In order to proceed to the formation of a bicyclic ring, compound **2a** was refluxed with acetic acid in *n*-butanol at 120ºC (**method A**).[60] In this case, the 5-monosubstituted (thio)barbituric compounds have a pKa higher than acetic acid, acting as a base. Thus, it was expected the formation of a protonated carbonyl which was further attacked by the nitrogen from the carbamide leading to a self-cyclization and generation of a 6-membered ring. The reaction proceeded as a suspension and no significant changes occorred according to the thin layer chromatography (TLC), although a change of the reaction colour was observed. The results of NMR spectra indicated the presence of only the starting material (**2a** and **2b**). The compound 1,3-diphenylbarbituric methyleneurea acid (**2c**) and 1,3-diphenylbarbituric methylenethiourea acid (**2d**) were submitted to the same conditions of the

method A. The reaction of each precursor proceeded as a solution and it was noticed some changes in the reactional mixture when comparing to the starting material (**2c-d**), on TLC during the reaction. On both cases, the reaction seemed complete after one day and the mixture was slowly cooled, which promoted the crystallization of golden-needled crystals afterwards. Hereafter, the formed crystals were filtered, dried and structurally analysed by ^{1}H NMR and ^{13}C NMR. The ^{1}H NMR spectra suggested the structures of the predicted final compounds (**4c-d**), showing a CH proton signal around 8.7 ppm, the appearance of a multiplet, around 7.57 and 7.24 ppm, indicating the aromatic groups linked to the nitrogens of the thiobarbituric moiety. Additionally, the protons signals of NH_2 group of the carbamide and thiocarbamide side group were not present on the ^{1}H NMR spectrum. According to the ^{13}C NMR, although it was possible to visualize the aromatic carbons around 124 and 140 ppm and the carbon-5 signal however, the ones related to the carbonyl and C=S groups did not appear in the spectra. These data did not confirmed the predicted structures of the desired pyrimido [4,5-*d*]pyrimidine compounds.

Considering that **method A** failed, it was performed a different approach involving the reaction of compound **2a** in acetic acid and *n*-butanol at 1:2.5 proportion, on the microwave (**method B**). Several studies mention the synthesis of several bicyclic rings, as pyrimido pyrimidines, by using a microwave method. The usage of the microwave can decrease significantly the duration of the reaction and higher reactional yields. The mixture was submitted to 140ºC and 10 bars pressure with continuous stirring for one hour. At the end of this time, the mixture was completely dissolved and a precipitate was formed as long as the mixture was cooling. The TLC did not show alterations between the precursor and the reactional solution. A ^{1}H NMR analysis was performed and it was verified the presence of compound **2a** as well as several impurities. Another microwave reaction was prepared changing some reactional conditions as the temperature (150ºC) and the absence of pressure. This second attempt lasted around 4 hours and was monitored by TLC between one to one hours. No significant changes were observed with the appearance of impurities mixed with starting material in the ^{1}H NMR spectrum.

An alternative strategy to produce pyrimido [4,5-*d*]pyrimidines involves a one-step reaction, combining simultaneously more than two starting materials in order to give a single product. This type of synthesis is denominated by Multicomponent Reaction(MCR's). Several procedures have been reported for the synthesis of pyrimidines, which involves a direct acid-catalysed reaction of diketones, aryl aldehyde and carbamide under acidic conditions. Mobinihhaledi *et al*. (2012) developed a MCR approach under solvent-free conditions to produce pyrimido [4,5-*d*]pyrimidines through a Biginelli-like reaction of a (thio)barbituric acid, an aryl aldehyde and a (thio)urea, in the presence of triethyl benzyl ammonium chloride (TEBAC) as a acid catalyst.[62] Therefore, it was made an attempt to synthesize the desired products through an adaptation of the method previously described in order to accomplish the self-condensation of compounds **2** to form compounds **4**. Thus, the precursor **2a** and TEBAC

were submitted to a reflux temperature using ethanol as a solvent (**method C**)[62]. The reactional mixture was kept for 3 days without significant changes according to TLC analysis. The ^{1}H NMR results also indicated the presence of starting material.

To synthesize pyrimido [4,5-*d*]pyrimidines derivatives from 5-arylidene thiobarbituric acid (**3**), a mixture of this precursor (**3a**) and urea was refluxed in ethanol with a catalytic amount of hydrochloric acid (Scheme 13 – method D). This procedure was also based on the Biginelli MCR but, instead of the involvement of three components as starting materials, only two were used due to the fact that the arylidene intermediates were prepared already. The reaction carried out as a suspension and no significant changes were verified while the reaction was being monitored. Considering all failed attempts on the pursuance of getting the proposed final compounds, one pot synthesis was performed following precisely the Biginelli protocol. A mixture of 1,3-diphenylthiobarbituric acid (**1b**), benzaldehyde and thiourea was refluxed in ethanol and few drops of concentrated hydrochloric acid were added (**scheme 13 - method E**)[62]. This strong acid was used to catalyse the reaction. All starting materials were dissolved into the ethanol however, as the reaction was advancing, an orange precipitated was formed. The reaction was kept under reflux for 3 days and the orange precipitate was filtered and dried afterwards. The structural analysis by ^{1}H and ^{13}C NMR, infrared spectroscopy and mass analysis. No structural data exhibited the desired final product but the open version.

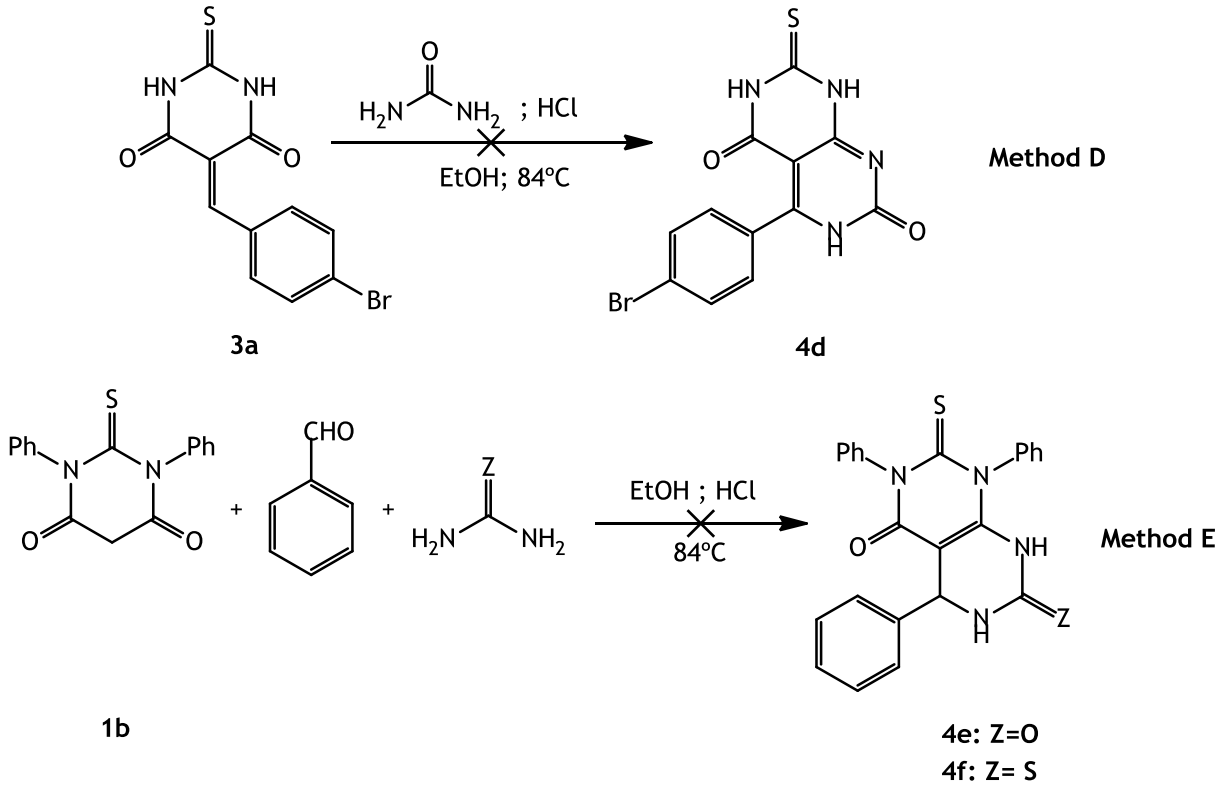

Scheme 13| Method D- Synthetic attempt for the preparation of pyrimido [4,5-*d*]pyrimidines from 5-(4-

bromo)benzylidene thiobarbituric acid; Method E- Attempt for the preparation of pyrimido [4,5-*d*]pyrimidines

3.1.5. Synthesis of predicted pyrimido [4,5-*b*]quinolines from 5-(2-nitro)benzylidenes

Besides the synthesis of new pyrimido [4,5-*d*]pyrimidines, it was proposed to product pyrimido [4,5-*b*]quinolones through the reduction of 5-(2-nitro)benzylidene (thio)barbituric acids (**3b**, **3c** and **3d**) previously prepared (Scheme 14). These precursors were refluxed with tin chloride di-hydrated ($SnCl_2.2H_2O$) and a catalytic amount of chloridric acid in ethanol. The reaction proceeded as a suspension and it completed in less than 30 minutes. The resulting product was submitted to a simple filtration and dried.

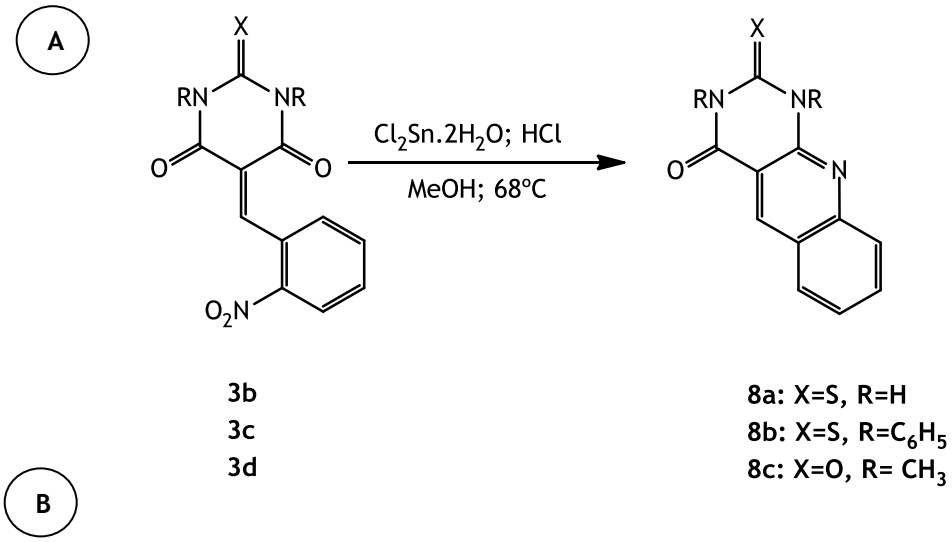

3b
3c
3d

8a: X=S, R=H
8b: X=S, R=C_6H_5
8c: X=O, R= CH_3

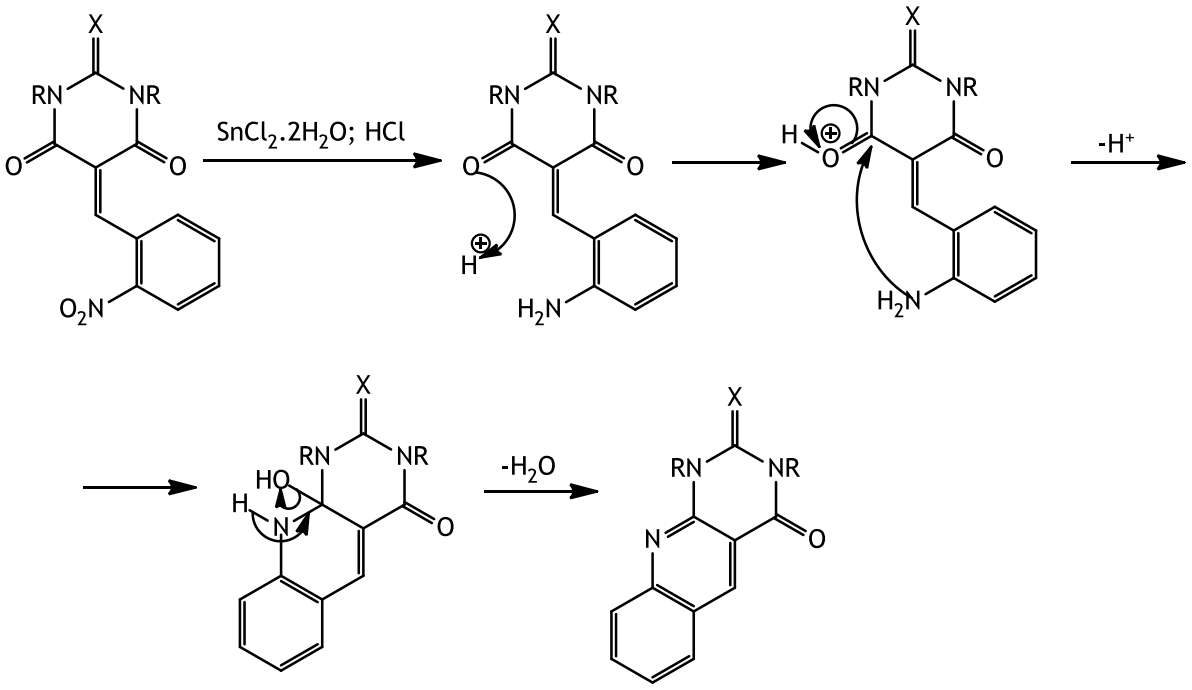

Scheme 14| A- Proposed preparation of pyrimido [4,5-*b*]quinolones; B- Proposed reaction mechanism of the formation for compounds **8a-c**

The obtained products presented yellow fluorescence at 366nm. The appearance of luminescence could be explained by the rigidity of the expected structure, attributed to the quinolone group, which avert the energy of the excited states from being lost by torsional vibrations of the molecule.[63] The formation of the quinolone ring could also be explained by the formation of an amino carbonyl group when the nitro group is reduced, which is often instable , undergoing to its further self-condensation.[64]

Structural analysis was performed by ^{1}H and ^{13}C NMR. Although the spectra showed pure compounds and presented most of the NMR signals expected, there were some points which did not confirm the suggested structure entirely due to a missing CH signal in proton NMR and a carbon in the ^{13}C NMR. It was suggested that the structure could have a symmetric configuration regarding that on compounds **8b** and **8c** was only attributed 5 protons and 3 protons on the assigned signals respectively. It was also proposed that the missing carbon could be overlapped in another carbon signal with higher intensity.

In order to figure out the achievement of the final pyrimido [4,5-*b*]quinolones desired, the precursor **3b** was reduced on the methylene double bond and a cyclocondensation attempt was proceeded afterwards. The reduction of the 5-(2-nitro)benzylidene thiobarbituric acid (**3b**) by treatment with $NaBH_4$ in methanol generated the compound **9** in good yield, succeeding the cyclization via nitro reduction in the same conditions as the previous protocol followed (Scheme 15). Thereafter, ^{1}H NMR data was acquired and the spectrum did not confirm the pretended structure, presenting several impurities only.

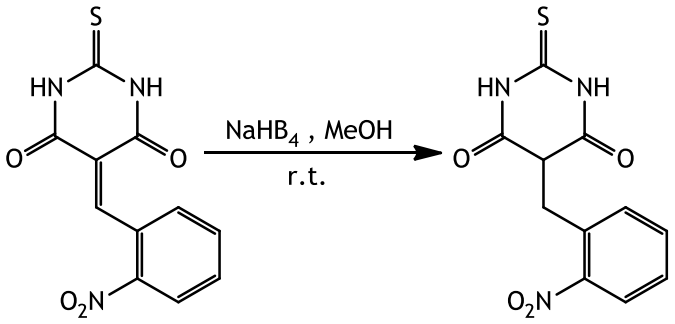

3b **9**

Scheme 15| Reduction of the methylene double bond of the compound **3b**

Further structural analysis, such as DEPT, HSQC, HMBC spectra, mass analysis and X-ray crystallography, performed by *João Serrano*, it was discovered that the final products obtained by this synthetic via were pyrimido spiro-indoles instead (Figure 16)[65]. This achievement could explain the missing NMR signals and the failed cyclization attempt of compound **9**.

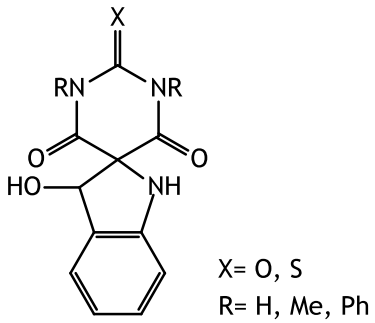

Figure 16 | Structure of the spiro-indole (thio)barbiturate derivatives

3.2. Antioxidant activity

The synthesized thiobarbituric and barbituric acids derivatives **2a-h** and **3b-d** were subjected to the free radical scavenging activity by 1,1-diphenyl-2-picrylhydrazyl) (DPPH) screening method according to a literature protocol [66]. On this assay, the freshly prepared DPPH solution exhibited a deep blue colour with maximum absorption at 517 nm. Thus, purple colour generally fades when an antioxidant is present in the solution. The method used in this work determines the antioxidant capacity by measuring the remaining amount of DPPH after 60 minutes reaction. The free radical scavenging capacity of all tested compounds were compared with Trolox as a standard control. Allopurinol was also submitted to this antioxidant assay as a XO inhibitor reference. The concentration of the test compounds used on this study was 30 μM and all experiments were performed in triplicate. Concentration-response curves were performed to the compounds that presented better antioxidant

scavenging activity The results of the screened compounds are summarized in the graphic 1 and the table 5.

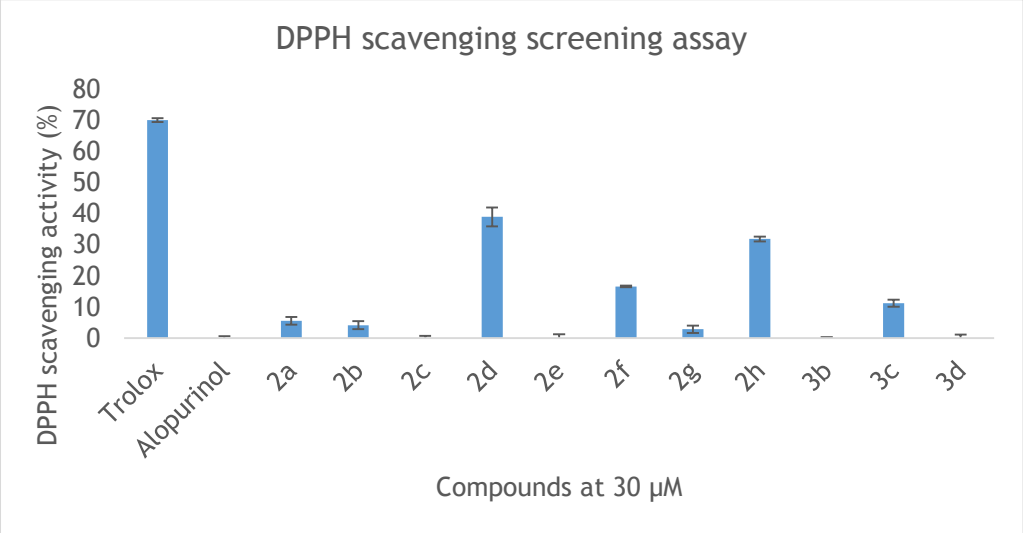

Graphic 1| DPPH free radical scavenging activity of the synthesized compounds

As it can be seen in table 5 and the graphic1, none of the tested compounds showed very high DPPH scavenging activity, demonstrating generally low values when compared with the standard compound Trolox. In fact, most of the thiobarbituric and barbituric acid derivatives exhibited DPPH scavenging activity, in a range 0-20%. Allopurinol and compounds **2c**, **2e**, **3b** and **3d** did not reveal activity at all whereas, compounds **2d** and **2h** exhibited 39% and 32% DPPH scavenging activity, respectively.

Although none of the tested compounds are considered good antioxidants agents, IC_{50} tests were performed for compounds **2d** and **2h**, and to Trolox, as a standard. This essay had the purpose to determinate the compound quantity that reduces 50% of the DPPH absorvance. Concerning the fact that the chosen compounds possess low antioxidant activity at 30 µM, presenting a screening under 50%, it was used 3 concentrations lower than 30 µM (1.0 µM, 7.5 µM and 15 µM) and 2 concentrations higher (50.0 µM and 100 µM). The concentrations applied to trolox were 0.1 µM, 1.0 µM, 7.5 µM, 15.0 µM, 30.0 µM and 50.0 µM. This test was proceeded in the same conditions of the previous one, by measuring the absorvance of the samples after 60 minutes of the beginning of the reaction. The IC_{50} values determined are presented on the table 5 and, to complement the study, graphic 2 demonstrates the DPPH scavenging activity along the compound concentrations used. Accordingly to the graphics on graphic 2, it is possible to see that the tested compounds have an IC_{50} value superior to the maximum concentration used (100 µM). The graphic correspondent to compound **2d** demonstrate a linear tendency with the increase of the compound concentration. However, the maximum DPPH reduction measured on the highest concentration was around 36%. The obtained values at 30 µM in the IC_{50} were not similar to the screening test performed

previously, demonstrating only 16% of DPPH scavenging instead of 39%. This can naturally put into question the veracity of the linear tendency of the obtained results in the graphic of the compound **2d**. The appearance of some antioxidant activity by 5-methylenethiourea 1,3-diphenylthiobarbituric acid can be explained by the presence of the benzyl and the C=S group of the pyrimidine ring. The C=S can transform itself into a thiol by tautomerization. This group can be able to catch the DPPH radical and afterwards, the aromatic ring permits the trapping of this radical.[67]

Relatively to the IC_{50} result of compound **2h**, it was not possible to determinate the concentration that has 50% DPPH scavenging on the tested concentration samples. The right graphic on graphic 2, demonstrates that, the reductive effect of this compound does not change significantly with concentrations higher than 30 μM with DPPH scavenging values on the same range until 100 μM. This can indicate that the compound **2h** cannot reduce DPPH more than 30-40%.

All 5-(2-nitro)benzylidene (thio)barbituric derivatives synthetised (**3b**, **3c** and **3d**) did not show relevant antioxidant activity being compound **3c** the only one who presented 11% of DPPH scavenging activity. Some substituted arylidene barbiturates have the ability to contribute with one electron to the DPPH free radical. The formation of the arylidene barbiturate radicals are normally stabilized by the resonance of the aromatic nucleus and by the substitutent present on the ring, converting themselves into harmless stable molecules.[9] The most active substituted positions at the benzyl ring are *para*- and *meta*- ones. Nitro is an electron-withdrawing group and it offers good stabilization to the free radicals when it is present at *para*- and *meta*-positions, being the first one the strongest. A suggested explanation regarding the lack of DPPH scavenging activity of the compounds **3b**, **3c** and **3d** is the fact that the nitro group is located at *ortho*-position and the stereochemistry involving it.[68]

Table 5| DPPH radical scavenging screening assay and determination of half inhibition concentrations (IC_{50}) in the compounds **2d and 2h**

Compound	% DPPH scavenging activity	IC_{50} values (μM)
Trolox	70,3 ± 0,646	38.37
Allopurinol	0,0 ± 0,663	------
2a	5,60 ± 1,252	------
2b	4,20 ± 1,314	------
2c	0,0 ± 0,802	------
2d	39,10 ± 3,068	>100

2e	0,0 ± 1,303	------
2f	16,70 ± 0,301	------
2g	2,90 ± 1,156	------
2h	32,00 ± 0,783	>100
3b	0,0 ± 0,319	------
3c	11,3 ± 1,148	------
3d	0,0 ± 1,130	------

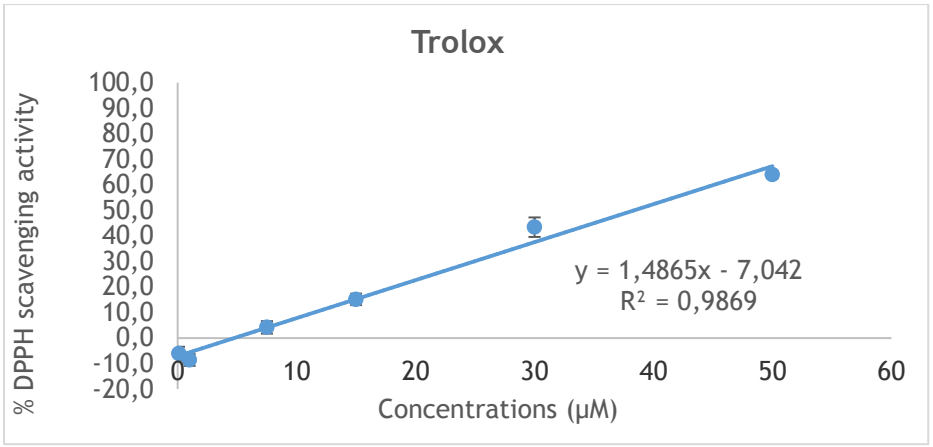

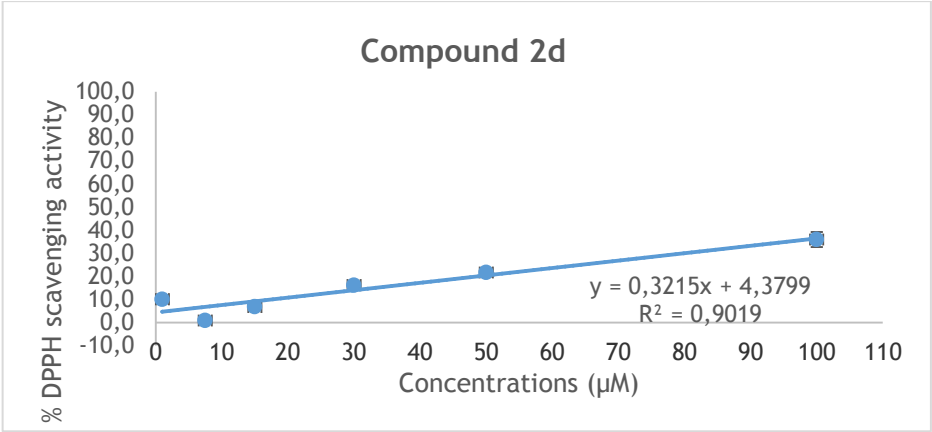

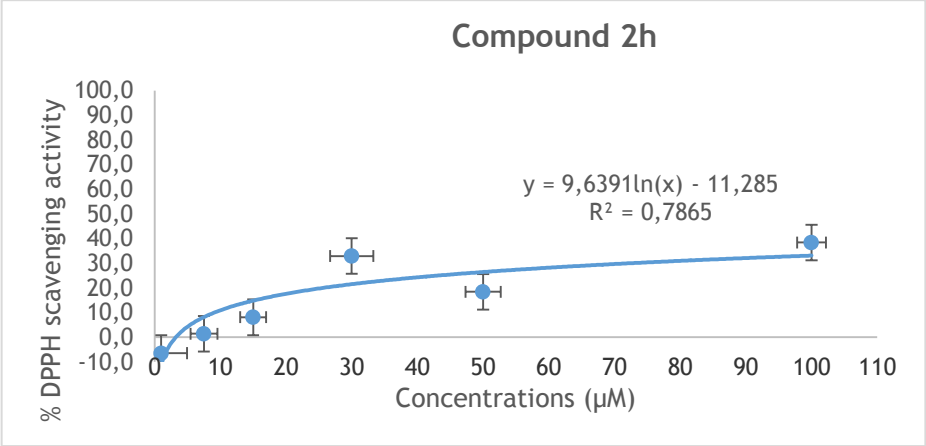

Graphic 2! Effect of compounds concentration and determination of the IC_{50} of the the DPPH scavenging activity in the positive control (Trolox) and compounds **2d** and **2h**

3.3. Xanthine Oxidase inhibition

After the preparation of pure 5-methylene(thio)ureas and 5-(2-nitro)benzylidene barbituric acids and their thio-analogues, the inhibitory activity was evaluated against bovine milk xanthine oxidase (XO) as described in literature[69]. In this assay a XO solution is added to a solution of the compound in the optimal conditions. Allopurinol was employed as reference inhibitor. The activity was evaluated in triplicate via spectrophotometric measurements. Firstly, a screening assay was performed at a concentration of 30 µM and the most active compounds were further considered for calculation of IC_{50} values. The inhibition effect of the tested molecules is displayed in the table 6 and graphics 3 and 4. In general, most of the target compounds did not exhibit potent inhibitory activity against XO, compared with allopurinol. Out of the 11 screened molecules, only compound **3d** was found to have a moderate activity against XO with 46% inhibition at 30µM.

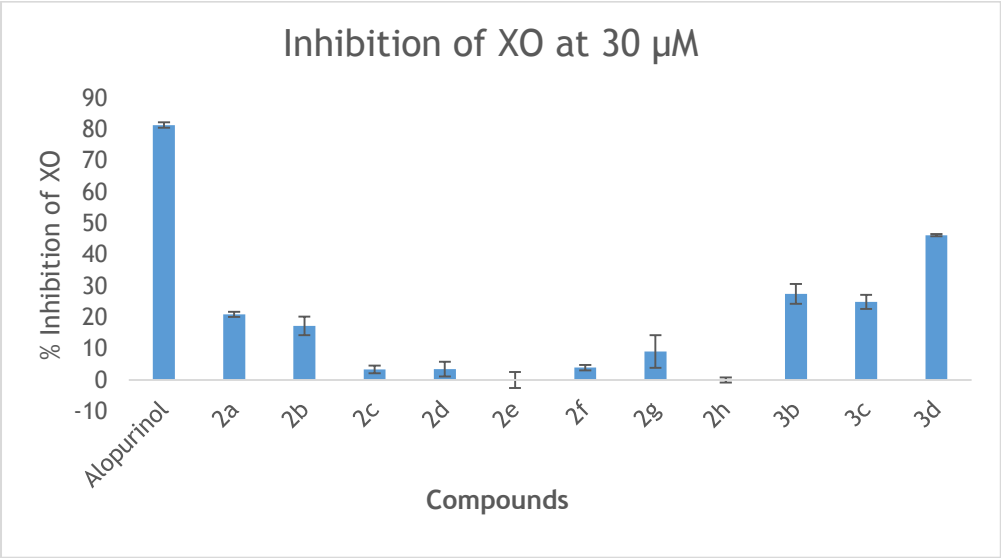

Graphic 3| XO inhibition screening activity of the synthesized compounds at 30 µM

The concentration required to inhibit 50% of the XO activity (IC_{50}) was determined for the compounds **2a**, **2b** and **3d** (Table 6 and Graphic 4). Regarding the results of the compound **3d**, it is possible to see that, when the IC_{50} was measured, the inhibition activity at a 30 µM concentration was higher than the obtained values of the screening assay, with 60% inhibition being observed. As it can be seen in the table, the concentration that is able to inhibit 50% of the tested enzyme was 24,1 µM and thus, this compound have a moderate XO inhibition effect. Previous studies mentioned the good XO inhibition in compounds with a nitro group on the phenyl ring, being the *ortho*-position the one associated to a lower IC_{50} when comparing the other benzyl ring positions.[70] The obtained IC_{50} results of compound **2a** and **2b** demonstrated a linear progression of the inhibition activity on the tested concentrations (1 – 100 µM). At the highest concentration used on this assay, the XO inhibition activity reached values around 36 and 39%. Therefore, it is possible to conclude that a higher compound concentration is required in both compounds to have a 50% inhibition effect on the XO.

Table 6| XO inhibitory activity assay and determination of IC_{50} values on the compounds **2a, 2b** and **3d**

Compound	XO inhibitory activity (%)	IC_{50} values (µM)
Allopurinol	81,44 ± 0,86	5,71
2a	20.96 ± 0,82	>100

2b	17.27 ± 2,98	>100
2c	3,41 ± 1,24	------
2d	3,49 ± 2,38	------
2e	0,0 ± 2,55	------
2f	3,96 ± 0,88	------
2g	9,11 ± 5,22	------
2h	0,0 ± 0,84	------
3b	27,55 ± 3,18	------
3c	24,93 ± 2,25	------
3d	46,28 ± 0,37	24,01

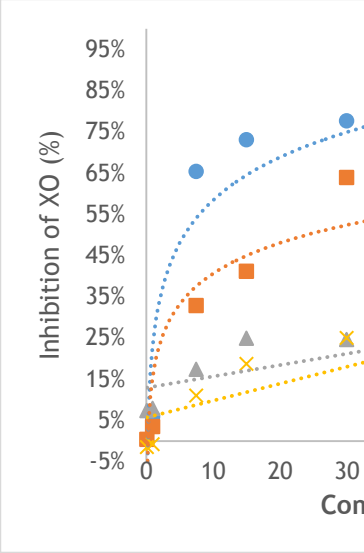

Graphic 4| Dose-response curves of the compounds 2a, 2b and 3d compared with allopurinol

3.4. Anti-proliferative evaluation

The anti-proliferation evaluation in different tumour cell lines have been broadly investigated for certain barbituric acid derivatives and their thio-analogues being the breast cancer studies one of the most explored. Terefore, it became interesting to explore the cytotoxicity of the synthesized compounds in human breast cancer cells, specifically in the MCF-7 cancer cell line.

In this study, a screening assay in the MCF-7 cancer cell line was performed in order to evaluate the cytotoxic effect of the synthetized compounds prepared in the course of this work. For this, the MCF-7 cell line was submitted to a culture process followed by the treatment with the test compounds. Temperature, pH, humidity, CO_2 and nutrients concentrations and contaminations are considered important factors in the maintenance and proliferation of cells meaning that the life cells culture is not so straightforward.[71] The effect of the synthesized compounds was compared with the positive control 5-fluorouracil (5-FU). The viability analysis was carried out through the 3-(4,5-dimethylthiazol-2-yl)-2,5-diphenyl tetrazolium bromide (MTT) method after 72 hours of the cell treatment with the compounds. The MTT method is a colorimetric, sensitive and reliable assay that quantifies the proliferation of cells. This assay relies on the capacity of mitochondrial dehydrogenases of viable cells to reduce MTT molecules, converting the yellow water-soluble molecule into an insoluble purple-blue formazan crystal. This product precipitates in the cellular cytosol and can be dissolved after cell lysis, whereas cells being dead or damaged, cannot transform MTT. For this reason, the biosynthesis of formazan crystals is considered proportional to the viable cell number.[72] The intensity of the purple colour was measured spectrophotometrically at 570 nm.

In this screening assay, all compounds were tested at 30 μM concentration and the obtained results are shown on the graphic 5. Throughout the analysis, it was possible to conclude that the screened compounds did not exhibited very relevant cytotoxic effects in the MCF-7 cell line, presenting cell viability values around 100 and 50%. Although the results did not showed promising anticancer activity, it is possible to visualize that 5-(2-nitro)benzylidene (thio)barbiturates (compounds **3b-d**) show lower cell proliferation results when compared to the 5-methyleneureas and thioureas barbiturates and their thio-analogues (compounds **2a-h**). Therefore, it was decided not to determine the IC_{50} because none of this tested compound presented prominent cytotoxic effect.

Despite theresults observed with these pyrimido [4,5-*d*]pyrimidine precursors, some research studies indicate some barbituric acid derivatives and thio-analogues as having good inhibition of tumour cell growth. For example, barbituric derivatives with enamine side groups linked to carbon-5 of this pyrimidine moiety showed significant anti-proliferative results in MCF-7 cells and other cancer cell lines.[73] Furthermore, when (thio)barbituric acids are linked in cancob-5 to a indole derivative, namely 1-aryl-2phenylindole, they exhibited good anticancer response. It was also assessed that the presence of the C=S group at carbon-2 of the pyrimidine ring was more tolerable on cancer cell lines than carbonyl group [74]. A patent also refers the excellent anti-proliferative in different types of cancer cell lines of 1,3-dibutyl thiobarbituric acid and 1,3-dibutyldihydro-2-thioxo-4,5,6-pyrimidinetrione compounds, indicating more than 90% of loss of cancer cell viability.[75]

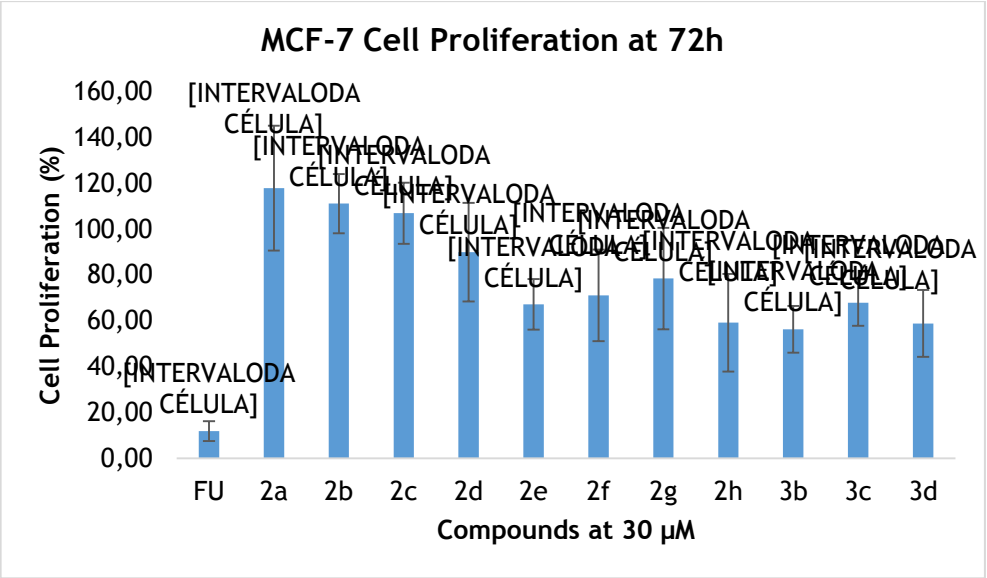

Graphic 5| Effect of the synthesized compounds in MCF-7 cell viability at 30 µM. *p<0,05 in relation to a negative control (t-Student test)

3.5. Molecular Docking

A molecular docking study was carried out to obtain information about the possible interactions between XO and the synthesised barbituric acids derivatives and their thio-analogues. The X-ray crystal structure of the enzyme from bovine milk was retrieved from Protein Data Bank (PDB).

Firstly, it was proceeded the validation method, which was performed using 1-[3-cyano-4-(2,2-dimethylpropoxy)phenyl]-1*H*pyrazole-4-carboxylic acid (Y-700)[76], the ligand crystalized in complex with the protein, and by comparison with results obtained in the literature for Allopurinol and Febuxostat, well-known inhibitors of XO. It is also important to mention that the crystalized ligand is a XO inhibitor. This ligand Y-700 was docked and the resulting conformation was similar with the crystalized ligand-protein complex, presenting a rote mean square deviation inferior to 2,00 Å (RMSD=0.75). (figure 17B) The results obtained from the inhibitors allopurinol and febuxostat were not in complete accordance with the values of the literature, indicating lower binding energy values.[79]

The table 7 demonstrate the results of the molecular docking of the ligand crystalized within the enzyme, the XO inhibitors and the synthetized compounds. As it can be seen, Febuxostat have the lowest binding energy among all and, relatively to the tested molecules, the values got around the range of allopurinol and febuxostat energies which means that these compounds could present a moderate or a good affinity to XO. From the tested molecules, compound **2b** showed the lowest binding energy. The interaction between the compounds and the active pocket of the enzyme was also evaluated in this molecular docking

study. Some compounds presented different types of interactions on the same residues of the XO active pocket. The main interactions between known-inhibitors and the binding site residues of the XO are underlined in table 7 and they are not in complete agreement with the literature data.[80-82] However, all tested compounds presented a lot of interactions with the same residues.

Each XO subunit contains a Molybdenum (Mo) metal. When XO substrate (xanthine) interacts at the XO binding site two electrons are transferred from xanthine to Mo (VI) reducing the metal to Mo (IV) while substrate oxygen reacts with FAD. The inactive modified enzyme complexed allopurinol evidences a lower valence state of Mo than in the unmodified enzyme. Hence, this complex formation prevents further electron uptake from xanthine being, apparently, the basis of the strong inhibitory action of purine analogues class of compounds[76]. Regarding to the table 7 most of the tested molecules interact with the described metal atom except compounds **Y-700, 2c, 2d, 3b, 3c** and **3d**.

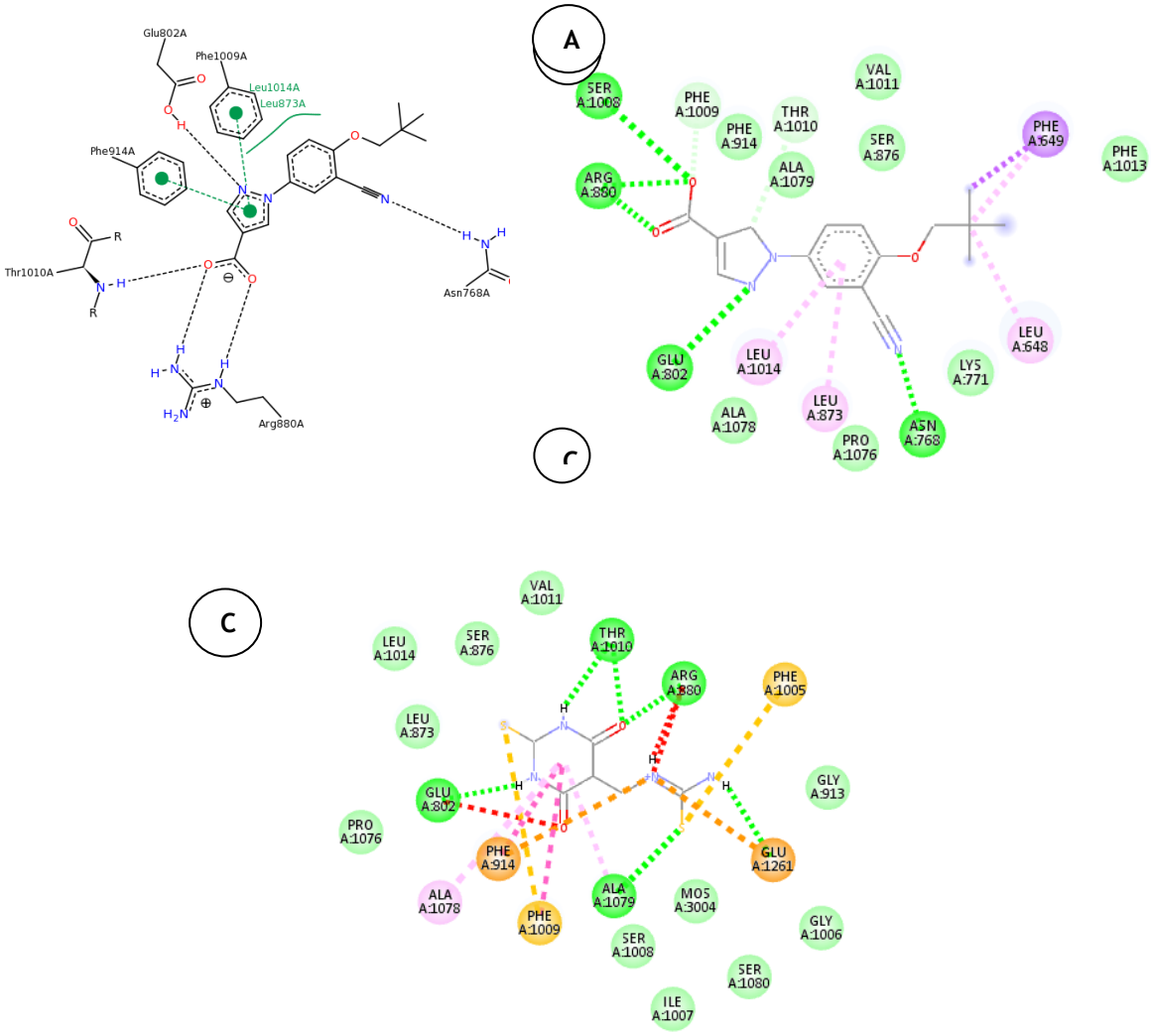

Figure 17| A – Real main interactions between Y-700 and XO68; B – Docked Y-700 structure interaction with XO; C- Docked test compound (**2b**) interactions win XO with the lowest binding energy value from all tested compounds; B and C were obtained by docking analysis through AutoDock Tools 1.5.6. software.

Table 7| Molecular docking results of the synthesized compounds with XO

Compound	Binding Energy	Residues present in main interactions
Y-700	-8.08	**GLU 802, VAL 1011, PHE 1009, SER 876,** LEU 873, THR 1010, ARG 880, **PHE 914**, SER 1008, **ALA 1078**, ALA 1079, **PHE 1013**, LYS 771, **LEU 648**, PRO 1076, ASN 768, **PHE 649**
Allopurinol	-6.24	**GLU 802, VAL 1011, PHE 1009, SER 876**, LEU 873, **LEU 1014**, THR 1010, ARG 880, **PHE 914**, SER 1008, **ALA 1078**, ALA 1079, MOS
Febuxostat	-8.70	**GLU 802, VAL 1011, PHE 1009, SER 876**, LEU 873, **LEU 1014**, THR 1010, ARG 880, **PHE 914**, SER 1008, ALA 1079, **ALA 1078, PHE 1013,** LYS 771, **LEU 648**, PRO 1076, ASN 768, THR 803, MOS
2a	-6.28	**GLU 802, VAL 1011, PHE 1009, SER 876**, **LEU 1014**, **PHE 914**, **ALA 1078**, ALA 1079, GLU 1271, MOS
2b	-8.31	**GLU 802, VAL 1011, PHE 1009, SER 876**, LEU 873, **LEU 1014**, THR 1010, ARG 880, **PHE 914**, SER 1008, **ALA 1078**, ALA 1079, PHE 1005, ILE 1007, SER 1080, GLY 1006, GLU 1261, GLY 913, **MOS**
2c	-8.09	**GLU 802, SER 876**, **LEU 1014**, LYS 771, **PHE 649**, ASN 768, LEU648
2d	-7.42	**GLU 802, VAL 1011, PHE 1009, SER 876**,LEU 873, **LEU 1014**, THR 1010, **PHE 914, PHE 1013**, LYS 771, PRO 1076, **PHE 649**, GLU 879, HIS 875, LEU 873
2e	-7.79	**GLU 802, VAL 1011, PHE 1009, SER 876**, LEU 873**, LEU 1014**, THR 1010, ARG 880, **PHE 914**, SER 1008, **ALA 1078**, ALA 1079, PRO 1076, PHE 1005, GLU 1261, **MOS**
2f	-7.13	**GLU 802, VAL 1011, PHE 1009, SER 876**, LEU 873, **LEU 1014**, THR 1010, ARG 880, **PHE 914**, ALA 1079**, ALA 1078**, PHE 1005, GLU 1261, **MOS**
2g	-7.10	**GLU 802, VAL 1011, PHE 1009, SER 876**, LEU 873, **LEU 1014**, THR 1010, ARG 880, **PHE 914, ALA 1078**, ALA 1079, LYS 771, **LEU 648**, PRO 1076, ASN 768, PHE 649**, MOS**

2h	-6.99	**GLU 802, VAL 1011, PHE 1009, SER 876**, LEU 873, **LEU 1014**, THR 1010, ARG 880, **PHE 914, ALA 1078**, ALA 1079**, LEU 648**, PRO 1076, ASN 768, **PHE 649**, ALA 910**, MOS**
3b	-7.93	**GLU 802, VAL 1011, PHE 1009, SER 876**, LEU 873, **LEU 1014**, **PHE 914**, LYS 771**, LEU 648, PHE 649**
3c	-6.93	**GLU 802, VAL 1011, PHE 1009, SER 876**, LEU 873**, LEU 1014**, **PHE 914**, LIS 771, **LEU 648**, PRO 1076, **PHE 649**, GLU 879, HIS 875, PHE 775
3d	-7.89	**GLU 802, VAL 1011, PHE 1009, SER 876**, LEU 873**, LEU 1014**, THR 1010, ARG 880, **PHE 914, ALA 1078**, ALA 1079, LYS 771, **LEU 648**, PRO 1076, **PHE 649**, ASN 768

4. Conclusions and Future Perspectives

In summary, in this work it was performed the synthesis of eight new 5-methylene(thio)urea (thio)barbiturates and three 5-(2-nitro)benzilidene derivatives with further evaluation of their antioxidant effects, XO inhibitory activity and their anti-proliferative properties. Moreover, *in silico* molecular docking was performed fitting the described compounds on the active binding centre of XO.

Although the initial aim was the preparation of pyrimido [4,5-*d*]pyrimidines, several 5-methylene(thio)urea (thio)barbiturate and 5-(2-nitro)benzilidene intermediates were synthesized with good yields. All spectra (NMR and IR) and MS-analysis data were consistent with the synthetized compounds, it would be interesting to perform an X-ray diffraction analysis to confirm the exact structure of the molecules. Several methods were performed in order to synthesised the desired bicyclic compounds with unsuccessful results.

The antioxidant activity of the synthesised compounds were evaluated using the DPPH scavenging method. In this assay none of the 5-methylene(thio)urea (thio)barbiturate and 5-(2-nitro)benzilidene derivatives exhibited high DPPH reducing powerand it was conclude that they are not good potential antioxidant agents.

The compounds were also evaluated as potential XO inhibitors, and it was observed that 5-(2-nitro)benzilidene 1,3-dimethylbarbituric acid (**3d**) had some inhibitory activity, whereas the other synthesised derivatives showed poorer results.

In the screening of the anti-proliferative effect through the MTT assay, it was found that the different synthesised compounds did not demonstrated significant cytotoxic activity in the MCF-7 cell lines thus, not affecting the cancer cell viability. In the future, it would be interesting to explore the cell viability in normal dermal skin cells (NHDF) in order to understand if the synthesised derivatives are harmful to the normal human cells.

Molecular docking studies were performed to predict the binding energies between the synthesised compounds and the active site of the XO using allopurinol and febuxostat as reference compounds. The study revealed binding energy values in the range of the two well-known inhibitors, leading to the conclusion that the synthesised compounds could potentially inhibit the XO enzyme.

As it was observed, the synthesised 5-methylene(thio)urea (thio)barbiturates have not demonstrated to be potential good XO inhibitors although the molecular docking study revealed the possibility of some inhibitory activity.

5. Experimental Section

5.1. Synthesis

5.1.1. General Data

Reagents and solvents were purchased from standard sources and purified and/or dried whenever necessary using standard procedures prior to use.

Thin layer chromatography (TLC) analysis was performed routinely using 0.20 mm Al-backed silica-gel Macherey-Nagel 60 F254 and Kieselgel 60Hf254/Kieselgel 60G (Merck) plates. The compounds were visualized using UV light (254 nm and 365 nm). Melting points were recorded with Electrothermal capillary tube melting analysis and are uncorrected. IR spectra were obtained using a Vertex 70 (Bruker Optics Inc., MA, USA) FTIR instrument. The FTIR measurements were made directly in solids with a horizontal attenuated total reflectance (ATR) accessory (MIRacle, Pike Technology, Inc, WI, USA). The transmittance spectra were recorded at a 4 cm^{-1} resolution between 4000 and 600 cm^{-1} using the OPUS 5.5 software (Bruker Optics Inc., MA, USA). ESI-MS was performed by direct injection using a Synapt G2 HDMS (Waters, MA, USA) instrument. NMR spectra were acquired using a Bruker Avance 400 MHz spectrometer (^{1}H NMR at 400 MHz and ^{13}C NMR at 100 MHz) and a Varian Mercury Plus 300 spectrometer, with tetramethylsilane (TMS) as internal standard. The chemical shifts (δ) are reported in parts per million (ppm) relative to TMS. Coupling constants (*J* values) are quoted in Hertz (Hz) and splitting multiplicities are described as s=singlet; d=duplet; t=triplet; q=quartet; or combinations of the above; or m=multiplet. Deuterated dimethylsulfoxide (DMSO-*d6*) was used as solvent.

5.1.2. Synthesis of 1,3-diphenylthiobarbituric acid

10.98 mmol of isothiocianate and 10.98 mmol of aniline were mixed with dichloromethane and triethylamine at room temperature with continuous stirring. A white precipitate was formed during the reaction The white precipitate was filtered and the filtrate was once more stirred in order to collect more precipitate and it was dried. 4.93 Mmol of the previous white precipitate (diphenylthiourea) was stirred at 60ºC with 5.71 mmol of malonic acid and 8.78 mmol of acetyl chloride for 40 min. Firstly, the reactional mixture was an homogeneous solution which then compacted into a yellow crystalline mass. The product was broken up into pieces and recrystallized with glacial acetic acid to afford green needled crystals.

Starting from diphenylurea, 1,3-diphenylthiobarbituric acid was obtained: η= 90%; mp= 252-253ºC; IR (vmáx/cm^{-1}): 3053, 2895, 1727, 1594, 1490, 1454, 1381, 1338, 1260, 1212, 1165, 1169, 1037, 1003, 747, 696, 687, 667. ^{1}H NMR (300MHz, DMSO-*d6*): δ (ppm) = 7.55 (m, 6H,CH_{ar}), 7.21 (d, 4H, *J*=7.3 Hz, CH_{ar}), 4.09 (s, 2H, CH_2). ^{13}C NMR (300MHz, DMSO-*d6*): δ (ppm) =181.6 (C=S), 163.3 (C=O), 138.8 (C_{ar}), 129.7 (CH_{ar}), 129.2 (CH_{ar}), 128.6 (CH_{ar}),41.2 (CH_2); mp= 252-253ºC

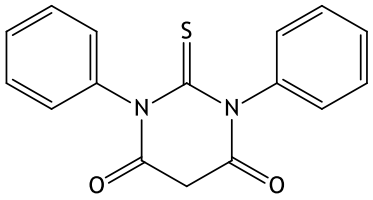

5.1.3. General procedure for the preparation of 5-methylene(thio)ureas (thio)barbiturates

0.500 mmol of (thio)barbituric acid and their 1,3-alkyl/aryl derivatives, 0.750 mmol trimethyl or triethyl *ortho*formate and 0.500 mmol of (thio)urea (1.0 eq.) were refluxed in *n*-butanol at 120ºC on continuous stirring. The reaction was monitored by TLC and it completed after 4 hours refluxing. Then, the reactional mixture was cooled and a precipitate product was formed. The product was filtered, washed in *n*-buthanol and dried at vacuum, to afford the following 5-methylene (thio)urea (thio)barbiturates

[(4,6-Dioxo-2-thioxoidene-1,3-diazinan-5-ylidene)methyl]urea (2a) obtained from thiobarbituric acid, triethyl *ortho*formate and urea resulting in a pure reddish solid.η= 77%; mp= decomposes; IR ($v_{máx}$/cm^{-1}): 3406, 3147, 2889, 1730, 1693, 1643, 1529, 1375, 1259, 1149, 815 – 757. ^{1}H NMR (400MHz, DMSO-*d6*): δ (ppm) = 12.19 (s, 1H, N*H*), 12.13 (1H, s, N*H*), 11,24 (1H, d, *J*= 13.2Hz, CH-N*H*-CO), 8.54 (1H, d, *J*= 13.1Hz, C*H*), 7,88 (1H, s, CO-NH_2), 7.56 (1H, s, CO-NH_2).^{13}C NMR (300MHz, DMSO-*d6*): δ (ppm) =96.1 (C), 151.03 (C-H), 152.0 (C=O), 161.3 (C=O), 163.0 (C=O), 178.5 (C=S), m/z= 214.01576.

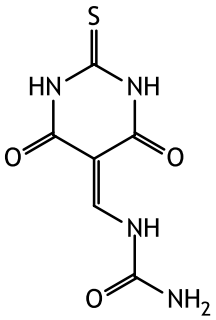

[(4,6-Dioxo-2-thioxoidene-1,3-diazinan-5-ylidene)methyl]thiourea (2b) obtained from thiobarbituric acid, trimethyl *ortho*formate and thiourea resulting in a pure reddish solid. η= 74%; mp= decomposes; IR ($v_{máx}$/cm^{-1}: 3284, 3136, 1695, 1664, 1574, 1506, 1413, 1259, 1143, 1012-997, 804.^{1}H NMR (300MHz, DMSO-*d6*): δ (ppm) = 12.27 (1H, s, N*H*), 12.18 (1H, s, N*H*), 11,94 (1H, d, *J*= 6.30 Hz, N*H*), 9.64 (1H, s, NH_2), 9.52 (1H, s, NH_2), 9.11 (1H, d, *J*= 6.30 Hz, C*H*). ^{13}C NMR (300MHz, DMSO-*d6*): δ (ppm) = 98.3 (C), 153.0 (C-H), 161.8 (C=O), 163.4 (C=O), 178.9 (C=S), 181.7 (C=S). *M*/z= 299.99336.

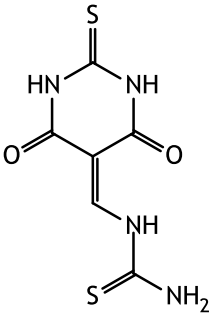

[(4,6-Dioxo-1,3-diphenyl-2-thioxoidene-1,3-diazinan-5-ylidene)methyl]urea (2c) obtained from 1,3-diphenylthiobarbituric acid, trimethyl *ortho*formate and urea resulting is a pure yellow solid product.η= 79%. mp= 261-265 ºC. IR ($v_{máx}$/cm^{-1}): 3469, 3307, 3182, 3060, 1735, 1689, 1649, 1560, 1471, 1328, 1265, 756, 692. ^{1}H NMR (300MHz, DMSO-*d6*): δ (ppm) = 11.48 (1H, d, *J*= 6.60 Hz, N*H*), 8.67 (2H, d, *J*= 6.15 Hz, C*H*), 7.76 (1H, s,NH_2), 7.58 (1H, s, NH_2) and 7.45-7.24 (10H, m, CH_{ar}).^{13}C NMR (300MHz, DMSO-*d6*): δ (ppm) = 97.2 (C), 128.4 (CH_{ar}), 128.9 (CH_{ar}), 129.2 (CH_{ar}), 129.3 (CH_{ar}), 129.4 (CH_{ar}), 129.6 (CH_{ar}), 139.7 (C_{ar}) 140.3 (C_{ar}), 152.2 (CH), 161.5 (C=O), 162.5 (C=O), 181.3 (C=S). M/z= 366.07856

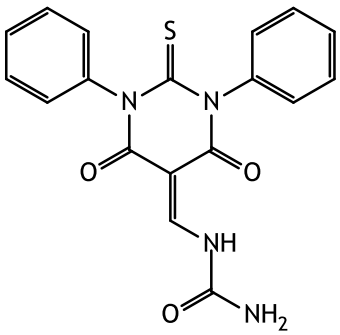

[(4,6-Dioxo-1,3-diphenyl-2-thioxoidene-1,3-diazinan-5-ylidene)methyl]thiourea (2d) obtained from 1,3-diphenylthiobarbituric acid, trimethyl *ortho*formate and thiourea resulting in a pure and orange solid. η= 85%; mp= 259-261 ºC. IR ($v_{máx}$/cm^{-1}): 3442, 3263, 3172, 3051, 1685, 1654, 1591, 1487, 1402, 1321, 1217, 1190, 1153, 823-688.^{1}H NMR (300MHz, DMSO-*d6*): δ (ppm) = 12.13 (1H, d, *J*= 6.30 Hz, N*H*), 9.72 (1H, s, NH_2), 9.44 (1H, s, NH_2), 9.28 (1H, d, *J*= 11.7 Hz, C*H*), 7.27 – 7.49 (10H, m, CH_{ar}). ^{13}C NMR (300MHz, DMSO-*d6*): δ (ppm) = 97.2 (C), 128.4 (CH_{ar}), 128.5 (CH_{ar}), 129.2 (CH_{ar}), 129.3 (CH_{ar}), 129.4 (CH_{ar}), 129.5 (CH_{ar}), 139.8 (C_{ar}), 140.5 (C_{ar}), 152.3 (CH), 161.2 (C=O), 162.5 (C=O), 181.3 (C=S), 181.6 (C=S). M/z= 382.05556.

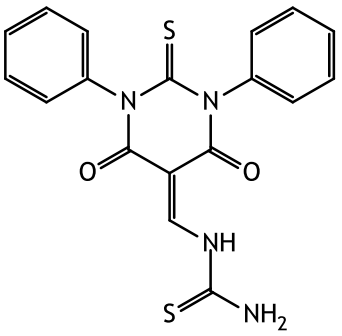

[(2,4,6-Trioxo-1,3-diazinan-5-ylidene)methyl]urea (2e) obtained from barbituric acid, trimethyl *ortho*formate and urea proceeding into further filtration with hot water and put to dry, affordinf a pure yellow solid. η= 71%; mp= 316-318 ºC; IR ($v_{máx}$/cm^{-1}): 3411, 3172, 1733-1703, 1629, 1569, 1384, 1305-1272, 792. ^{1}H NMR (400MHz, DMSO-*d6*): δ (ppm) = 11.10 (1H, d, *J*= 6.60 Hz, N*H*), 11.06 (1H, s, N*H*), 10.97 (1H, s, N*H*), 8.51 (1H, d, *J*= 6.45 Hz, C*H*), 7.83 (1H, s, NH_2), 7.46 (1H, s, NH_2). ^{13}C NMR (300MHz, DMSO-*d6*): δ (ppm) = 95.5 (C), 150.3 (C-H), 151.0 (C=O), 152.7 (C=O), 163.9 (C=O), 165.6 (C=O). M/z= 198.13672.

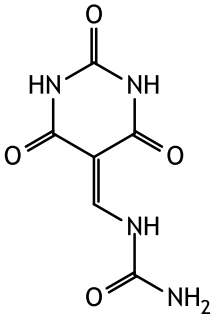

[(2,4,6-Trioxo-1,3-diazinan-5-ylidene)methyl]thiourea (2f) obtained from barbituric acid, trimethyl *ortho*formate and thiourea resulting in a pure light-brown solid. η= 86%. mp=317-320 ºC. IR ($\nu_{máx}$/cm^{-1}): 3280, 3217, 3145, 3045, 2808, 1733-1701, 1645, 1571, 1438-1407, 1247, 1024, 783.^{1}H NMR (300MHz, DMSO-*d6*): δ (ppm) = 11.84 (1H, d, *J*= 6.15 Hz, N*H*), 11.15 (1H, s, N*H*), 11.03 (1H, s, N*H*), 9.53 (1H, s, NH_2), 9.45 (1H, s, NH_2), 9.08 (1H, d, *J*= 6.15 Hz, C*H*). ^{13}C NMR (300MHz, DMSO-*d6*): δ (ppm) = 97.4 (C), 150.9 (C-H), 152.0 (C=O), 163.7 (C=O), 165.6 (C=O), 181.9 (C=S). M/z= 214.0860

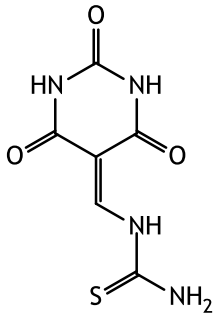

.

[(1,3-Dimethyl-2,4,6-trioxo-1,3-diazinan-5-ylidene)methyl]urea (2g) obtained from 1,3-dimethylbarbituric acid, trimethyl *ortho*formate and urea resulting in a pure yellow solid. η= 52%. mp= 248-250 ºC. IR (vmáx/cm-1): 3371, 3278, 3197, 1704, 1666-1635, 1560, 1406, 1371, 1255, 1085. ^{1}H NMR (300MHz, DMSO-*d6*): δ (ppm) = 11.23 (1H, d, J= 6.60 Hz, N*H*), (1H,s, NH), 8.61 (1H, d, J=6.45 Hz, C*H*), 7.82 (1H, s, NH_2), 7.47 (1H, s, NH_2), 3.18 (3H, s, CH_3), 3.16 (3H, s, CH_3). ^{13}C NMR (300MHz, DMSO-*d6*): δ (ppm) = 27.5 (CH_3), 28.1 (CH_3), 95.4 (C), 151.1 (C-H), 151.7 (C=O), 152.6 (C=O) 162.4 (C=O), 163.7 (C=O). M/z= 226.07006.

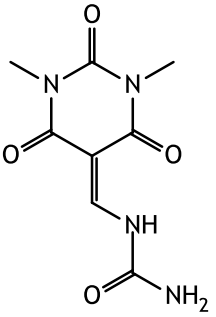

[(1,3-Dimethyl-2,4,6-trioxo-1,3-diazinan-5-ylidene)methyl]thiourea (2h) obtained from 1,3-dimethylbarbituric acid, trimethyl *ortho*formate and thiourea resulting in a pure yellow solid. η= 89%. mp= 267-270ºC. IR (vmáx/cm^{-1}): 3290, 3145, 1716, 1635, 1589, 1469-1429, 1338, 1230, 1186, 1086, 798-754. ^{1}H NMR (300MHz, DMSO-*d6*): δ (ppm) = 11.95 (1H, d, J= 6.15 Hz, N*H*), 9.59 (1H, s, NH_2), 9.48 (1H, s, NH_2), 9.19 (1H, d, J= 6.3 Hz, C*H*), 3.20 (3h, s, CH_3), 3.18 (3H, s, CH_3). ^{13}C NMR (300MHz, DMSO-*d6*): δ (ppm) = 27.7 (CH_3), 28.3 (CH_3), 97.3 (C), 151.6 (C-H), 152.8 (C=O), 162.2 (C=O), 167.8 (C=O), 181.5 (C=S). M /z= 242.04716.

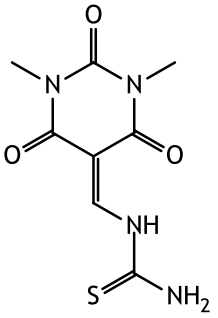

5.1.4. General procedure for the preparation of 5-arylidene thiobarbituric acids

0.500 mmol of thiobarbituric acid and his *N,N'*-diphenyl derivative was refluxed with 0.500 mmol of aromatic aldehydes in water. The reaction proceeded as a suspension with continuous stirring and it was followed by TLC (eluent: DCM/MeOH (20%)). The reaction was completed after 3 hours and the product was filtered after the reaction was warmed and washed with cold water and ethyl ether, to afford the following compounds:

5-[(4-Bromophenyl)methylidene]-2-thioxoidene-1,3-diazinane-4,6-dione (3a) obtained from thiobarbituric acid and 4-bromobenzaldehyde resulting into a pure yellow solid. η= 71%. mp= 230-232ºC. IR (vmáx/cm^{-1}): 3240, 3095, 3078, 1739, 1620, 1562, 852-787. ^{1}H NMR (300MHz, DMSO-*d6*): δ (ppm) = 12.50 (1H, s, N*H*), 12.39 (1H, s, N*H*), 8,31 (1H, s, C*H*), 7.74-8.30 (4H, m, CH_{ar}). ^{13}C NMR (300MHz, DMSO-*d6*): δ (ppm) =119.9 (C), 127.9 (C_{ar}-Br), 131.1 (CH_{ar}), 131.7 (C_{ar}), 134.4 (CH_{ar}), 153.0 (CH), 152.8 (C=O), 160.4 (C=O), 162.7 (C=O), 178.7 (C=S).

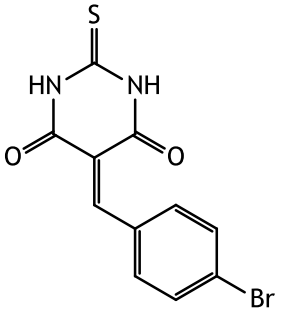

5-[(2-Nitrophenyl)methylidene]-2-thioxoidene-1,3-diazinane-4,6-dione (3b) obtained from thiobarbituric acid and 2-nitrobenzaldehyde resulting into a pure yellow solid. η= 89%. mp= 239-241ºC. IR ($v_{máx}$/cm^{-1}): 3255, 3157, 2876, 1719, 1693, 1627, 1604, 1540, 1514, 1439, 1352, 1288, 1204, 1141, 1064, 785, 759, 733, 699, 678.^{1}H NMR (400MHz, DMSO-*d6*): δ (ppm) = 12.56 (1H, s, N*H*), 12.33 (1H, s, N*H*), 8.63 (1H, s, C*H*), 8.24 (1H, dd, *J*= Hz, CH_{ar}), 7.80 (1H, td, *J*= Hz, CH_{ar}), 7.69 (1H, td, *J*= Hz, CH_{ar}), 7.62 (1H, dt, *J*= Hz, CH_{ar}). ^{13}C NMR (300MHz, DMSO-*d6*): δ (ppm) = 120.6 (C), 124.0 (CH_{ar}), 130.3 (CH_{ar}), 130.4 (CH_{ar}), 131.6 (C_{ar}), 133.7 (CH_{ar}), 146.3 (C_{ar}), 153.3 (CH), 159.2 (C=O), 160.6 (C=O), 179.1 (C=S).

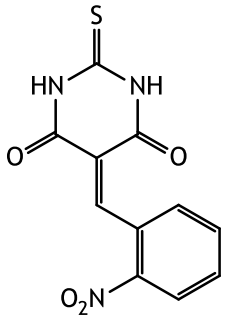

5-[(2-Nitrophenyl)methylidene]-1,3-diphenyl-2-thioxoidene-1,3-diazinane-4,6-dione (3c) obtained from 1,3-diphenylthiobarbituric acid and 2-nitrobenzaldehyde resulting into a pure yellow solid. η= 90%. mp= 235ºC. IR ($v_{máx}$/cm^{-1}): 3032, 1717, 1692, 1625, 1607, 1592, 1520, 1487, 1454, 1396, 1354, 1326, 1265, 1190, 1174, 1156, 1070, 1023, 963, 923, 902, 868, 842, 781, 768, 753, 723, 705, 692, 676, 667. ^{1}H NMR (400MHz, DMSO-*d6*): δ (ppm) = 8.80 (1H, s, C*H*), 8.19 (1H, d, *J*= 8.2Hz, CH_{ar}), 7.71 (1H, t, *J*=7.5 Hz, CH_{ar}), 7.59 (2H, t, *J*=7.9 Hz, CH_{ar}), 7.45 (2H,t, *J*=7.6Hz, CH_{ar}) 7.40-7.29 (6H, m, CH_{ar}), 7.20 (2H, d, *J*=7.6 Hz, CH_{ar}). ^{13}C NMR

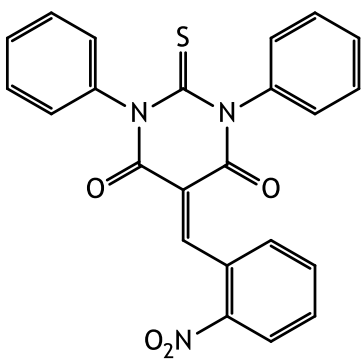

(300MHz, DMSO-*d6*): δ (ppm) = 121.7 (C), 124.6 (CH_{ar}), 128.6 (CH_{ar}), 128.8 (CH_{ar}), 129.3 (CH_{ar}),129.4 (CH_{ar}), 129.5 (CH_{ar}), 130.6 (CH_{ar}), 130.9 (CH_{ar}), 132.2 (C_{ar}), 134.5 (CH_{ar}), 140.2 (C_{ar}), 140.5 (C_{ar}), 146.7 (C_{ar}), 155.5 (CH), 159.3 (C=O),160.8 (C=O),181.9 (C=S).

1,3-Dimethyl-5-[(2-nitrophenyl)methylidene]-1,3-diazinane-2,4,6-trione (3d) obtained from 1,3-methylbarbituric acid and 2-nitrobenzaldehyde resulting into a pure yellow solid. η= 93%. mp = 158-159ºC. IR ($v_{máx}/cm^{-1}$); 3028, 2950, 1603, 1518, 1416, 1377, 1342, 1323, 1161, 1092,1057, 961, 862, 831, 788, 773, 754, 737, 708, 692, 668, 608. ^{1}H NMR (400MHz, DMSO-*d6*): δ (ppm) = 8.70 (1H, s, C*H*), 8.25 (1H, dd, *J*= Hz, C*H*$_{ar}$), 7.80 (1H, dt, *J*= Hz, C*H*$_{ar}$), 7.69 (2H, dt, *J*= Hz, C*H*$_{ar}$), 7.53 (1H, dd, *J*= Hz, C*H*$_{ar}$), 3.26 (3H, s, CH_3), 3.07 (3H, s, CH_3). ^{13}C NMR (400MHz, DMSO-*d6*): δ (ppm) = 28.3 (CH_3), 28.9 (CH_3), 120.6 (C),124.5 (CH_{ar}), 130.5 (CH_{ar}), 130.6 (CH_{ar}), 132.5 (C_{ar}), 134.4 (CH_{ar}), 146.6 (C_{ar}), 151.2 (C=O), 154.1 (CH),160.4 (C=O), 161.7 (C=O).

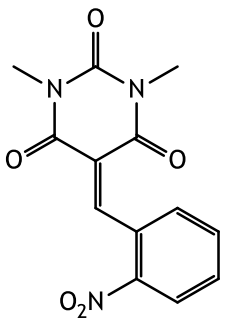

5.1.5. Preparation of the 5-[(2-nitrophenyl)methyl]-2-thioxoidene-1,3-diazinane-4,6-dione

0.36 mmol of 5-[(2-Nitrophenyl)methylidene]-2-thioxoidene-1,3-diazinane-4,6-dione was dissolved in 10 mL of anhydrous ethanol, and 1.0 mmol of $NaBH_4$ was added three times. The reaction was stirred at room temperature for 3h. After completion of the reaction, the ethanol was evaporated under reduced pressure. To the obtained residue, 10 mL of water was added and the solution obtained was neutralised. The precipitated solid was filtered and recrystallized with methanol. η= 30%. IR ($v_{máx}/cm^{-1}$): 3230, 3141, 2891, 1721, 1687, 1621, 1600, 1535, 1516, 1436, 1355, 1281, 1203, 1145, 1070, 782, 755, 730, 694. ^{1}H NMR (400MHz, DMSO): δ (ppm) = 12.16 (2H, s, N*H*), 7.93 (1H, d, *J*= Hz, C*H*$_{ar}$), 7.58 (1H, t, *J*= Hz, C*H*$_{ar}$), 7.45 (1H, t, *J*= Hz, C*H*$_{ar}$), 7.22 (1H, d, *J*= Hz, C*H*$_{ar}$), 3.84 (2H, s, CH_2). ^{13}C NMR (300MHz, DMSO): δ (ppm) = 24.7 (CH_2), 49.0 (C), 91.9 (C), 124.6 (CH_{ar}),127.6 (CH_{ar}), 129.9 (CH_{ar}), 133.7 (CH_{ar}), 135.0 (C=O),149.7 (C_{ar}), 161.2 (C=O), 174.0 (C=S).

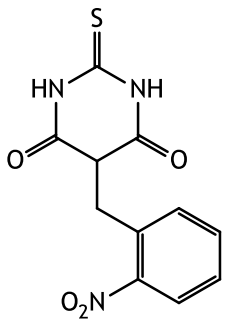

5.1.6. Procedure attempts for the preparation of pyrimido [4,5-*d*]pyrimidines

Method A1: 0.136 mmol of [(4,6-dioxo-2-sulfanylidene-1,3-diazinan-5-ylidene)methyl]urea **(2a)** / [(4,6-dioxo-2-sulfanylidene-1,3-diazinan-5-ylidene)methyl]thiourea **(2b)** were refluxed in 10.0 mL of *n*-butanol and 4.0 mL of acetic acid for 3 days. The reaction proceeded as a suspension and was monitored by TLC. No differences were found on TLC plaques and the proton NMR showed the presence of starting material only.

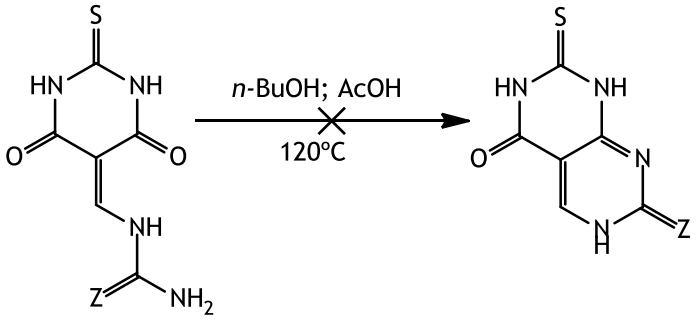

2a
2b
Z= O, S

4a
4b

Method A2: 0.136 mmol [(4,6-dioxo-1,3-diphenyl-2-sulfanylidene-1,3-diazinan-5-ylidene)methyl]urea **(2c)** / [(4,6-dioxo-1,3-diphenyl-2-sulfanylidene-1,3-diazinan-5-ylidene)methyl]thiourea **(2d)** were refluxed in 10.0 mL of *n*-butanol and 4.0 mL of acetic acid at 120ºC for 24 hours. All starting material dissolved and reaction proceeded as solution. The mixture was monitored by TLC. After completion of the reaction, the solution was cooled and the generated precipitate was filtered and dried. Although the TLC's plaques showed spots with different Rf's, the mass analysis results showed starting material only.

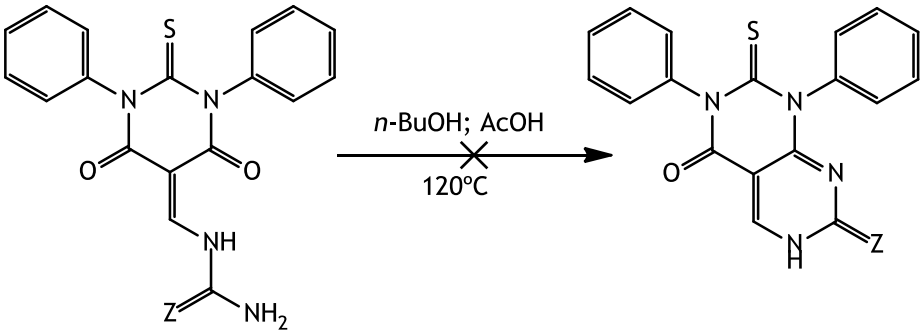

2c
2d
Z= O, S

4b
4c

Method B: In a mixture of 3.5 mL of *n*-butanol and 1.4 mL of acetic acid was added 20,0 mg of [(4,6-dioxo-2-sulfanylidene-1,3-diazinan-5-ylidene)methyl]urea **(2a**) in a microwave tube. The reaction mixture was subjected to microwave irradiation with continuous stirring between 2 and 4 hours at high power, 10 bars pressure and 140ºC temperature. The process of the reaction was monitored at intervals of 1 hour without any progresses being observed by TLC plaques.

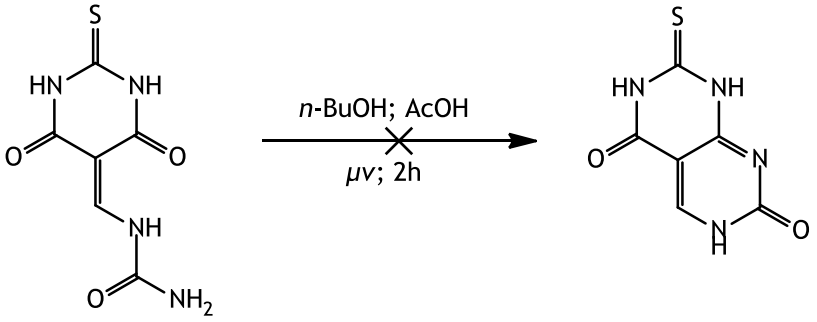

2a **4a**

Method C: 0.233 mmol of [(4,6-dioxo-2-sulfanylidene-1,3-diazinan-5-ylidene)methyl]urea **(2a) and** 10.0 mg of triethyl benzyl ammonium chloride (TEBAC) were dissolved in 2.00 mL of ethanol. The mixture was refluxed with continuous stirring at 84ºC for 42 hours. The reaction was monitored by TLC and no differences were found on silica plaques after its elution. The ^{1}H NMR results showed the presence of starting material only.

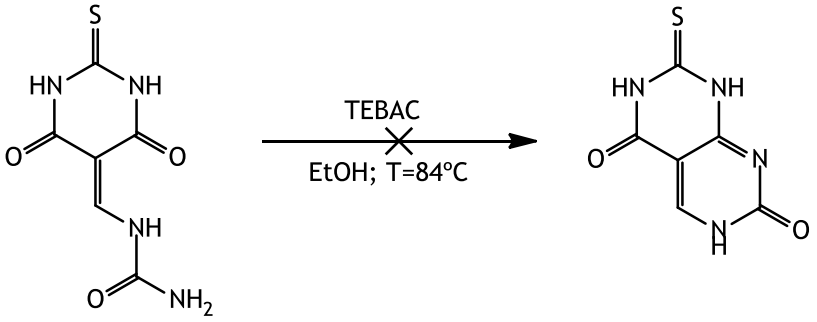

1a **4a**

Method D: A mixture of 0,693 mmol of 5-[(4-Bromophenyl)methylidene]-2-sulfanylidene-1,3-diazinane-4,6-dione and 1,040 mmol of urea was refluxed in ethanol with a catalytic amount (a few drops)of hydrochloric acid with continuous stirring. The reaction was monitored by TLC and no differences were found on silica plaques after its elution.

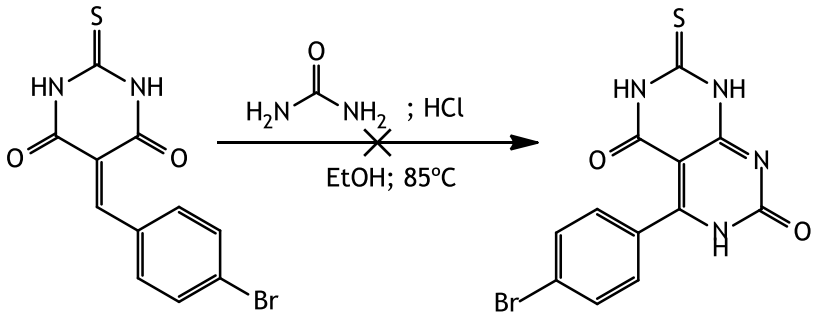

3a **4a**

Method E: 0.337 mmol of 1,3-diphenylthiobarbituric acid (**1a**) was dissolved in 0.337 mmol of benzaldehyde and 0.337 mmol of urea / thiourea in ethanol with a catalytic amount of hydrochloric acid at 84ºC. After 10 min, a precipitate started to be formed. The reaction was monitored by TLC and it ended after 3 hours. Although the TLC plaques showed some Rf's differences and the proton and carbon NMR's spectra indicated the desired product, the mass analysis did not confirm the structure.

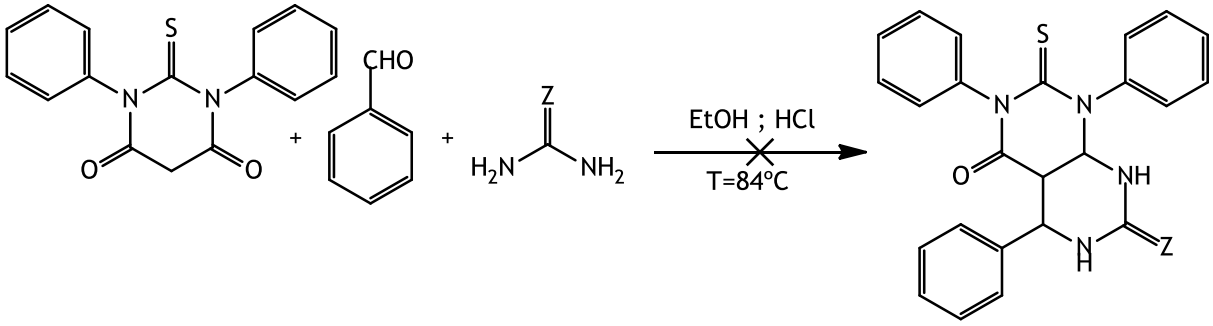

1a

Z= O, S

4a

5.1.7. General procedure for the preparation of spiro-indole (thio)barbiturates

0.400 mmol of 5-(2-nitro)benzylidene thiobarbiturates derivatives, 0.200 mmol of di-hydrate tin(II) chloride and 0.70 mL of concentrated chloridric acid in 10 mL of methanol was refluxed at 68ºC with continuous stirring for 40 min. The reaction proceeded as a suspension resulting in a fluorescent solid yellow powder. The final product was filtered and dried.

3'-Hydroxy-6-thioxoidene-1',3'-dihydrospiro[1,5-diazinane-3,2'-indole]-2,4-dione (10a) obtained from 5-[(2-nitrophenyl)methylidene]-2-sulfanylidene-1,3-diazinane-4,6-dione (**3b**) resulting in a fluorescent yellow solid with 45% yield. η= 45%. ^{1}H NMR (400MHz, DMSO-*d6*): δ (ppm) =11.05 (2H, s, NH), 7.87 (1H, d, *J*= 8.8 Hz, CH_{ar}), 7.34 (1H, d, *J*= 9.0 Hz, CH_{ar}), 7.21 (1H, dd, *J*= 8.9, 6.3 Hz, CH_{ar}), 6.73 (1H, dd, *J*= 8.7, 6.3 Hz, CH_{ar}). ^{13}C NMR

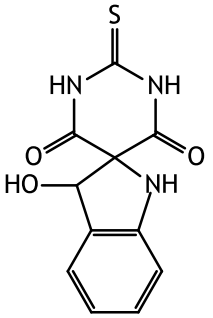

(300MHz, DMSO-*d6*): δ (ppm) = 85,4 (C), 113,5 (CH_{ar}), 114.6 (C), 119.7 (CH_{ar}), 130.7 (CH_{ar}), 156.7 (C=O), 161.4 (C(OH)), 166.5 (C=O), 174.9 (C=S).

3'-Hydroxy-1,5-diphenyl-6-thioxoidene-1',3'-dihydrospiro[1,5-diazinane-3,2'-indole]-2,4-dione (10b) obtained from 5-[(2-nitrophenyl)methylidene]-1,3-diphenyl-2-sulfanylidene-1,3-diazinane-4,6-dione (**3c**) resulting in a fluorescent yellow solid. η= 70%, ^{1}H NMR (400MHz, DMSO--*d6*): δ (ppm) = 7.80 (1H, d, *J*=8.8 Hz, CH_{ar}), 7.40 (4H, *J*=7.7 Hz, CH_{ar}), 7.35 (1H, d, *J*=8.9 Hz, CH_{ar}), 7.29 (2H, t, *J*=7.4 Hz, CH_{ar}), 7.24-7.19 (5H, m, CH_{ar}), 6.72 (1H, dd, *J*=8.9, 6.2 Hz, CH_{ar}). ^{13}C NMR (300MHz, DMSO-*d6*): δ (ppm) = 85.8, 113.6 (CH_{ar}), 114.8 (C), 119.8 (CH_{ar}), 120.8 (CH_{ar}), 127.4 (CH_{ar}), 128.9 (CH_{ar}), 130.0 (CH_{ar}), 130.7 (CH_{ar}), 142.3 (C), 156.6 (C), 160.1 (C=O), 166.7 (C), 179.0 (C=S).

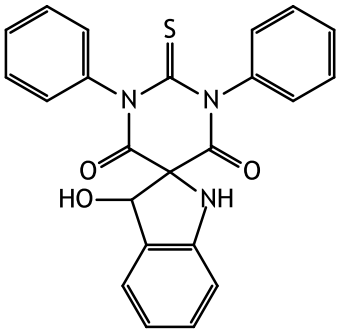

3'-Hydroxy-1,5-dimethyl-1',3'-dihydrospiro[1,5-diazinane-3,2'-indole]-2,4,6-trione (10c) obtained from 1,3-dimethyl-5-[(2-nitrophenyl)methylidene]-1,3-diazinane-2,4,6-trione (3d) resulting in a fluorescent yellow solid with 69% yield. η= 70%, ^{1}H NMR (400MHz, DMSO-*d6*): δ (ppm) = 7.86 (1H, dt, *J*= 8.8, 1.1 Hz, CH_{ar}), 7.36 (1H, dt, *J*= 8.0, 1.0 Hz, CH_{ar}), 7.28 (1H, ddd, *J*= 8.9, 6.2, 1.1 Hz, CH_{ar}), 6.80 (1H, ddd, *J*= 8.9, 6.2, 1.1 Hz, CH_{ar}), 5.71 (1H, ddd, *J*= 8.8, 6.3, 0.9 Hz, CH_{ar}), 3.16 (6H, s, CH_3). ^{13}C NMR (400MHz, DMSO-*d6*): δ (ppm) = 27.6 (CH_3), 55.0 (C), 112.9 (CH), 114.8 (C_{ar}), 120.0 (CH), 125.6 (CH), 131.1 (CH), 152.3 (C=O), 155.9 (C=O), 160.9 (C(OH)), 167.4 (C=O).

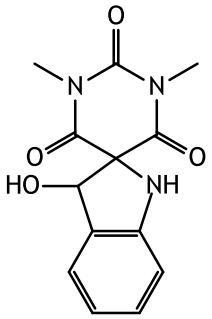

5.2. Biological Studies

5.2.1. Antioxidant assay: DPPH (1,1-diphenyl-2-picrylhydrazyl) free radical scavenging activity

5.2.1.1. Preparation of compound solutions

All compounds were dissolved in dimethyl sulfoxide (DMSO) in a concentration of 10 mM and stored at 4ºC. From this mother solution, several solutions were prepared by their adequate dilutions in ethanol before each assay, ensuring a 30 µM concentration in each well for the initial screening and concentrations of 1.0, 7.5, 15.0, 30.0, 50.0 and 100 µM for concentration-response curves.

5.2.2.1. DPPH Assay

The antioxidant activity was determined spectrophotometrically by measuring the reduction extension of DPPH by the tested compounds. The reaction started with the addition of 100 µL of the sample solution and 100 µL of the DPPH solution (0.2 Mm). The reduction capacity was followed by measuring the absorvance at 517 nm after 20 and 60 minutes. Between the absorvance measures, the solutions were kept in the dark. The absorvance of the negative control was determined by substituting the sample solutions for ethanol, whereas the Trolox was used as the positive control. A blank sample was performed for each compound by changing the DPPH for ethanol in order to discount the absorvance of each compound. Each study were performed in triplicate and the radical scavenging activity of each compound was calculated using the following equation:

$$\%\text{Reduction} = [1-(\text{Abs}_{\text{sample}} - \text{Abs}_{\text{balnk}}/\text{Abs}_{\text{negative control}})]x100$$

After the initial screening of each compound at 30µM, it was calculated de IC_{50} for the two best compounds and Trolox.

5.2.2. *In vitro* xanthine oxidase inhibition assays

5.3.1.1. Preparation of compounds solutions

All tested compounds were dissolved in DMSO in a concentration of 10 mM. From this mother solution, a 30 µM concentration solution was prepared for screening assays and a 50 µM concentration to prepare the samples for the concentration-response curves. The xanthine mother solution with 10 mM concentration was prepared in an aqueous solution of 25 mM of NaOH. All mother solutions were stored at 4ºC. Before each experience, several dilutions from the mentioned solutions were prepared in 50 mM dihydrogen fosfate buffer (pH 7.4), ensuring a concentration of 30 µM in each well on the screening essay and 0.1, 1.0, 7.5, 15.0, 30.0, 50.0, and 100.0 µM for the concentration-response curve essay. The final DMSO concentrations of 1% was insured so it would not interfere with the enzyme activity.

5.3.1.2. Xanthine oxidase inhibition assay

The xanthine oxidase activity oxidase was determined spectrophotometrically by measuring the rate of hydroxylation of the substrate (xanthine) into uric acid, which is a colourless end product of the reaction and shows absorption at 295 nm. In each assay, 50 µL of tested solution and 50 µL of XO suspension from the bovine serum (0.1 U/mL) were added in a well, being pre-incubated at 37ºC for 5 minutes. The reaction started by introducing 150 µL of xanthine (0,42 mM) and further incubated for 10 minutes. Absorvance was measured minute by minute, mixing it slowly 20 seconds before each measure. Buffer was used as the negative control and allopurinol as the positive control. To discount the absorvance of the compounds, a blank sample was measured, consisting by 50 µL of the tested solution and 200 µL of buffer. Each study were performed in triplicate and the inhibitory percentage of each sample was calculated using the followed equation:

$$\% \text{ Inhibition} = [1-(Abs_{\text{sample}} - Abs_{\text{blank of the sample}}/Abs_{\text{negative control}})]x100$$

After the initial screening of each compound at 30µM, it was calculated de IC_{50} for the for the compounds that exhibited moderate inhibition values.

5.2.3. Cell studies

5.2.3.1. Cell cultures

In this study was used a cell line from human breast carcinoma (MCF-7) obtained from American Type Culture Collection (ATCC; Manassas, VA, USA). This cell line was cultured in 75 or 175 cm^2 culture flasks at 37ºC in a humidified air incubation with 5% CO_2. MCF-7 cells were cultured with high-glucose Dulbecco's modified Eagle medium (DMEM) supplemented with 10% fetal bovine serum (FBS; SigmaAldrich, Inc.) and 1% antibiotic/antimycotic (10,000 U/mL penicillin G, 100 mg/mL streptomycin and 25 µg/mL anfothericin B)(Ab; SigmaAldrich, Inc.). The cells used in the experiments were used in passages 26 to 28. The medium was renewed every 2-3 days until cells reach confluence. When cells reached 90-95% confluence, they were detached by gentle trypsinization and, before the experiments, viable cells were counted by trypan-blue exclusion assay and adequately diluted in the complete culture medium.

5.2.3.2. Preparation of compounds solutions

All compounds were dissolved in dimethyl sulfoxide (DMSO) in a concentration of 10 mM and stored at 4ºC. From this mother solution, 30 µM solutions were prepared by their adequate dilution in the complete culture medium before each experiment. The maximum DMSO concentration in the studies was 1% and previous experiments revealed that this solvent level has no significant effect in cell proliferation (data not shown).

5.2.3.3. MTT cell proliferation assay

Cells treatment with the compound

After trypsinization and cells counting, 100 µL of cell suspension in medium with an initial density of $2x10^4$ cells/mL was seeded in 96-well culture plates (Nunc, Apogent, Denmark) and left to adhere for 48h. After adherence, the appropriate medium was replaced by several solutions of the compounds in study (30µM concentration), using untreated cells as negative controls, for approximately 72h. Each experiment was performed in quadruplicate and independently repeated at least two times.5-FU was used as a positive control.

MTT assay

The *in vitro* anti-proliferative effects were evaluated by the MTT assay (3-(4,5-dimethylthiazol-2-yl)-2,5-diphenyltetrazoliumbromide)(Sigma Aldrich), by measuring the extent of reduction of MTT. After the incubation period (72h) the medium was removed, 100 µL of phosphate buffer saline (NaCl 137 mM; KCl 2.7 mM, Na_2HPO_4 10 mM and, KH_2PO4 1.8 mM in distilled water and pH adjusted to 7.4) were used to wash the cells and then 100 µL of the MTT solution (5mg/mL), prepared in the appropriate serum-free medium, was added to each well, followed by 4h incubation at 37ºC. Thereafter, the MTT containing medium was removed and the formazan crystals were dissolved in DMSO. The contents of each cell were transferred to a reading plate and the absorbance was measured at 570nm using a microplate reader Anthos 2020 (Alfagene). Cell viability values were expressed as percentages relatively to the absorbance determined in the cells used as controls.

5.2.3.4. Statistics

The MTT assays were performed in quadruplicate and independently repeated at least two times. The acquired data were expressed as a mean± standard deviation (SD). *t*-Student test was applied to determine statistical significance ($p<0,05$) in cell proliferation results. These calculations were performed using the Microsoft Excell 2013 software.

5.4. Molecular Docking

The compounds **2a-h** and **3b-c** of this present project were subjected to molecular docking studies, as well as the drugs allopurinol and febuxoxtat (reference compounds), using the AutoDock Tools program (version 1.5.6) with Lamarckian genetic algorithm. The 2D-structure of the synthesized ligand molecule were drawn using the ChemDraw Pro 12.0 program and converted to energy minimized 3D structures using the Marvin Scketch 15.11.9

software (ChemAxon, Budapest, Hungary). The enzyme used in this studies was Xanthine Oxidase (XO) and the method was validated before the compounds molecular studies.

The crystal structure of XO from bovine milk (PDB code 1VDV) with the inhibitor 1-[3-cyano-4-(2,2-dimethylpropoxy)phenyl]-1*H*pyrazole-4-carboxylic acid (code Y-700) was obtained from Protein Data Bank. The protein and the correspondent ligand were isolated with Chimera 1.9rc software. Therefore the preparation, parameters definition and results analysis were performed using AutoDock Tools 1.5.6. The docking simulations were carried out using AutoDock 4.0 package with AutoGrid4 and AutoDock4. AutoGrid4 defines the active site map, where the docking is processed, and generate all needed calculations, and AutoDock4 performs the docking simulation itself.

The XO protein was prepared by adding Gasteiger charges, emerging of n-polar hydrogens and removing the water molecules. The rigid roots of each compound were defined automatically. Ligand parameters were maintained as default. The active pocket was selected by a grid box with 60 x 60 x60 dimensions and 0.300 Å spacing around the co-crystalized ligand thus, ensuring that the tested compounds occupy the defined space. For the execution of the grid, it was added a parameter file "AD4_Parameter.dat", an library archive, The box size was relatively maintained for each ligand. All other parameters were the standard except the number of conformations. To each compound, 10 conformations were generated in order to achieve more feasible results.

6. References

1. Enroth C., Eger B. T., Okamoto K, Nishino T, Nishino T, Pai EF. Crystal structures of bovine milk xanthine dehydrogenase and xanthine oxidase : structure-based mechanism. *Proceeding of the National Academy of Sciences*. 97(20), 10723-10728 (2000);
2. Harrison, R. Structure and Function of Xanthine Oxidoreductase : Where Are We Now ?. *Free Radical Biology & Medicine*. 33(6), 774–797 (2002);

3. Harrison, R. Milk xanthine oxidase : Properties and physiological roles. *International Diary Journal*. 16, 546–554 (2006);
4. Nishino T., Okamoto K., Eger B. T., Pai E. F., Nishino T. Mammalian xanthine oxidoreductase – mechanism of transition from xanthine dehydrogenase to xanthine oxidase. *The FEBS Journal*. 275, 3278–3289 (2008);
5. Kistić, D. A., Dimitrijević, D. S., Stojanović, G. S., Palić, I. R., Đorđević, A., Ickovski, J. D. Xanthine Oxidase: Isolation, Assays of Activity, and Inhibition. *Journal of Chemistry*, 2015, 1-8 (2015);
6. Harrison R. Physiological roles of xanthine oxidoreductase. *Drug Metabolism Reviews*. 36(2), 363–375 (2004);
7. B-Rao, C., Kulkarni-Almeida, A., Katkar, K. V., Khanna, S., Ghosh, U., Keche, A., Shah, P., Srivastava, A., Korde, V., Nemmani, K. V. S., Deshmukh, N. J., Dixit, A., Brahma, M. K., Bahirat, U., Doshi, L., Sharma, R., Sivaramakrishnan, H., Identification of novel isocytosine derivatives as xanthine oxidase inhibitors from a set of virtual screening hits, *Bioorganic & Medicinal Chemistry. 20*, 2930-2939 (2012);
8. Sarawek, Sasiporn. Xanthine Oxidase Inhibition and Antioxidant Activity of an Artichoke Leaf Extract (*Cynara scolymus L.*) and its Compounds. *University of Florida*, 22-23 (2007);
9. Lu, J., Yao, Q, Chen, C. 3, 4-dihydroxy-5-nitrobenzaldehyde (DHNB) is a potent inhibitor of xanthine oxidase : A potential therapeutic agent for treatment of hyperuricemia and gout, *Biochemical Pharmacology*. 86(9), 1328–37 (2013);
10. Nivorozhkin, A., Szabo, C. Therapeutic Effects of Xanthine Oxidase Inhibitors : Renaissance Half a Century after the Discovery of Allopurinol, *Pharmacological Reviews*. 58(1), 87–114 (2006);
11. Borges, F., Fernandes, E., Roleira, F. Progress towards the Discovery of Xanthine Oxidase Inhibitors. *Current Medicinal Chemistry*. 9, 195–217 (2002);
12. Rodrigues, M. V. N., Barbosa, A.F., Silva, J. F., Santos, D. A., Vanzolini, K. L., Moraes, M. C., Corrêa, A. G., Cass, Q.B. 9-Benzoyl 9-deazaguanines as potent xanthine oxidase inhibitors. *Bioorganic & Medicinal Chemistry*. 24(2), 226–231 (2016);
13. Gupta, S., Rodrigues, L. M., Esteves, A.P., Oliveira-Campos, A. M. F., Nascimento, M. J., Nazareth, N., Cidade, H., Neves, M. P., Fernandes, E., Pinto, M., Cerqueira, N. M. F.S., Brás, N. Synthesis of *N*-aryl-5-amino-4-cyanopyrazole derivatives as potent xanthine oxidase inhibitors. *European Journal of Medicinal Chemisty*. 43, 771–780 (2008);
14. Oettl, K., Reibnegger, G., Pteridines as inhibitors of xanthine oxidase : structural requirements. *Biochimica et Biophisica Acta*, 1430, 387–395 (1999);
15. Rastelli, G., Costantino, L., Albasini, A., Campi, V. 1997. A Model of the Interaction of Substrates and Inhibitors with Xanthine Oxidase. *Journal of American Chemical Society*. 119, 3007–3016 (1993);

16. Ernst, M. E., Fravel, M. A., Febuxostat : A Selective Xanthine-Oxidase / Xanthine Dehydrogenase Inhibitor for the Management of Hyperuricemia in Adults with Gout. *Clinical Therapeutics*. 31(11), 2503–2518 (2009);
17. Takano, Y., Hase-Aoki, K., Horiuchi, H., Zhao, L., Kasahara, Y, Kondo, S., Becker, M. A. Selectivity of febuxostat, a novel non-purine inhibitor of xanthine oxidase / xanthine dehydrogenase. *Life Sciences*. 76, 1835–47 (2005);
18. Ishibuchi, S., Morimoto, H., Oe, T., Ikebe, T., Inoue, H., Fukunati, A., Kamezawa, M., Yamada, I., Naka, Y. Synthesis and Structure-Activity Relationships of 1-Phenylpyrazoles as Xanthine Oxidase Inhibitors. *Bioorganic & Medicinal Chemistry Letters*. 11, 879–882 (2001);
19. Wang, S., Yan, J., Wang, J., Chen, J., Zhang, T., Zhao, Y., Xue, M., Synthesis of some 5-phenylisoxazole-3-carboxylic acid derivatives as potent xanthine oxidase inhibitors. *European Journal of Medicinal Chemistry*. 45(6), 2663–2670 (2010);
20. Guan, Q., Cheng, Z., Ma, X., Wang, L., Feng, D., Cui, Y., Bao, K., Wu, L., Zhang, W. Synthesis and bioevaluation of 2-phenyl-4-methyl-1 , 3-selenazole-5- carboxylic acids as potent xanthine oxidase inhibitors. *European Journal of Medicinal Chemistry,* 85, 508–516 (2014);
21. Chen, S., Zhang, T., Wang, J., Wang, F., Niu, H., Wu, C., Wang, S. Synthesis and evaluation of 1-hydroxy / methoxy-4-methyl-2-phenyl- 1 h -imidazole-5-carboxylic acid derivatives as non-purine xanthine oxidase inhibitors. *European Journal of Medicinal Chemistry*. 103, 343–353 (2015);
22. Nepali, K., Singh, G., Turan, A., Agarwal, A., Sapra, S., Kumar, R., Banerjee, U. C., Verma, P. K., Satti, N. K., Gupta, M. K., Suri, O. P. Dhar, K. L. A rational approach for the design and synthesis of 1-acetyl-3,5-diaryl-4,5-dihydro(1*H*)pyrazoles as a new class of potential non-purine xanthine oxidase inhibitors. *Bioorganic & Medicinal Chemistry*. 19(6), 1950–1958 (2011);
23. Nepali, K., Agarwal, A., Sapra, S., Mittal, V., Kumar, R., Banerjee, U. C., Gupta, M. K, Satti, N. K., Suri, O. P., Dhar, K. L. *N*-(1,3-diaryl-3-oxopropyl)amides as a new template for xanthine oxidase inhibitors. *Bioorganic &. Medicinal Chemistry*. 19(18), 5569–5576 (2011);
24. Dhiman, R., Sharma, S., Singh, G., Nepali, K., Mohinder, P., Bedi, S. Full paper design and synthesis of aza-flavones as a new class of xanthine oxidase inhibitors. *Archiv der Pharmazie Chemistry in Life Sciences*. 24 346, 7–16 (2013);
25. Singh, H., Sharma, S., Ojha, R., Gupta, M. K, Nepali, K., Bedi, P. M. S. Synthesis and evaluation of naphthoflavones as a new class of non purine xanthine oxidase inhibitors. *Bioorganic & Medicinal Chemistry Letters.*, 1–6 (2014);
26. Baeyer, A., *Annalen der Chemie und Pharmacie*, 131, 291-302 (1864);

27. Neumann, Donna, The Design and Synthesis of Novel Barbiturates of Pharmaceutical Interest (2004). *University of New Orleans, Thesis and Dissertations*. Paper 1040;

28. Mahmudov, K. T., Kopylovich, M. N., Maharramov, A. M., Kurbanova, M. M., Gurbanov, A.V., Pombeiro, A. J. L. Barbituric acids as a useful tool for the construction of coordination and supramolecular compounds, *Coordination Chemistry Reviews*, 265, 1-37 (2014);

29. Bojarski, J. T., Mokrosz, J. L., Barton, H. J., Paluchowska, M. H. Recent progress in barbituric acid chemistry, *Advances in Heterocyclic Chemistry*, 38, 229-297 (1985);

30. Garcia, H. C., Campos, M. T. C., Edwards, H. G. M., de Oliveira, L, F. C. Vibrational and structural properties of barbiturate anions in supramolecular compounds. *Vibrational Spectroscopy,* 86, 134–142 (2016);

31. Lutoshkin, M. A., Golovnev, N. N., Acid-base properties and keto-enol equilibrium of a 5-substituted derivative of 1,3-diethyl-2-thiobarbituric acid. *Heterocyclic Community*. 22(2), 111–116 (2016);

32. Volonterio, A., Zanda, M., Chimica, C.N.R., Quilico, S.A., Mancinelli, V. Multicomponent, One-Pot Sequential Synthesis of 1, 3, 5- and 1,3,5,5-Substituted Barbiturates, *The Journal of Organic Chemistry,* 73 7486–7497 (2008);

33. Ganem, B. Strategies for Innovation in Multicomponent Reaction Design. *Accounts of Chemical Research,* 42(3), 463–472 (2009);

34. Shimo, K., Wakamatsu, S. A New Barbituric Acid Synthesis in Liquid Ammonia-Alkali Hidroxide. II. Condensation of Malonamide Derivatives with Ethyl Carbonate. *Journal of Organic Chemistry*, 24, 19-21 (1959);

35. Botsi,S., Tsolomitis, A. One or two-step acid mediated cyclocondensation: Process for the preparation of 5-carbethoxy-2-thiouracils from diethyl ethoxymethylenemalonate and thioureas. *Heterocyclic Communications*, 229–234 (2007);

36. Bouhlel A, Curti, C., Vanelle, P. New Methodology for the Synthesis of Thiobarbiturates mediated by Manganese (III) Acetate. *Molecules*, 17, 4313–4325 (2012);

37. Kidwai, M,, Venkataramanam, R., Garg, R.K., Bhushan, K.R. Novel one pot synthesis of new pyranopyrimidines using microwaves, *Journal of Chemical Research,* S, 586-587 (2000);

38. Kappe, C.O, Dallinger, D. The impact of microwave synthesis on drug discovery. *Nature Reviews – Drug Discovery*, 5, 51–64 (2006);

39. Shaker, R.M., Ishak, E.A. Barbituric Acid Utility in Multi-Component Reactions. *Zeitschrift für Naturforschung B: A Journal of Chemical Sciences,* 66, 1189-1201 (2011);

40. Ziarani, G.M., Aleali, F., Lashgari, N. Recent applications of barbituric acid in multicomponent reactions. *Royal Society of Chemistry Advances,* 6, 50895-50922 (2016);

41. Ivantsova, M.N., Tokareva, M.I., Mironov, M.A. Multicomponent Interphase Synthesis of Heterocyclic Compounds (Review). *Chemistry of Heterocyclic Compounds*, 48, 584-600 (2012);

42. Kidwai, M., Singhal, K., Kukreja, S. One-Pot Green Synthesis for Pyrimido[4 ,5- *d*] pyrimidine Derivatives. *Zeitschrift für Naturforschung B: A Journal of Chemical Sciences*, 62, 732–736 (2007);

43. Ko, S., Sastry, M.N.V., Lin, C., Yao, C. Molecular iodine-catalyzed one-pot synthesis of 4-substituted-1,4-dihydropyridine derivatives via Hantzsch reaction. *Tetrahedron Letters*. 46, 5771–5774 (2005);

44. Muñoz-Lopez, F., Ucha-Udabe, R., Alamo, C. The history of barbiturates a century after their clinical introduction. *Neuropsychiatric Disease and Treatment*, 4, 329-343 (2005);

45. Bialer, M. Chemical properties of antiepileptic drugs (AEDs). *Advanced Drug Delivery Reviews*, 64, 887-895 (2012);

46. Kim, S., Pudzianowski, A. T., Leavitt, K. J., Barbosa, J., McDonell, P. A., Metzler, W. J., Rankin, B. M., Liu, R., Vaccaro, W., Pitts, W. Structure-based design of potent and selective inhibitors of collagenase-3 (MMP-13), *Bioinorganic & Medicinal Chemistry Letters*, 15, 1101-1106 (2005);

47. Foley, L. H., Palermo, R., Dunten, P., Wang, P. Novel 5,5-Disubstitutedpyrimidine-2,4,6-triones as Selective MMP Inhibitors. *Bioinorganic & Medicinal Chemistry Letters*, 11, 969-972 (2001);

48. Suzuki, H., Kneller, M. B., Rock, D.A., Jones, J.P., Trager, W.F., Rettie, A.E. Active-site characteristics of CYP2C19 and CYP2C9 probed with hydantoin and barbiturate inhibitors. *Archives of Biochemistry and Biophysics*, 429, 1–15 (2004);

49. Maquoi, E., Sounni, N.E., Devy, L., Olivier, F., Frankenne, F., Krell, H., Grams, F., Foidart, J., Noël, A. Anti-Invasive, Antitumoral and Antiangiogenic Efficacy of a Pyrimidine-2,4,6-trione Derivative, An Orally Active and Selective Matrix Metalloproteinases Inhibitor. *Clinical Cancer Research*, 10, 4038–4047 (2004);

50. Sokmen, B. B., Ugras, S. Antibacterial, Antiurease and Antioxidant Activities of some Arylidene Barbiturates. *Applied Biochemistry and Biotecnology*, 171. 2030–2039 (2013);

51. Haldar, M. K., Scott, M. D., Sule, N., Srivastava, D. K., Mallik, S. Synthesis of Barbiturate-Based Methionine Aminopeptase-1 Inhibitors. *Bioinorganic & Medicinal Chemistry Letters*, 18 (7), 2373-2376 (2008);

52. Dhorajiya, B. D., Ibrahim, A. S., Badria, F. A., Dholakiya, B. Z. Chemistry design and synthesis of novel nucleobase-based barbiturate derivatives as potential anticancer agents. *Medicinal Chemistry Research*, 23, 839–847 (2014);

53. Bhaskarachar, K. K, Vijayakumar, B., Hegde, S., Balakrishna, J. P., Reddy, S. Y. Design, synthesis and anticancer activity of functionalized spiro-quinolines with barbituric and thiobarbituric acids. *Medicinal Chemistry Research*, 24, 3516–3528 (2015);

54. Palmucci, J., Mahmudov, K. T., Guedes da Silva, M. F. C., Marchetti, F., Pettinari, C., Petrelli, D., Vitali, L. A., Quassinti, L., Bramucci, M., Lupidi, G., Pombeiro, A. J. L. DNA and BSA Binding, Anticancer and Antimicrobial Properties of Co (II), Co (II/III), Cu (II) and Ag (I) Complexes of Arylhydrazones of Barbituric Acid. *Royal Society of Chemistry Advances*, 1-26 (2015);

55. Alcerreca, G., Sanabria, R., Miranda, R., Arroyo, G., Tamariz, J., Delgado, F. Preparation of benzylidene barbituric acids by infrared irradiation in absence of solvent. *Synthetic Communications,* 30 (7), 1295-1301 (2000);

56. N. Seyyedi, F. Shirini, M.S. Nikoo Langarudi, DABCO-based ionic liquids: green and recyclable catalysts for the synthesis of barbituric and thiobarbituric acid derivatives in aqueous media, *Royal Society of Chemistry Advances*, 6 44630-44640 (2016);

57. M. Kuanar, B.K. Mishra, Applicability of Williams-Norrington model for quantitative structure spectra relationship, Indian Journal of Chemistry, Section A: Inorganic, Bio-inorganic, Physical, *Theoretical & Analytical Chemistry*, 34, 721-723 (1995);

58. M.K. Haldar, M.D. Scott, N. Sule, D.K. Srivastava, S. Mallik, Synthesis of barbiturate-based methionine aminopeptidase-1 inhibitors, *Bioorganic & Medicinal Chemistry Letters*, 18, 2373-2376 (2008);

59. Khan, K. M., Ali, M., Ajaz, A., Perveen, S., Choudhary, M. I. Synthesis of 5-arylidene barbiturates : a novel class of DPPH radical scavengers. *Letters in Drug Design & Discovery,* 5 , 286–291 (2008);

60. Thokchom, H. S.,Nongmeikapam, A. D., Laitonjam, W. S. Synthesis of fused pyrazolo-, isoxazolo-, pyrimido- and pyridopyrimidines. *Canadian Journal of Chemistry,* 83, 1056-1062 (2005).

61. Mobinikhaledi, A., Mosleh, T., Foroughifar, N. Triethyl benzyl ammonium chloride (TEBAC) catalysed solvent-free one-pot synthess of pyrimido [4,5-*d*]pyrimidines. *Research Chemical Intermed.*, 41, 2985-2990 (2015);

62. Faidallah, H. M., Khan, K. A. Synthesis and biological evaluation of new barbitutric and thiobarbituric acids: fluoro analogs of benzenesulfonamidas as antidiabetic and antibacterial agents. *Journal of Fluor Chemistry*, 142, 96-104 (2012).

63. Zollinger, Heinrich. *Color Chemistry: Syntheses, Properties and Aplicaions of Organic Dyes and Pigments*. 2nd edition, VCH, Weinheim, New York, Basel, Cambridge;

64. Desbène-Finck, K.A. S., Giorgi-Renault, P. H. S. A new synthetic approach to functionalize pyrimido [4,5-*b*]quinoline-2,4(1H, 3H)-diones via a three-component one-pot reaction. *Molecular. Diversity,* 14, 123–130 (2010);

65. Serrano, J., *Novos espiro(tio)barbituratos: Síntese, caracterização e avaliação biológica* (Master thesis). Universidade da Beira Interior, Covilhã, Portugal (2016);

66. Zhao, M., Zhu, D., Sun-Waterhouse, D., Su, G., Lin, L., Wang, X., Dong, Y. In vitro and in vivo studies on adlay-derived seed extracts: phenolic profiles, antioxidant activities,

serum uric acid suppression and xanthine oxidase inhibitory effects. *Journal of Agricultural and Food Chemistry*, 62, 7771-7778 (2014)

67. Dhorajiya, B. D., Dholakiya, B. Z., Ibrahim, A. S., Badria, F. A. 2014. Nucleobase-Based Barbiturates: Their Protective Effect Against DNA Damage Induced by Bleomycin-Iron, Antioxidant and Lymphocyte Transformation Assay. *BioMedical Research International*, 1-7 (2014);
68. Mohammed, K., Ali, M., Wadood, A., Khan, M., Arif, M, Perveen, S., Choudhary, M. I., Voelter, W. Molecular Modeling-based Antioxidant Arylidene Barbiturates as Urease Inhibitors. *Journal of Molecular Graphics and Modelling*, 30, 153–156 (2011);
69. Gupta, S, Rodrigues, L.M., Esteves, A.P., Oliveira-Campos, A.M., Nascimento, M.S., Nazareth, Cidade, N. H., Neves, M.P., Fernandes, E., Pinto, M., Cerqueira, N.M., Brás, N., Synthesis of *N*-aryl-5-amino-4-cyanopyrazole derivatives as potent xanthine oxidase inhibitors, *European Journal of Medicinal Chemistry*, 43, 771-780 (2008);
70. Khan, K. M., Khan, M., Karim, A., Taha, M., Ambreen, N., Gojayev, A., Perveen, S., Choudhary, M. I. Xanthine Oxidase Inhibition by 5-Aryledene *N*,*N*'- Dimethylbarbituric Acid Derivatives. *Journal of Chemical Society of Pakistan*, 35(2), 495–498 (2013);
71. Giard, D. J., Aaronson, S. A., Todaro, G.J., Arnstein, P., Kersey, J. H., Parks, W.P. 1973. *In vitro* Cultivation of Human Tumors : Establishment of Cell Lines Derived from a Serie of Solid Tumors. *Journal of National Cancer Institute,* 51(5), 1417–1423 (1973);
72. Stockert, J. C., Blázquez-Castro, A., Ca, M., Horobin, R. W. MTT assay for cell viability : Intracellular localization of the formazan product is in lipid droplets. *Acta Histochemica,*. 114, 785–796 (2012);
73. Singh, P., Kaur, J., Paul, K. Pyrimidin-2,4-diones with Amines : Anti-cancer and Metal Sequestering Properties. *Indian Journal of Chemistry*. 47, 291–296 (2008);
74. Laxmi, S. V., Rajitha, G., Rajitha, B., Rao, A. J. Photochemical synthesis and anticancer activity of barbituric acid, thiobarbituric acid, thiosemicarbazide and isoniazid linked to 2-phenyl indole derivatives. *Journal of Chemical Biology*, 9, 57–63 (2016)
75. Gulliya, K. S., Anti-cancer uses for barbituric acids analogues, US Patent 5674870, 7th October,1993, p.14;
76. Fukunari, A., Okamoto, K., Nishino, T., Eger, B. T., Pai, E. F. Y-700 [1-[3-Cyano-4-(2,2-dimethylpropoxy)phenyl]-*1H*pyrazole-4-carboxylic Acid]: a Potent Xanthine Oxidoreductase Inhibitor with Hepatic Excretion. *The Journal of Pharmacology and Experimental Therapeutics*, 311 (2), 519–528 (2004);
77. Bajaj, K., Burudkar, S., Shah, P., Keche, A., Ghosh, U. Lead Optimization of Isocytosine-derived Xanthine Oxidase Inhibitors. *Bioorganic & Medicinal Chemistry Letters*, 23(3), 834–838 (2013);

78. Beedkar, S. D., Khobragage, C. N., Chobe, S. S., Dawane,B. S., Yemul, O. S. Novel thiazolo-pyrazolyl derivatives as xanthine oxidase inhibitoes and free radical scavengers. *International Journal of Biological Macromolecules*, 50, 947-956 (2012);
79. Shukla, S., Kumar, D., Ojha, R., Gupta, M. K., Nepali, K., Bedi, P. M. S. 4,6-diaryl / heteroarylpyrimidin-2(1H)-ones as a New Class of Xanthine Oxidase Inhibitors. *Arch. Pharm. Chem. Life Sci*, 347, 486–495 (2014);
80. B-Rao, C., Kulkarni-Almeida, A., Katkar, K. V., Khanna, S., Ghosh, U. Identification of novel isocytosine derivatives as xanthine oxidase inhibitors from a set of virtual screening hits. *Bioorganic & Medicinal Chemistry*, 20(9), 2930–2939 (2012);
81. Ya, J., Zhang, G., Hu, Y., Ma, Y. Effect of luteolin on xanthine oxidase: Inhibition kinetics and interaction mechanism merging with docking simulation, *Food Chemistry*, 141, 3766-3773 (2013);
82. Ali, H. I., Fujita, T., Akaho, E. A comparative study of Autodock and pmf scoring performances, and SAR of 2-substituted pyrazolotriazolopyrimidines and 4-substituted pyrazolopyrimidines as potent xanthine oxidase inhibitors. *J Comput Aided Mol Des*, 24, 57–75 (2010);

6. Publications

Panel Communications within the scope of this dissertation

Cavalheiro E., Keurulainen L., Yli-Kauhaluoma J., Moreira V., Silvestre S., Almeida P., Synthesis of 5-methylene(thio)urea (thio)barbiturates as portential xanthine oxidase inhibitors, Abstract book of IX Annual-CICS-UBI Symposium (2016) (attachment 2).

Panel Communications outside the scope of this dissertation

Catarro M., Cavalheiro E, Serrano J., Silvestre S., Almeida P., Development of new *ortho*-(alkylthio)-*N*-acetanilidas as potential anticancer drugs, Abstracts book of IX Annual CICS-UBI Symposium (2016) (attachment 3)

Ramos S. S, Catarro M., Cavalheiro E., Serrano J., Silvestre S., Almeida P., Looking for new 2-(alkylthio)-*N*-4-nitroanilines resembling Nimesulide analogues as potential anti drugs, III Jornadas da Química e Bioquímica, University of Beira Interior (attachment 4)

~

7. Attachments

Attachment 1 – Compounds Structure Support

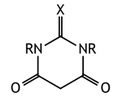

1a: X=S, R=H
1b: X=S, R=Ph
1c: X=O, R=H
1d: X=O, R=Me

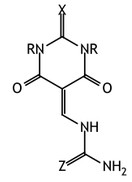

2a: X=S, R=H, Z=O
2b: X=S, R=H, Z=S
2c: X=S, R=Ph, Z=O
2d: X=S, R=Ph, Z=S
2e: X=O, R=H, Z=O
2f: X=O, R=H, Z=S
2g: X=O, R=Me, Z=O
2h: X=O, R=Me, Z=S

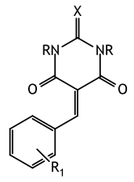

3a: X=S, R=H, R_1= 4-Br
3b: X=S, R=H, R_1= 2-NO_2
3c: X=S, R=Ph, R_1= 2-NO_2
3d: X=O, R=Me, R_1= 2-NO_2

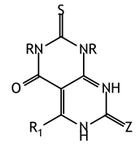

4a: R=H, Z= O, R_1=H
4b: R=Ph, Z=O, R_1=H
4c: R=Ph, Z=S, R_1=H
4d: R=H, Z=O, R_1=4-Br-Ph
4e: R=Ph, Z=O, R_1=Ph
4f: R=Ph, Z=O, R_1=pH

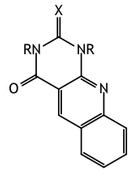

8a: X=S, R=H
8b: X=S, R=Ph
8c: X=O, R=Me

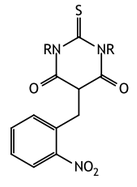

9

Attachment 2 – Abstract of the Panel Communication in the IX Anunal CICS Symposium about this project.

SYNTHESIS OF 5-METHYLENE(THIO)UREA (THIO)BARBITURATES AS POTENTIAL XANTHINE OXIDASE INHIBITORS

Cavalheiro E.,[1] Keurulainen L.,[2] Yli-Kauhaluoma J.,[2] Moreira V.,[2] Silvestre S.,[3] Almeida P.[1,3]

[1] Department of Chemistry, University of Beira Interior, Covilhã, Portugal; [2] Division of Pharmaceutical Chemistry and Technology, Faculty of Pharmacy - University of Helsinki, Helsinki, Finland; [3]CICS-UBI - Health Sciences Research Centre, University of Beira Interior, Covilhã, Portugal

Barbituric acids have an important role on the development of new drugs. Nowadays, these derivatives can be used as sedatives, hypnotics, anticonvulsants and anesthetics. Most of these pharmacological properties are due to different side groups attached on the carbon C5 of the pyrimidine ring.[1]
Some studies indicate that barbiturates can inhibit the xanthine oxidase (XO) enzyme.[2] This enzyme plays an important role in purines metabolism by transforming hypoxanthine to xanthine and then to uric acid. As the overproduction of uric acid is linked to gout disease it is of high interest to inhibit XO.
In order to find new XO inhibitors with improved potency and reduced side effects, several 5-methylene(thio)barbiturates linked to (thio)urea **2** were synthetized starting from (thio)barbituric acid derivatives and *N,N*-derivatives **1.**

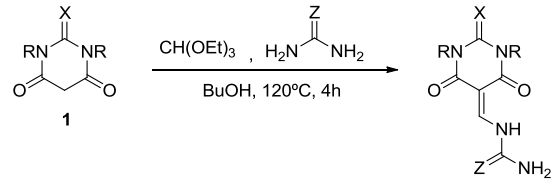

R= H, Me, Ph; X=O, S; Z= O, S

All synthesized compounds were structurally characterized and their computational molecular docking studies were performed.

Keywords: barbiturate derivatives, xanthine oxidase

References: [1] Mahmudov *et al.*, *Coordination Chemistry Reviews* **2014**, *265*, 1-37. [2] Khan *et al.*, *Journal of the Chemical Society of Pakistan* **2013**, *35*, 495-498.

Acknowledgements: This work is supported by FEDER funds through the POCI - COMPETE 2020 - Operational Programme Competitiveness and Internationalisation in Axis I - Strengthening research, technological development and innovation (Project No. 007491) and National Funds by FCT - Foundation for Science and Technology (Project UID/Multi /00709).

Attachment 3 – Abstract of the Panel Communication of a project outside the scope of this dissertation

DEVELOPMENT OF NEW *ORTHO*-(ALKYLTHIO)-*N*-ACETANILIDES AS POTENCIAL ANTICANCER DRUGS

Catarro M. [1], Cavalheiro E. [1], Serrano J. [1], Silvestre S. [1], Almeida P. [1]

[1] *CICS-UBI – Health Sciences Research Centre, University of Beira Interior, Covilhã, Portugal*

Several studies have demonstrated an overexpression of ciclooxygenase-2 (COX-2) in solid cancers. COX-2 is responsible, namely, for the production of prostaglandin-E_2 (PGE-2), which has been associated with tumor progression, invasiveness and angiogenesis. Thus, it is expectable that COX-2 inhibitors including nimesulide and its analogues can exhibit anticancer properties by targeting COX-2. [139]

Recently, several *ortho*-(alkylchalcogen)-*N*-acetanilides structurally resembling nimesulide were synthesized and their potential anticancer activity was evaluated. In fact, *in vitro* cell proliferation studies in human breast (MCF-7) and prostate (LNCaP) cancer cell lines as well as on normal human dermal fibroblasts (NHDF) showed a selective antiproliferative activity for tumoral cells with prominence to the LNCaP cell line and the most potent compounds were O- and/or N-benzylic and -hexyl acetanilides.[138]

In the present work and taking in mind already known groups that potentiate the antiproliferation activity of nimesulide analogues,[138] a set of new 6-nitro and 6-acetamide *ortho*-(alkylthio)-*N*-acetanilides **1** were prepared, in which 2,4-dimethylbenzyl, methylcyclohexyl and/or hexyl are linked to thio and/or to amide group.

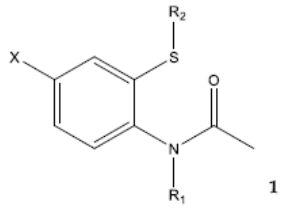

1

X = NO_2, $NHCOCH_3$
R_1 and/or R_2 = Hexyl, 2,4-dimethylbenzyl, methylcyclohexyl

The COX-2 docking studies and biological evaluation through the MTT cell proliferation assay in MCF-7, LNCaP and NHDF cell lines were performed, confirming the potential interest of these new nimesulide analogues as anticancer drugs.

Keywords: *ortho*-(alkylthio)-*N*-acetanilides, nimesulide analogues, anticancer activity

References: [1] Zhong B. *et al.*, *Bioorganic & Medicinal Chemistry Letters* **2011,** *21*, 5324-5327.

[2] Ramos S. S *et al.*, *Tetrahedron* **2014,** *70*, 8930-8937.

Acknowledgements: This work is supported by FEDER funds through the POCI - COMPETE 2020 - Operational Programme Competitiveness and Internationalisation in Axis I - Strengthening research,

technological development and innovation (Project No. 007491) and National Funds by FCT - Foundation for Science and Technology (Project UID/Multi /00709).

Attachment 4 – Abstract of the Panel Communication of a project outside the scope of this dissertation

Looking to new 2-(alkylthio)-*N*-formyl-4-nitroanilines resembling Nimesulide analogues as potential anticancer drugs

Ramos S.S.(1,2), Catarro M.(1,3), Cavalheiro E.(1,3), Serrano J.(1,3), Silvestre S.(3), Almeida P.(1,3)
(1)Department of Chemistry, University of Beira Interior, 6200-001 Covilhã, Portugal; (2)UMTP-UBI - Unit of Textile and Paper Materials, University of Beira Interior, 6200-001 Covilhã, Portugal; (3)CICS-UBI - Health Sciences Research Centre, University of Beira Interior, 6200-506 Covilhã, Portugal.

Nimesulide is a widely used nonsteroidal anti-inflammatory drug (NSAID) having also analgesic and antipyretic properties.
Several studies have demonstrated an overexpression of COX-2 in solid cancer malignancies, increasing the producing of Prostaglandin-2 (PGE2) and therefore potentiating the development of the cancer cells. Since NSAIDs including Nimesulide and its derivatives inhibited COX-2, it is expectable that these compounds are potentially benefit in both cancer development prevention and anticancer once developed. Nimesulide itself is known to possess anticancer properties.
Even before its discovery and until nowadays, a lot of work has been developed to modify the different moieties constituting the nimesulide skeleton, looking for new potent and more selective COX-2 inhibitors and, more recently, for new anticancer agents.
Recently, as part of our efforts to definitively clarify the identity of the products resulting from the hydroxylation of 2-methylbenzoazolium iodides, we described a new synthesis of *ortho*-(alkylchalcogen)-*N*-ethylacetanilides resembling Nimesulide analogues.[1]
Thus, looking for new Nimesulide analogues with potentially anti-cancer properties and taking in mind this new synthetic approach to prepare *ortho*-(alkylchalcogen)-*N*-alkylanilides, we ended a simple way to obtain 2-(alkylthio)-*N*-formyl-4-nitroanilines starting from 6-nitrobenzothiazole. The formilanilides so obtained already protected with a formyl group can be easily converted in other anilides by hydrolysis followed by acylation.
All this new anilides were structurally characterized by ^{1}H and ^{13}C NMR and FTIR. The *in vitro* cytotoxicity of this anilides against human breast (MCF-7) and prostate (LNCaP) cancer cell lines as well as normal human dermal fibroblasts (NHDF) will be evaluated looking for new and potent anti-cancer drugs.

[1] S. S. Ramos, L. V. Reis, R. E. F. Boto, P. F. Santos, P. Almeida, "Synthesis and Dynamic Study of New *ortho*-(alkylchalcogen)acetanilide atropisomers. A second look at the hydrolysis of quaternary 2-methylbenzazol-3-ium salts", Tetrahedron Letters, 2013, 54(40), 5441–5444.

KEY-WORDS: Nimesulide analogous, anticancer activity, new synthetic approach

Acknowledgments: This work was financed by COMPETE (Project Pest-C/SAU/UI0709/2011).